# ELECTRODEPOSITION ON MAGNESIUM ALLOY DIECASTING

by

KATY YEE-YUNG WAN

A thesis submitted for the degree of Doctor of Philosophy of the University of Aston in Birmingham.

April 1986.

THE UNIVERSITY OF ASTON IN BIRMINGHAM

TITLE: ELECTRODEPOSITION ON MAGNESIUM ALLOY DIECASTING

AUTHOR: KATY YEE-YUNG WAN

DEGREE: Ph.D.

DATE: APRIL 1986

## SUMMARY

Magnesium alloy diecasting AZ91CC*, AZ61CC*, AZ91HC** and AZ71HC** were electroplated using different pretreatment sequences which incorporated conventional zincate immersion processes. Satisfactory peel adhesion in excess of 7.7 $KNm^{-1}$ was achieved on AZ61CC using a sequence which was designated Canning. The comparatively low adhesion achieved on the AZ91HC was due to its poor surface quality as cast.

Growth of deposits was monitored using a strip-and-analysis technique and the morphology of the various deposits were studied using scanning electron microscopy. Different pretreatment sequences resulted in different surface responses for the alloys but all alloys behaved in a similar manner in a particular sequence with regard to potential time-curves and the rate of zinc deposition.

The role of fluoride in both the second stage solution and zinc immersion stages of the Canning pretreatment sequence was studied using techniques listed above and Auger electron spectroscopy. Complete coverage of the magnesium alloy surface with immersion zinc was achieved when fluoride was absent from the zincating solution. However, a zero adhesion value was indicated in both thermal cycling and peel tests. The presence of fluoride in the immersion zinc solution suppressed the rate of zinc deposition and affected the time taken to reach equilibrium during potential-time determinations. A mechanism is suggested to explain the significance of fluoride additions to the processing solutions.

pH and composition of the zincating solution had a significant effect on the time taken to produce the step observed in the potential/time curves and hence equilibrium potential. Immersion zinc deposition occurred rapidly at first but then changed to a lower uniform rate at a point corresponding approximately to the step in the potential/time curve.

Although the minimum levels of adhesion, using the Canning sequence, varied from 7.72 $KNm^{-1}$ for alloy AZ61CC to 1.54 $KNm^{-1}$ for alloy AZ91HC, all the alloys revealed ductile failure characteristics in the surface layer of the substrate after peel testing. Plated magnesium alloys exhibited good corrosion resistance when appropriately pretreated and overplated with adequate nickel chromium coatings. The immersion zinc layer was not preferentially attacked when pits penetrated to the coating/substrate interface. Hemispherical pits formed and attack on the substrate was severe.

Of the pretreatment sequences investigated, the Canning one was the most promising with respect to peel adhesion and corrosion behaviour.

KEY WORDS : ELECTRODEPOSITION, MAGNESIUM, FLUORIDE

* CC Cold chamber

** HC Hot chamber

CONTENTS

CONTENTS

CONTENTS

CONTENTS

CONTENTS

List of Tables

List of Figures

List of Figures

List of Figures

List of plates

List of plates

List of plates

List of plates

List of plates

List of plates

# CHAPTER 1 LITERATURE REVIEW

## 1.1 METALLURGICAL ASPECTS OF MAGNESIUM AND MAGNESIUM ALLOYS

Magnesium is widely distributed in the earth's crust and sea in the form of its compounds, but because of its high affinity for oxygen and chlorine, the metal was not isolated until 1808. Davy[1] achieved this by the distillation of mercury from a magnesium mercury amalgam which he had made electrolytically from a moist paste of magnesium oxide MgO and mercury oxide HgO. About twenty-five years later, Faraday obtained magnesium by direct electrolysis of impure magnesium chloride $MgCl_2$. However, one of the first essentials for success in magnesium electrolysis was discovered in 1852 by Bunsen[2] who prepared and electrolysed the pure anhydrous $MgCl_2$ salt. To dehydrate the salt, he added ammonium chloride $NH_4Cl$ and heated the mixture to redness several times with fresh additions of $NH_4Cl$. The process would not proceed smoothly and losses due to formation of basic chloride would occur if the melt was not anhydrous. In 1828, Bussy[1] made magnesium by reduction of anhydrous $MgCl_2$ with potassium. These early experiments foreshadowed the two types of extraction process which are now used commercially - electrolysis and thermal reduction.

Many people first encounter magnesium as ribbon or powder, and suppose it to be readily inflammable and dangerous to handle, but in fact magnesium will not ignite until the melting point has been exceeded and continual heat is required to maintain the combustion.

The lightness of magnesium is a remarkable property. Its specific gravity is 1.74 as compared with 2.7 for aluminium and 7.8 for iron. Lightness is almost always a virtue in the use of metals, especially when employed as constructional and engineering material. The comparison between the physical properties of magnesium and aluminium are given in Table 1 [3,4,5].

The density of magnesium is about 2/3 that of aluminium while their Young's moduli are approximately the same. The specific rigidity of magnesium is therefore 1.5 times that of aluminium. However, the pure metal magnesium is not valuable in most technological applications. As in the case of other metals, alloying of magnesium has been used to obtain higher strength, ductility, workability, corrosion resistance, low density and castability.

In general, the strength of magnesium alloys is lower than aluminium alloys, but taking the difference in densities into account, the specific strengths of the two materials are about the same. There is therefore an incentive to use

Table 1 PHYSICAL PROPERTIES OF MAGNESIUM AND ALUMINIUM

| | Magnesium | Aluminium |
|---|---|---|
| Atomic number | 12 | 13 |
| Atomic weight | 24.32 | 26.97 |
| Crystal structure | C.P.H. | F.C.C. |
| Colour | silver white | tin white |
| Specific gravity | 1.74 | 2.7 |
| Density | 1740 Kg $m^{-3}$ | 2700 Kg $m^{-3}$ |
| Melting point | 650°C | 658°C |
| Boiling point | 1130°C | 2270°C |
| Specific heat | 1.03 J/g°C | 0.90 J/g°C |
| Thermal conductivity | 159 W/m°C | 210 W/m°C |
| Coeff. of linear expansion (20-100°C) | 26.1 X $10^{-6}$/°C | 24.0 X $10^{-6}$/°C |
| Latent heat of fusion | 371.8 J/g | 386.9 J/g |
| Latent heat of vapourization | 4760 J/g | 9462 J/g |
| Electrical conductivity | 37% IACS | 62 - 62.9% IACS |
| Magnetic susceptibility | 0.55 X $10^{-6}$ | 0.60 X $10^{-6}$ |
| Young's modulus of elasticity | 64.5 X $10^{9}$ N $mm^{-2}$ | 68.3 X $10^{9}$ N $mm^{-2}$ |
| Tensile strength (general purpose die castings) | 125 - 255 N $mm^{-2}$ | 150 - 310 N $mm^{-2}$ |

Data taken from Ross[3], BS 2970:1972[4] and BS 1490:1970[5].

magnesium alloys to replace those of aluminium in a variety of engineering applications.

### 1.1.1 GENERAL EFFECTS OF ALLOYING ADDITIONS

Magnesium alloys usually contain aluminium, zinc and manganese, and the general effects of the alloying additions are discussed below (6-14).

#### 1.1.1.1 ALUMINIUM

The Mg-Al phase diagram is shown in Fig. 1. Approximately 2% aluminium is soluble in magnesium at room temperature and this increases to 12% at 430 °C. Intermetallic compounds $\alpha$, $\beta$ and $\gamma$ are formed in the range 40-60% aluminium and some of these phases will be precipitated during cooling from the melt in alloys containing more than 2% aluminium. It is also possible to age hardened Mg-Al alloys using appropriate solution treatment and age-hardening sequences. Aluminium hardens the alloy with some grain refinement but gives a long freezing range leading to casting porosity in many cases, which leads to some of the problems encountered in this project. Up to 10% aluminium is usually added to increase strength, hardness and castability.

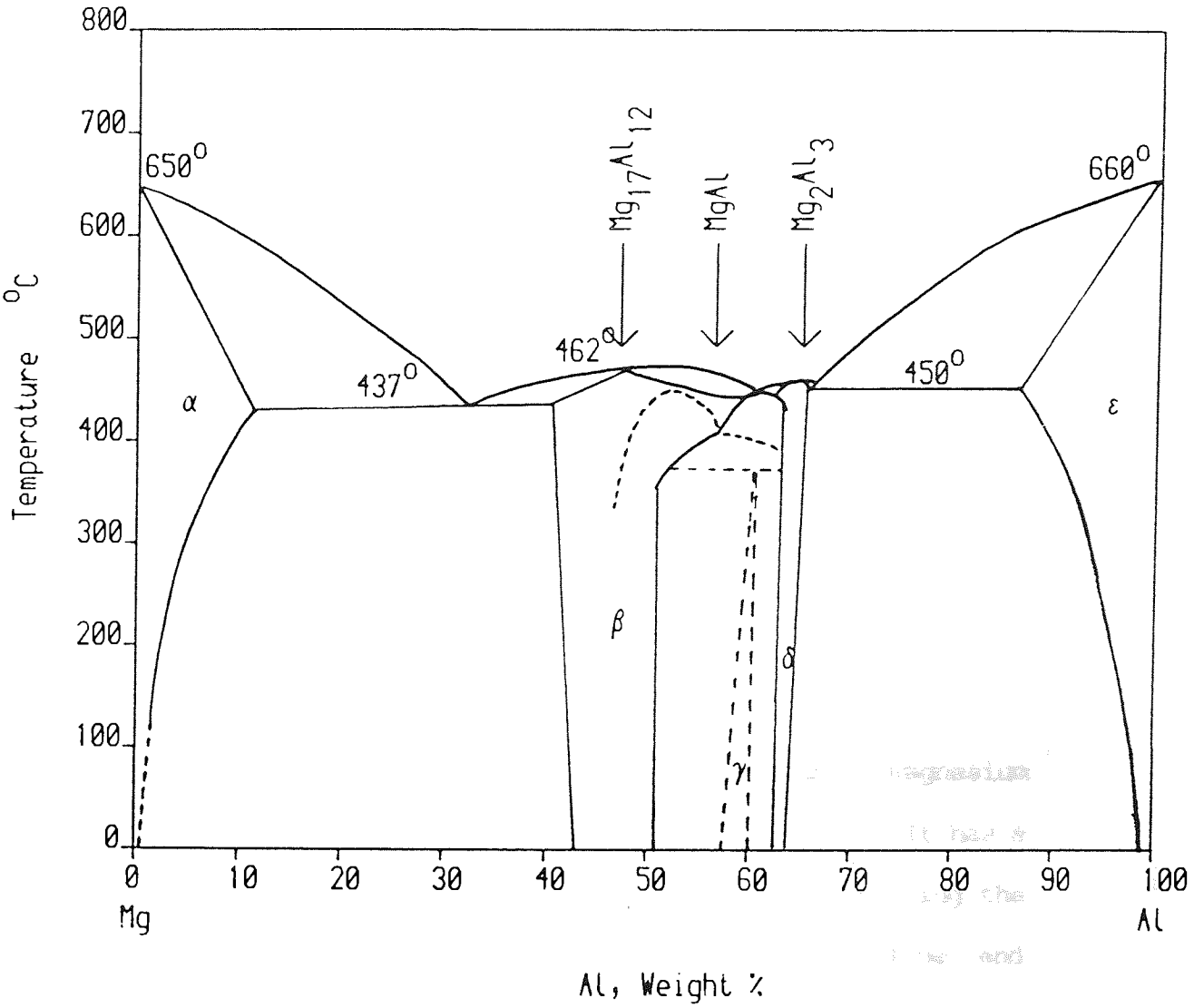


β - $Mg_{17}Al_{12}$

γ - MgAl

δ - $Mg_2Al_3$

Magnesium rich solid solution is called α, and successively more solute rich phases are termed β, γ and δ etc.

(9)

Fig.1 Phase diagram of Mg-Al alloy .

### 1.1.1.2 ZINC

Addition of zinc confers grain refinement and improves castability and corrosion resistance. Up to 1% of zinc is commonly added. Magnesium alloys containing more than 1% zinc are very prone to weld cracking and hot shortness. Zinc is chiefly added as a third constituent to the magnesium aluminium group, giving a general improvement in properties and facilitating foundary work.

### 1.1.1.3 MANGANESE

Manganese has little effect on the strength of magnesium alloys, but improves the corrosion resistance. It has a tendency to coarsen the grain size, thus reducing the fatigue strength. Up to 2% manganese is used alone, and considerably less in conjunction with aluminium and zinc.

## 1.1.2 EFFECTS OF SOME IMPURITIES

Iron, nickel and copper are the three common impurities in magnesium. They all have adverse effects on corrosion resistance of magnesium alloys. Hanawalt et al [15] found

that the amount of these impurities was the factor of primary importance in determining the corrosion rate of magnesium and its alloys in sodium chloride solutions. They found that for pure magnesium, the corrosion rate increased rapidly as the content of iron, copper and nickel was increased beyond 170, 1300 and 5 ppm respectively; they are therefore called the tolerance limits for these three impurities.

The copper and nickel content of magnesium alloys can be controlled by careful monitoring of scrap additions in melting and by the specification of low nickel content in the alloys from which melting equipment is fabricated (16). Also manganese and zinc are the important alloying elements for reducing the corrosion rate of magnesium and Mg-Al alloys containing appreciable amounts of iron.

## 1.2 PRODUCTION OF MAGNESIUM ALLOY CASTINGS

In the last ten years, world production of magnesium has increased as illustrated by information gathered from the metal bulletin years 1971-1981 [17]. Methods for the production of magnesium alloy castings resemble in general those adopted for other metals. However the conditions differ in many respects depending on the type of casting processes employed.

### 1.2.1 PRESSURE DIE CASTING OF MAGNESIUM ALLOYS

The process involves metal flow at high velocity induced by the application of pressure, and because of this high velocity, filling of complex cavities can be achieved.

In die casting, the die is closed and locked. Molten metal is delivered by a pump, which may be cold or heated to the temperature of the molten magnesium, (the casting temperature ranges from 600 °C to 700 °C). The pump plunger is then advanced to drive the metal quickly through the feeding system while the air trapped in the die escapes through vents. Sufficient metal is introduced to overflow the die cavities and develop some flash as the extraneous metal solidifies. Pressure is applied to the remaining

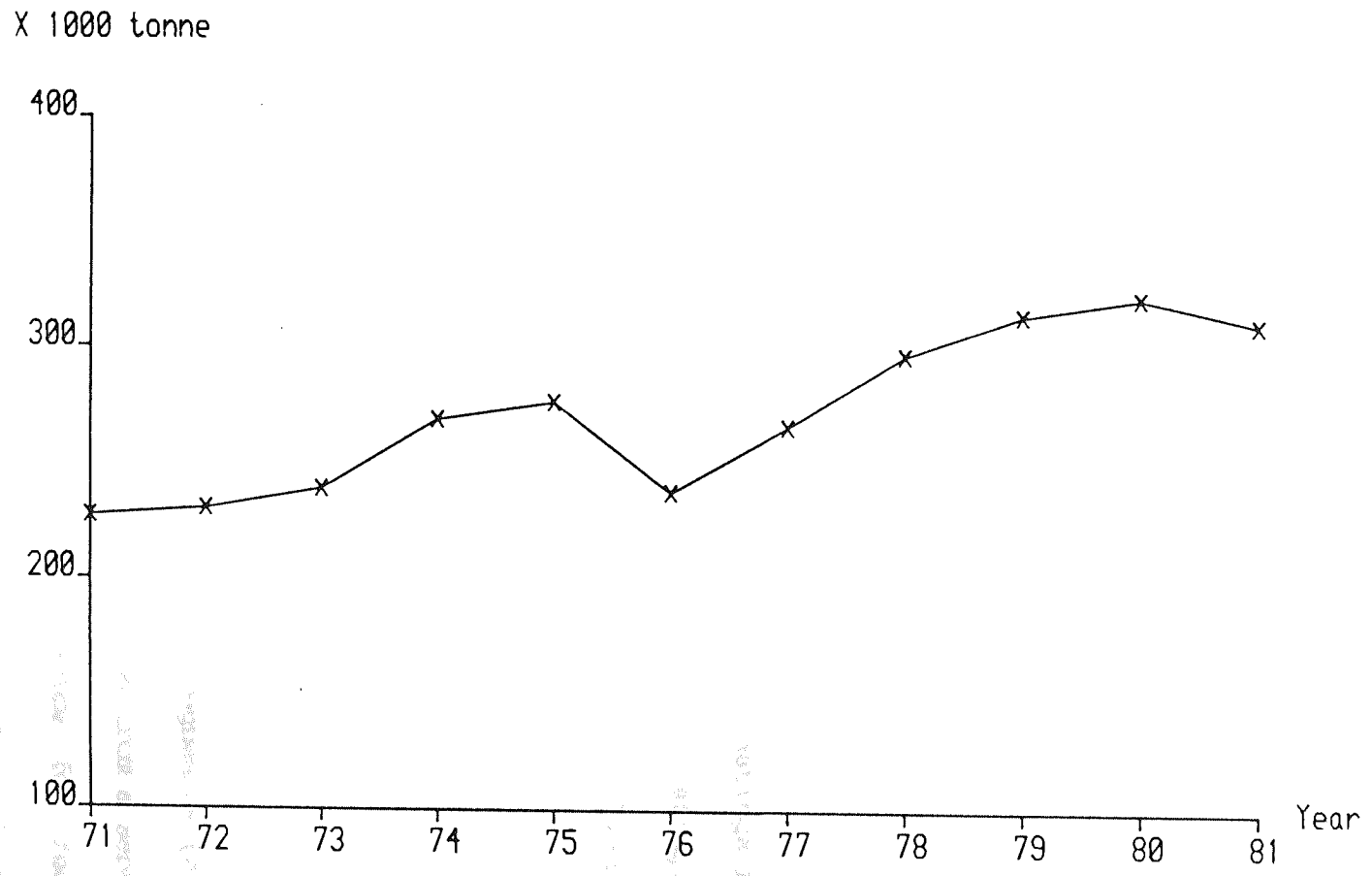


Fig.2 World production of magnesium during the years 1971-1981 (17).

metal and is maintained through a specified dwell time as the casting solidifies. Finally the die is opened and the casting ejected [18-21].

The low density and the low volume heat capacity of magnesium alloys mean that the die must be filled quickly. Thus, less heat is needed to be extracted by the mould per shot than with rival metals, thereby opening the way to greater productivity. Since iron does not alloy readily with magnesium, castings are not liable to stick in the dies which are made of cast iron. Die lubrication can sometimes be almost eliminated, (magnesium is sensitive to overlubrication which often causes black swirls) [13]. Moreover, the high stiffness to weight ratio of magnesium encourages the design of large thin-walled castings in the metal [22]. There are two procedures for die casting, with machines corresponding to them. They are the cold-chamber and the hot-chamber processes.

### 1.2.1.1 COLD CHAMBER PRESSURE DIE CASTING

In cold chamber pressure die casting, the magnesium (either molten or pasty) is baled into the machine from a separate crucible. An automatic metering device for feeding controlled volumes of metals into the shot well may be attached to the cold chamber machine in order to achieve

higher casting rates, uniformity of quality and less operator fatigue [23]. A conventional horizontal cold chamber machine with an automatic metering device is shown in Fig. 3 [24].

1.2.1.2 HOT CHAMBER PRESSURE DIE CASTINGS

In hot chamber pressure die casting, a well of the molten metal is connected directly with the die cavity. The pressure for the movement of the metal into the cavity comes from a piston which operates partially or completely bathed in the liquid metal as shown in Fig. 4 [25]. Although the piston in the cold chamber is in periodic contact with the liquid metal, it does not have to withstand the continuous erosion and heat of that in the hot-chamber machine. Thus the material requirement is much less demanding, e.g. tungsten alloy steel is necessary for the piston used in the Hot chamber process [26].

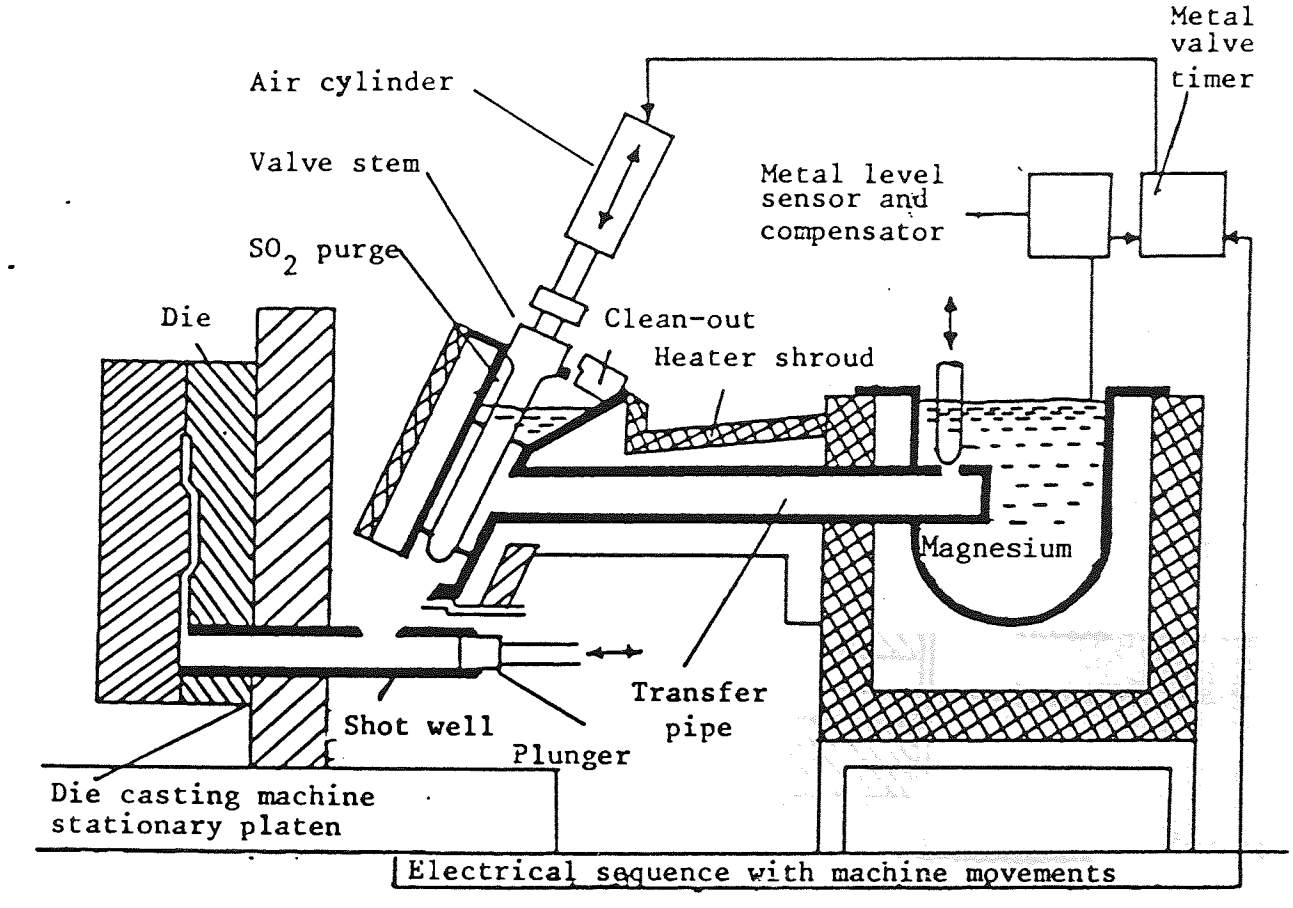


Fig. 3 A conventional horizontal cold chamber casting machine with an automatic metering device[24].

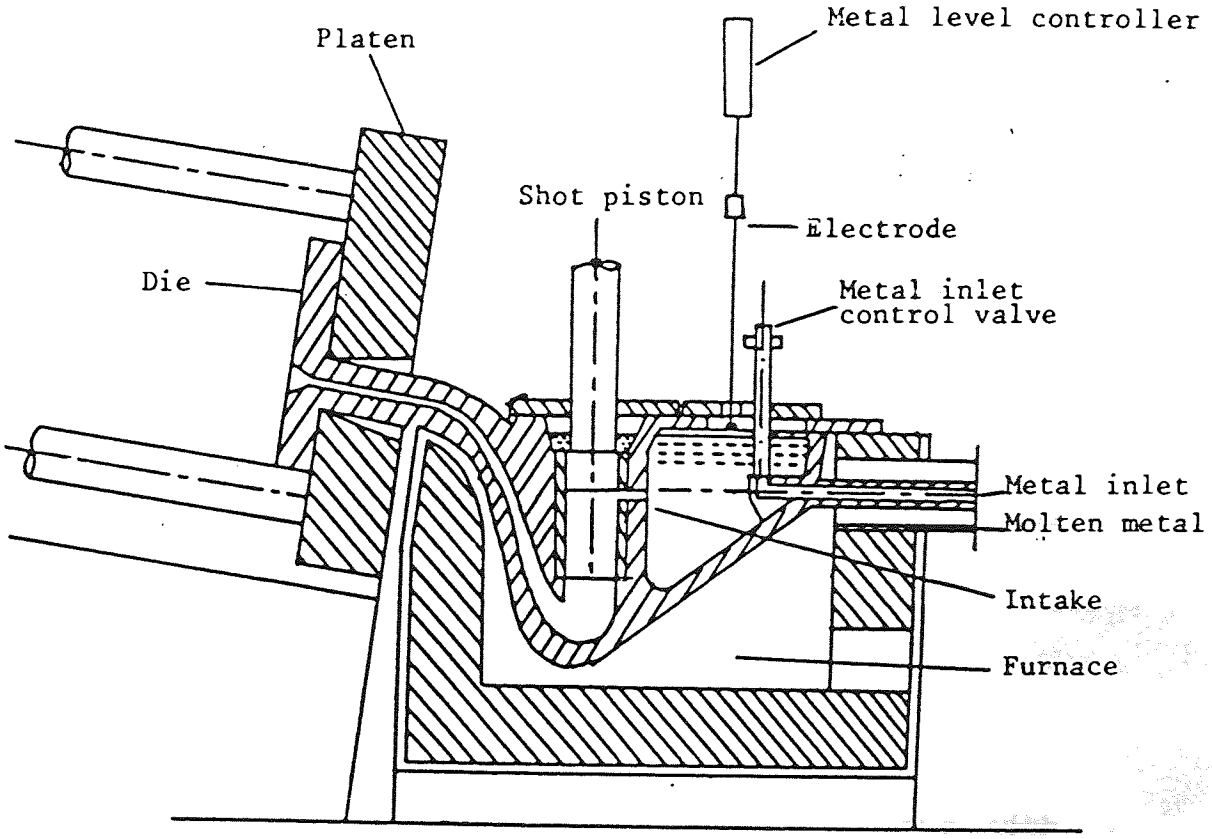


Fig.4 A hot chamber die casting machine.(25)

### 1.2.1.3 GENERAL COMPARISON OF HOT AND COLD CHAMBER DIE CASTING

With cold chamber machines maintenance costs are lower because moving parts are not continually immersed in molten metal, pressure can be higher and metal temperature lower. Casting can generally be made sounder, though not necessarily stronger. Fatigue properties are usually better. Due to the method of filling, the cold pressure die castings are more likely to show cold shuts, flow lines and underfilled parts. On the other hand, productivity is higher with hot chamber machines. Large thin-walled castings can be made, resulting in less scrap. Metal losses are reduced and closing pressures and die wear are also lessened.

The hot pressure die casting's finish improves with increasing die temperature, and above approximately 250 $^{o}$C, flow lines should disappear. However, increasing die temperature brings with it more risks of cracking and trouble with parts sticking in the die.

Barton and Bakui [27] found that magnesium pressure die castings did not exhibit the same pore-free chilled surface as did those in aluminium and zinc. The observation is probably more true of cold chamber castings in magnesium alloy, which have high aluminium content,(approximately 9%),

than it would be of hot chamber casting of alloys of lower aluminium content. Cold chamber castings in AZ91 (9% Al and 1% Zn) frequently show aluminium-rich inverse segregation at the surface [28]. This can give rise to problems in surface treatment.

### 1.2.2 CAST ALLOYS IN CURRENT USE

There are several systems of magnesium alloys for sand and pressure die casting: magnesium-aluminium-manganese with or without silicon or zinc (AM, AS and AZ respectively), magnesium-zinc-zirconium with and without rare earth metals (ZK, ZE, EZ), magnesium-thorium-zirconium with and without zinc (HK, HZ, ZH) [29]. Among these alloys, AZ91 (i.e. 9% aluminium and 1% zinc) is the most popular for die casting, and is studied in this present project.

#### 1.2.2.1 Mg-Al-Zn ALLOY CASTINGS

The magnesium-aluminium-zinc (AZ) alloys are equivalent to British standard BS MAG 1, 3 and 7 which are classified as general purpose alloys [30]. This group of alloys offer a wide range of properties for general or commercial application and should be considered first when selecting an

alloy for a particular application. The castability of these alloys is good and the final selection of the specific composition is based on tests of the finished castings since most of the die castings are used in the as-cast condition. Table 2 shows the chemical composition and mechanical properties for general purpose magnesium alloy die castings[4].

MAG 3 or specified as AZ91 alloy is the most commonly used alloy for high pressure die castings for commercial applications. The mechanical strength of AZ91 die castings is high; their corrosion resistance and soundness are satisfactory. The major problems in magnesium alloy die castings are hot cracking and shrinkage. Mann's[32] study of the die casting of several alloys and pure magnesium indicates that the smaller the solidification temperature range interval, the less the shrinkage and crack susceptibility. AZ91 alloys have a fairly long solidification range (about 135 °C) but, with good die design, cracking can held to a minimum. Die temperature and holding time are also variable in the minimization of hot cracking. However Hepfer[33] believed that it is impossible to satisfactorily electroplate AZ91 die castings by the zinc immersion process, the reason being that areas of segregates of $Mg_{17}Al_{12}$ are formed on the surface of most castings which contain heavy sections. The areas of segregation, being higher in aluminium content and thus more

cathodic than the rest of the surface of the castings, cause the zinc to plate more rapidly by immersion on the areas of segregation than on the rest of the metal surface. The rapidly plated zinc deposit on these areas is spongy and non-adherent. As a result the subsequent electrodeposits tend to be non-adherent in these areas. In order to obtain adherent electrodeposits on die castings which contain this type of segregation, it is necessary to selectively remove the segregation from the surface of the casting prior to electroplating. However, the method is costly and the surface finish would be generally adversely affected if the segregates were heavy. An alloy containing less aluminium and having the required die casting and mechanical properties would therefore be preferred. For this reason, Norsk Hydro (33) introduced AZ61 (approximately 6% Al and 1% Zn) and this is thought to be a compromise. However, the castability is inferior due to the low content of aluminium. Consequently AZ71 (approximately 7% aluminium and 1% zinc) is therefore claimed to give good hot chamber castability and plating characteristics.

Table 2 CHEMICAL COMPOSITION AND MECHANICAL PROPERTIES FOR Mg-Al-Zn ALLOY DIE CASTINGS.

| Designation | Al | Zn | Mn | Cu | Si | Fe | Ni | Mg | | 0.2% Proof stress, min | Tensile strength | Elongation |
|---|---|---|---|---|---|---|---|---|---|---|---|---|
| BSI | % | % | % | % | % | % | % | % | | $N\ mm^{-2}$ | $N\ mm^{-2}$ | % |
| MAG1 | 7.5 – 9.0 | 0.3 – 1.0 | 0.15 – 0.4 | 0.15 | 0.3 | 0.05 | 0.01 | REM | M | 85 | 185 | 4 |
| | | | | 0.4 max | | | | | TB | 80 | 230 | 10 |
| MAG3 | 9.0 – 10.5 | 0.3 – 1.0 | 0.15 – 0.4 | 0.15 | 0.3 | 0.05 | 0.01 | REM | M | 100 | 170 | 2 |
| | | | | 0.4 max | | | | | TB | 85 | 215 | 5 |
| | | | | | | | | | TF | 130 | 215 | 2 |
| MAG7 | 7.5 – 9.5 | 0.3 – 1.5 | 0.15 – 0.8 | 0.35 | 0.4 | 0.05 | 0.02 | REM | M | 85 | 170 | 2 |
| | | | | 0.4 max | | | | | TB | 80 | 215 | 5 |
| | | | | | | | | | TF | 110 | 215 | 2 |

* REM - remainder, M - as cast, TB - solution treated only, TF - solution treated & ppt. treated.

Data taken from BS 2970:1972[4].

## 1.3 GENERAL CORROSION BEHAVIOUR OF MAGNESIUM AND MAGNESIUM BASE ALLOYS

Magnesium has high chemical reactivity as indicated by its highly electronegative potential (Table 3)[3]. However it does have good resistance to atmospheric exposure which is attributed to the formation of an oxide film which is highly protective.

The corrosion resistance of magnesium and its alloys is dependent on film formation in the medium to which the alloys are exposed. The rate of formation in solution, or chemical change of the film varies with the medium, and also with the metallic alloying elements or impurities present in the magnesium. Magnesium alloys react similarly to magnesium with respect to humidity and time of exposure. The surface film however contains a higher percentage of the hydroxides of the alloying metals than would be expected from the composition of the alloy. This is particularly true for magnesium alloys containing aluminium, manganese, or zinc[34].

Table 3 ELECTROLYTIC POTENTIALS OF SEVERAL METALS WITH RESPECT TO S.H.E.*

| Metal | Potential V |
|---|---|
| Mg | -2.37 |
| Al | -1.69 |
| Zn | -0.76 |
| Cr | -0.56 |
| Cd | -0.40 |
| Ni | -0.25 |
| Pd | -0.13 |
| $H_2$ | arbitrary zero |
| Cu | +0.34 |
| Pt | +12.0 |

* Electrode potential at 25°C with the base metal in contact with its divalent ions at normal activity and taking the corresponding hydrogen electrode potential as zero.

Data taken from R.B.Ross, Material Specification Handbook.(3)

1.3.1 ATMOSPHERIC CORROSION

Bengough and Whitby[35] have made tests of three years duration, in which various magnesium alloys were exposed outdoors, unprotected from the rain, at Teddington, England. A slow increase in weight was noticed, even in dry periods. The increase was followed by a decrease during rainy periods. They suggested that the hydroxide or carbonate film lost protection by conversion to highly soluble $MgSO_4$ and $MgSO_3$ which were then washed away by the rain. The actual weight-loss corrosion rates over the period were less than 1 mg $dm^{-2}$ per day, which is of the same order of magnitude as the rate for a metal such as zinc under similar conditions. The magnesium alloy specimens were finely pitted.

Also according to Whitby[36], the rate of indoor tarnishing of magnesium and its alloys is largely controlled by the relative humidity. The rate of attack increases with humidity to a point where, at 90% of saturation, the attack was rapid. The primary reaction is the formation of magnesium hydroxide. A secondary reaction with carbon dioxide converts the hydroxide to a hydrated carbonate. Secondary reactions of the surface decrease its porosity and provide some measure of protection[37]. However the corrosion products formed on magnesium at Teddington after 400 days had a higher sulphate content than that obtained

indoors. There was also more carbonaceous matter and metal oxides in the corrosion products formed outdoors.

Depending on the environment, variable analyses of corrosion products may be obtained. Carbon dioxide absorption by the water layer on the metal with subsequent reaction with $Mg(OH)_2$ to form the double salt is believed to play an important part in the corrosion and tarnishing of magnesium [34].

## 1.3.2 CORROSION IN SOLUTIONS

The potential-pH equilibrium diagram [38] of magnesium was consulted since it provides a thermodynamic framework for electrochemical reactions involving an aqueous solution. Fig. 5 indicates that magnesium dissolves readily as $Mg^{++}$ in solutions with pH up to 10 and magnesium hydroxide has an equilibrium pH of 10.2-10.6. It is too strong a base to ionise as an acid, and therefore magnesium is quite resistant to strong bases. The resistance of magnesium to solutions of pure bases in water rather closely resembles its resistance to pure water, but the good resistance of magnesium to pure water at room temperature is impaired by continued absorption by the water of carbon dioxide from the atmosphere [39].

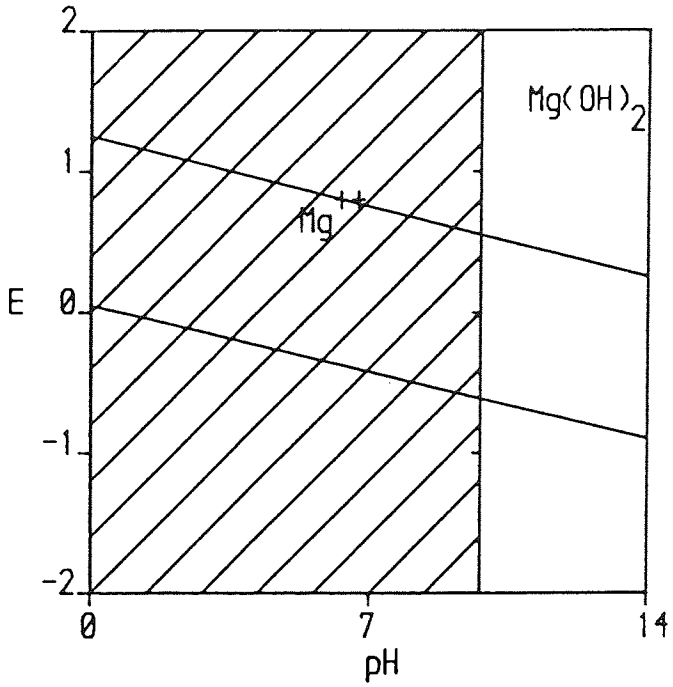


Corrosion by dissolution.

Passivation by oxide or hydroxide layer.

(38)

Fig.5 Pourbaix diagram of magnesium .

Almost all organic and mineral acids attack magnesium and its alloys except hydrofluoric and chromic. Action may be so strong as to be described as violent in hydrochloric and nitric acids. On the other hand, the resistance is very good against hydrofluoric acid due to the formation of a relatively insoluble and highly protective film of $MgF_2$. HF does not attack magnesium to an appreciable extent at concentrations above approximately 2% [34,39,40]. Pure chromic acid attacks magnesium and its alloys at a very slow rate, but the presence of small amounts of chloride or sulphate ions greatly increases the rate, and there is some tendency for intercrystalline attack [41]. Boiling 20% chromic acid is widely used for cleaning corrosion products from magnesium and its alloys because of the solubility of $Mg(OH)_2$ and resistance of magnesium to the acid.

Magnesium and its alloys exhibit good resistance to attack by alkalies as mentioned previously. Dilute solutions show negligible attack at temperatures up to the boiling point according to Loose [34], and 50% sodium hydroxide or other caustic solutions produce little attack at temperatures up to about 60 °C.

## 1.4 SURFACE PROTECTION OF MAGNESIUM ALLOYS

The selection of a suitable finishing system depends on the service environment, particularly with respect to oxygen, moisture, chloride and temperature. Magnesium is more susceptible than other common metals to galvanic corrosion owing to its electronegativity. However, galvanic corrosion of magnesium is possible only if bare magnesium is in intimate contact with another bare metal. Therefore galvanic corrosion can be avoided by separating the two metals with a film of paint, sealant, or a metal more compatible with magnesium.

Protection and decorative treatments applied to magnesium alloys may be divided into the following groups [42,43] :

(a) Chemical treatment

(b) Hard anodizing

(c) Surface sealing

(d) Painting

(e) Electroplating

### 1.4.1 CHEMICAL TREATMENTS

Chemical treatments include acid pickling, chromating and fluoride anodizing. These merely clean or passivate the

surface to some extent, and in most cases provide a base for subsequent painting where required.

1.4.1.1 ACID PICKLING AND CHROMATING

Castings are normally delivered from the foundry in the chromated condition and generally do not require cleaning other than degreasing. If, however, they are in a very bad condition, e.g. prolonged storage in a humid atmosphere, it will probably be necessary to shot blast or wire brush them. A dip in 2.5% nitric acid removes the oxidized surface so that they can be rechromated (44).

Chromating is a process of passivating the surface of magnesium so that it will retain its condition unchanged over a reasonable period. The film developed also makes a very good base for painting and increases the durability of paint applied to the surface (45). There are many baths suitable for carrying out this operation, which is a simple dip process, but none has any outstanding advantage other than convenience of application (46,47,48). In appendix 1, the formulations of two chromating baths are shown (44):

(1) The acid chromate bath is a rapid dip process suitable for rough castings.

(2) The chromium-manganese bath is a milder one which does not affect machined tolerances but which requires a longer process time.

### 1.4.1.2 FLUORIDE ANODIZING

In fluoride anodizing, the casting is anodized at high voltage in 10-30% ammonium hydrogen fluoride ($NH_4HF_2$) solution. As long as cathodic particles remain exposed on the surface, current can flow, but once these particles are dislodged and magnesium is covered with a complete skin of magnesium fluoride ($MgF_2$), the resistance becomes considerable. Accordingly the voltage is increased until 90-120 V is reached; and the operation is completed after 10-15 min. or when the current density has fallen below 0.5 $A/dm^2$. A uniform white or greyish white film should be formed on the surface of the casting [46,47,49].

### 1.4.2 HARD ANODIZING

The hard anodizing process is applied in much the same way as in fluoride anodizing. The voltage is increased to about 90V before the end of the process by which time the insulating coating has become almost complete and the

current has fallen to a very low value. With the full treatment, the process adds about 25μm of coating to the surface. Huber[50] studied the anodizing of magnesium in a normal sodium hydroxide (NaOH) solution and obtained the results summarized in Fig. 6. When anodically treated magnesium alloys are painted, the combination coating offers maximum protection against corrosion under severe conditions, including immersion in fresh water and exposure to outdoor industrial and marine atmosphere.

### 1.4.3 SURFACE SEALING

This process, devised by Higgins[46] involves baking residual moisture out of the pores and other surface imperfections and applying a stovable epoxy resin coating whilst the component is still hot. To obtain good results, the time and temperature of baking and stoving must be sufficient, otherwise the film may be porous with poor adherence. Therefore one of the limitations of this process is that stoving temperature is rather high for close tolerance machined castings.

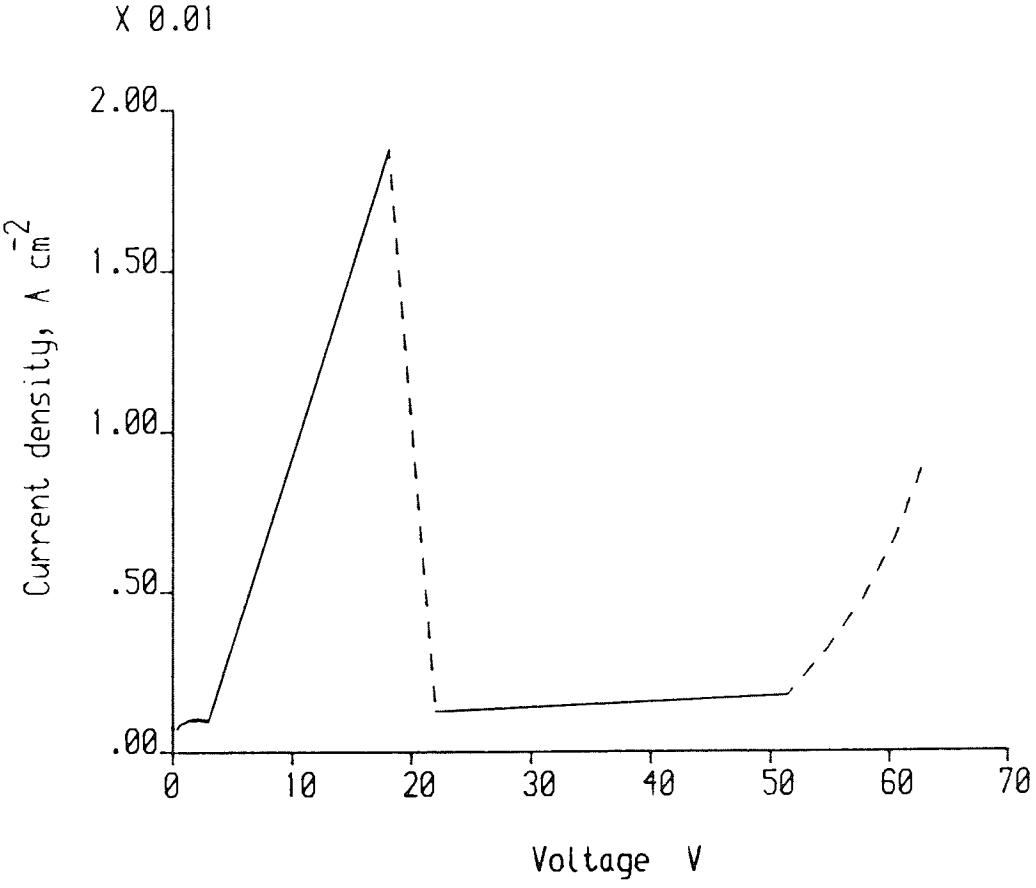


| 0.3-3.0 V | 3.0-20 V | 20-50 V |
|---|---|---|
| passive after initial attack | thicker Film with Oxygen evolution | invisible thin (high voltage only) |
| light grey | dark grey | light grey adherent film if voltage gradually increased |
| $Mg(OH)_2$ | | $MgO \longrightarrow Mg(OH)_2$ |

(50)

Fig.6 Relationship between applied voltage and film characteristics (anodizing magnesium in N NaOH)

### 1.4.4 PAINTING

Fig. 7 shows the various pretreatment and painting sequences for magnesium components. In principle the painting of magnesium hardly differs from that of other metals. The alkaline nature of magnesium hydroxide $Mg(OH)_2$ however makes it desirable to use paints based on alkyd resins rather than linseed oil, and to carry out the painting on freshly prepared surfaces. A chromate treatment is generally desirable before painting both to passivate the surface to some extent against corrosion with formation of $Mg(OH)_2$, and also to provide a key for the paint film. Since no paint is permanent and all deteriorate slowly (or sometimes quickly) paints therefore need to be applied frequently [51].

### 1.4.5 ELECTROPLATING

Electroplating on magnesium base alloys can be considered as a more expensive method of surface protection compared with other finishing systems. However, if it is preferred or necessary to obtain a surface that provides wear and corrosion resistance together with a bright attractive finish on consumer products, plating may be essential. Such application of plated magnesium can be found in automobiles, transcribing machines and rule cases [52].

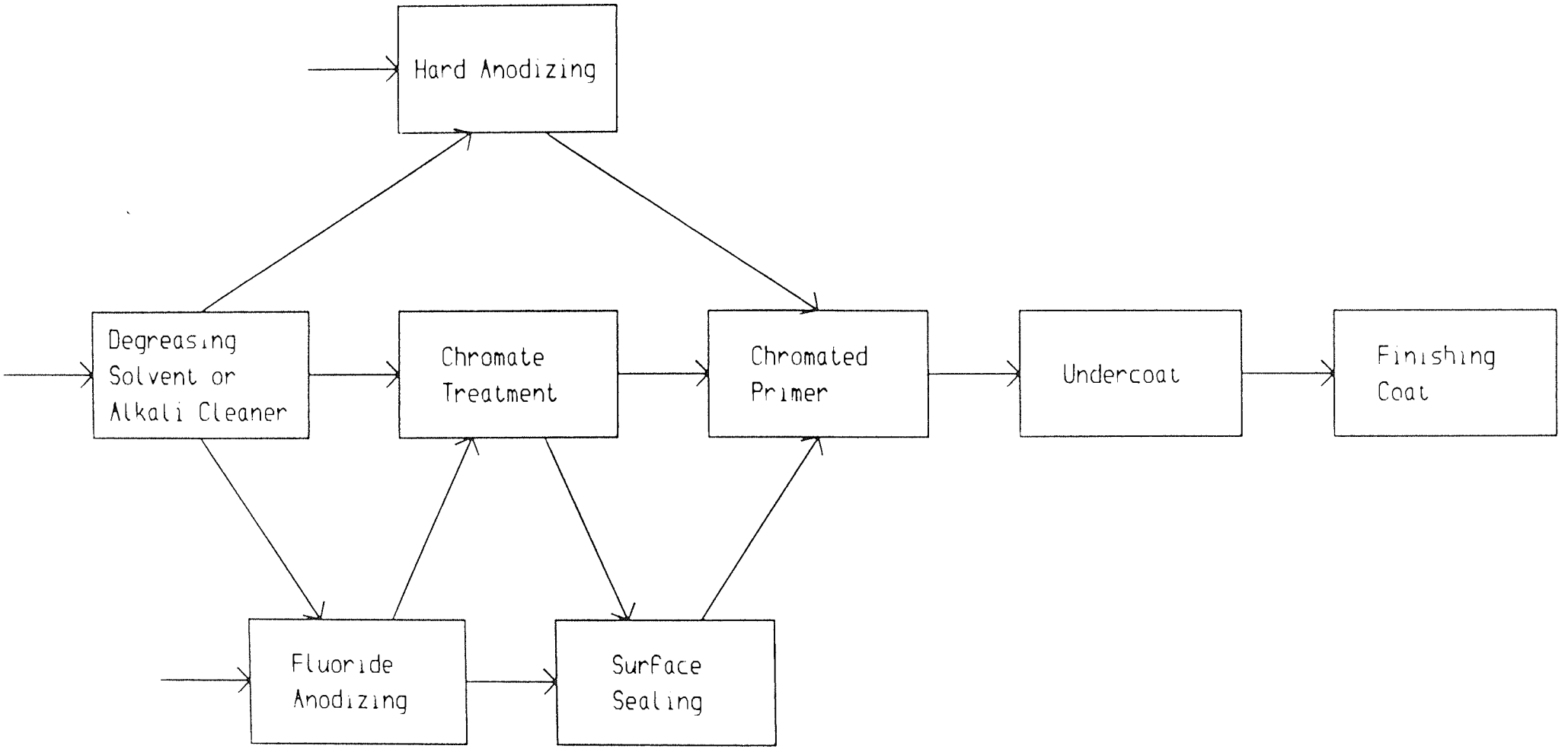


Fig.7 Various pretreatment and painting sequences for magnesium compounds.

Several processes have been developed for electroplating on magnesium and its alloys. The majority of the processes have limitations such as poor adhesion to the basis metal, adaptability to specific magnesium alloys or they are too critical to assure success on a production basis. Of these, the two processes that appear most promising are the zinc immersion treatment and the special chemical etching process. Details are given in Section 1.5.

## 1.5 CURRENT STATUS ON ELECTROPLATING OF MAGNESIUM ALLOYS

Attempts in the past to develop a successful practical process have not been, in general, too encouraging. Various methods have been advanced and are mentioned in the patent literature for obtaining electrodeposits in both aqueous and non-aqueous media [53-61].

Although during the last 30 years, many sources including the Dow Chemical Company [62,63] have claimed that magnesium alloys can be electroplated successfully, yet magnesium in general and magnesium die castings in particular are still little used in plated form. Satisfactory process sequences have yet to be developed for certain alloys and a universal process for all alloys has not been achieved. This is because the numerous alloys exhibit very different microstructures and electrochemical behaviour. The difference in chemical properties between the two alloys AZ91 and AZ61 can be demonstrated by a simple chromate dip. The chromate film formed on AZ91 die castings is uneven in colour and, in some areas, the metal surface is covered with a powdery grey coating owing to aluminium-rich segregation. The same part cast in alloy AZ61 develops a decorative yellow chromate coating [56].

More recently, Oslen[33] of Norsk Hydro a.s. has claimed that by using a more suitable alloy (AZ71) which can be die cast commercially, it is possible to simplify and improve the plating process.

Various processes of current commercial significance are based on the use of an immersion zinc deposit prior to the application of the electrodeposited coating and the deposition of a nickel undercoat by the special chemical etching process. Both processes were developed by DeLong of the Dow Chemical Company.

### 1.5.1 THE DOW PROCESSES

Nickel and zinc are the only metals that are plated directly on to magnesium. The preparation of magnesium for electroplating is similar in principle to many other metals. First, magnesium must be cleansed to remove all surface contaminants. Then, depending on the surface finish desired, it must be conditioned, e.g. polishing and buffing, shot or sand blasting, pickling, and barrel finishing. The surface contaminants resulting from these treatments can be removed by alkaline soak cleaning, vapour degreasing or emulsion cleaning. The magnesium is then chemically activated before either nickel or zinc is deposited.

### 1.5.1.1 THE CHEMICAL ETCHING PROCESS

The deposition of nickel on magnesium is preceded by two acid etching treatments, one in a chromic-nitric acid solution and the other in a solution of hydrofluoric acid. These pretreatments of magnesium, in combination with the deposition of an electroless nickel undercoat, are generally referred to as the chemical etching process. Fig. 8 shows the flow chart of the Dow process for the deposition of electroless nickel undercoat on magnesium. The two etching treatments produce surface pits which provide mechanical anchorage for the plated deposits. After the nickel undercoat is applied to the roughened surface, any standard electrodeposits or electroless deposits may also be applied over the initial nickel deposit. However, some users have reported that the direct electroless nickel procedure does not produce quite as high a level of adhesion as zinc immersion [61,63,64,65]. It should be noted that Puippe [66] has very recently claimed that by modifying the chemical nickel bath, it is possible to carry out an ion exchange reaction between nickel and magnesium. This is done in such a manner that an adherent magnesium oxide layer develops which not only limits the dissolution of the basis metal, but also provides a suitable undercoat for the bonding of the nickel deposit. The deposit is produced from an electroless nickel solution which functions by means of a Hypophosphite reducing agent.

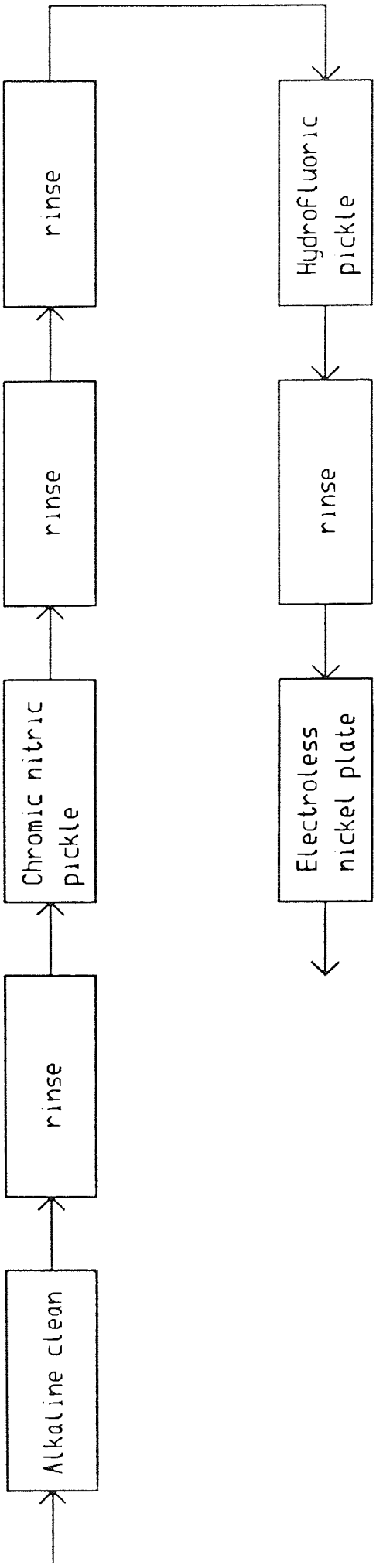


Fig.8 The Dow process for the deposition of electroless nickel.

### 1.5.1.2 THE ZINC IMMERSION TREATMENTS

After the surface of the magnesium alloy has been alkaline cleaned, acid pickled and surface activated, a thin layer of zinc about 2.5µm thick is deposited by galvanic deposition. This is protected by an electrodeposit of copper from a copper cyanide bath. After this copper strike has been applied, other metals can be electrodeposited in the customary manner. Fig. 9 shows one of the flow charts of the Dow processes for electroplating of magnesium. The operation may be summarized as follows:

1) Surface conditioning
2) Activating
3) Zinc immersion
4) Copper plating
5) Subsequent plating (using standard procedures)

#### 1.5.1.2.1 Surface conditioning

All metals to be plated require careful surface preparation to establish a satisfactory base for electroplating. The surface must be free from all contaminants such as heavy oxide layers, graphite-base lubricants and previously applied chromate coatings which are frequently applied for storage protection. To clean a surface of these contaminants, the surface is pickled. DeLong (67) has

recommended a number of pickling solutions for the conditioning of castings, two of which were:

a) a 15 second to 3 minute immersion at room temperature in an aqueous solution consisting of 180 g/l chromium trioxide ($CrO_3$), 40 g/l of ferric nitrate and 3.5 g/l of potassium fluoride or

b) a 30 second to 1 minute immersion at room temperature in concentrated phosphoric acid (85%) solution.

1.5.1.2.2 ACTIVATING

Not only is the surface activation treatment an added precaution to remove any traces of surface contamination and to remove any thin films left by prior pickling, but also to produce a minimum of etching in order to avoid a roughness in the subsequent electrodeposits. In the Dow procedure, a patented aqueous solution containing 200 ml/l of 85% phosphoric acid and 100 g/l of either sodium, potassium or ammonium bifluoride is employed. This solution should remove average surface contamination without causing a roughening etch, as well as activating the magnesium surface to receive the zinc coating (68).

1.5.1.2.3 ZINC IMMERSION COATING

The key to electrodeposition on magnesium and magnesium alloys is the zinc immersion coating. When applied correctly the zinc coating is also the layer to which subsequent deposits adhere. The success of the whole procedure is largely dependent on how well this step is controlled. In order to obtain an adherent zinc coating on magnesium by immersion, DeLong has emphasized the necessity of removing the magnesium hydroxide film and depositing the metal at a slow and controlled rate.

Investigations have revealed that alkaline pyrophoshates, particularly below pH 11, react readily with magnesium hydroxide to form water soluble compounds (62-65,69). It is also found that a small quantity of fluorides work effectively as inhibitors to control and produce a zinc deposit that has a finer grain size (no detailed explanation has been given for this mechanism). Since lithium fluoride is soluble only to the required concentration level and is self-regulating, it is the preferred addition.

THE STANDARD ZINC IMMERSION BATHS

The standard zinc immersion baths (62-65) are based on aqueous solutions of pyrophosphates, a zinc salt and a

fluoride, with a small amount of carbonate added to adjust the alkalinity within the recommended range.

| | |
|---|---|
| zinc sulphate, monohydrate | 30 g/l |
| tetrasodium pyrophosphate | 120 g/l |
| potassium fluoride | 7 g/l |
| or sodium fluoride | 5 g/l |
| or lithium fluoride | 3 g/l |
| sodium carbonate | 5 g/l |

An aqueous solution of tetrasodium pyrophosphate at pH below 11, functions as a complexing agent in that it readily reacts with magnesium oxide and magnesium hydroxide surface films to form water soluble complexes. By effecting this film removal in a metallic salt solution (in this case, zinc) an adherent metallic deposit can be obtained by galvanic deposition.

$$1 \quad Mg \longrightarrow Mg^{++} + 2e^{-}$$

$$2 \quad Zn^{++} + 2e^{-} \longrightarrow Zn$$

$$3 \quad Mg + Zn^{++} \longrightarrow Zn + Mg^{++} \quad \text{overall}$$

Neither glass nor ceramic equipment is recommended for use in the activating and zincating stages due to the presence of fluorides, which may form fluorosilicates with glasses or ceramics. The baths can then be contaminated and

subsequently the deposit. Plastic containers and equipment were therefore used in this project.

The bath is operated at 80-85 °C at pH 10.2-10.4 and is mildly agitated during use to avoid stratification. The time for treatment is 3 to 10 minutes, but the optimum time for aluminium-containing alloys is 5-7 minutes. The time should be no longer than that required for complete coverage of the surface with a continuous zinc coating because beyond this point, loosely adherent zinc deposits may form (70). However, the necessity for complete coverage will be discussed later.

1.5.1.2.4 COPPER PLATING

Immediately after the application of the zinc coating, the work is transferred to a cyanide-type copper bath. The thickness of the copper deposit depends on the subsequent plate and the kind of bath in which it will be plated. If the work is to be subsequently plated in an alkaline bath, then copper deposits of 2.5μm are adequate. However, if an acid type bath is used, copper deposits of 7.5μm are required to protect the magnesium surface from chemical attack. With castings where complexity of design or a highly porous surface is present a slightly greater thickness of copper deposit may be required.

Periodic current reversal is recommended with the cyanide copper bath in order to achieve maximum brightness and smooth deposits[71]. It is preferable to plate on the forward cycle for the first 30 seconds to 1 minute and then apply the coating using alternating forward and reverse cycles, 15 seconds forward and 3 seconds reverse. This procedure builds up an initial layer of copper before deplating occurs. It is important that the work makes electrical contact with the cathode bar before being immersed in the plating baths. Current density of 2.5 $Adm^{-2}$ is recommended.

### 1.5.1.3 PROPERTIES OF ELECTROPLATED MAGNESIUM ALLOY DIE CASTINGS BY THE DOW PROCESS

#### ADHESION

It is claimed[72] that the adhesion of the electrodeposits appears to be good and equivalent to that normally obtained with good practice on zinc base die castings.

Copper-nickel-chromium plated cast parts will withstand heating up to 230 $^{o}C$ without a general lifting or blistering of the deposits.

CORROSION RESISTANCE

When deposits, such as nickel and copper, are applied directly to a magnesium surface, magnesium, being cathodic to these metals, would be expected to corrode at a fairly rapid rate unless the deposits are pore free. However, DeLong has pointed out that the presence of an intermediate zinc layer, as obtained in the zinc immersion process, between the magnesium and a more noble deposit, will enhance a system's protective value, with the galvanic cell action being reduced to a minimal value.

Corrosion tests were carried out on plated zinc, aluminium and magnesium base die castings by Caldwell et al (73) in 1949. One of the conclusions was that the zinc alloy was the best as a base for copper-nickel-chromium plate since it appeared to have the least number of corrosion pits and corrosion products after lengthy static exposure at different sites. The magnesium die casting alloy (AZ91) was second and the aluminium alloy third. However, good plating can now be achieved on aluminium and its alloys using the Bondal Process *(74,75,76) which enables many different electrodeposits to be applied directly without intermediate brass or copper plating.

* one of W. Canning Ltd.'s proprietary processes.

## 1.5.2 THE NORSK HYDRO PROCESS

A new process based on the zinc immersion process by DeLong was invented recently by Olsen and Halvorsen of Norsk Hydro a.s. [77].

They found that the pretreatment prior to the zinc immersion coating in the Dow process can only work well on homogeneous materials such as sheets and extrusions, but on castings and especially pressure die castings, it is difficult to achieve a satisfactory coating quality [78]. The reason for this is that the activating bath used in the process after pickling, a solution of phosphoric acid or other acid solutions, as recommended in the patent, produces an etched structure followed by the formation of a magnesium fluoride ($MgF_2$) film on or around the intermetallic phases ($Mg_{17}Al_{12}$). These phases are aluminium-rich (approximately 40% aluminium) and thus more cathodic than the rest of the surface of the coating as mentioned earlier in section 1.2.4.1. This leads to the formation of a non-uniform immersion zinc coating. In order to achieve coverage over the entire surface, increase in treatment time and/or temperature is necessary. This however, involves local over-zincating, resulting in a porous zinc deposit and gives poor adhesion of the subsequent metallic coating.

It may be possible to omit pickling and activating steps in the Dow process by applying efficient mechanical cleaning to the metal surface prior to degreasing and zincating. Such operations, however, would seem rather costly and difficult where pressure die castings are concerned because most articles have complex designs with narrow recesses.

A two-step activating process was suggested in which the articles are first treated in a solution of oxalic acid, then rinsed in water and transferred for subsequent activation into a pyrophosphate bath prior to chemical zinc coating. The treatment processes comprise the following steps:

1) Mechanical pretreatment
2) Degrease in organic solvents
3) Two-step activation
    i) pickling/activating in oxalic acid
    ii) activating in an alkali metal pyrophosphate
4) Chemical zinc precipitation
5) Electrolytical metal coating

Steps 1, 2, 4, and 5 are well known and similar to the Dow process. The flow chart of the Norsk Hydro process is shown in Fig. 10.

THE DOW PROCESS

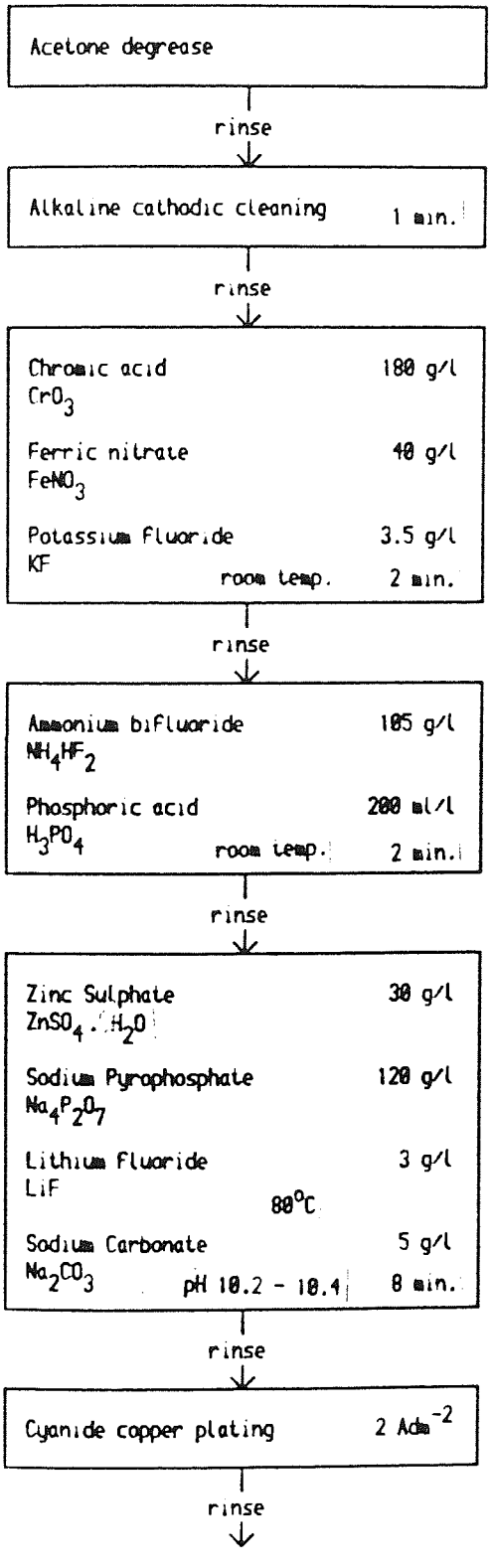


Fig.9 Flow chart for the Dow process.

THE NORSK HYDRO PROCESS

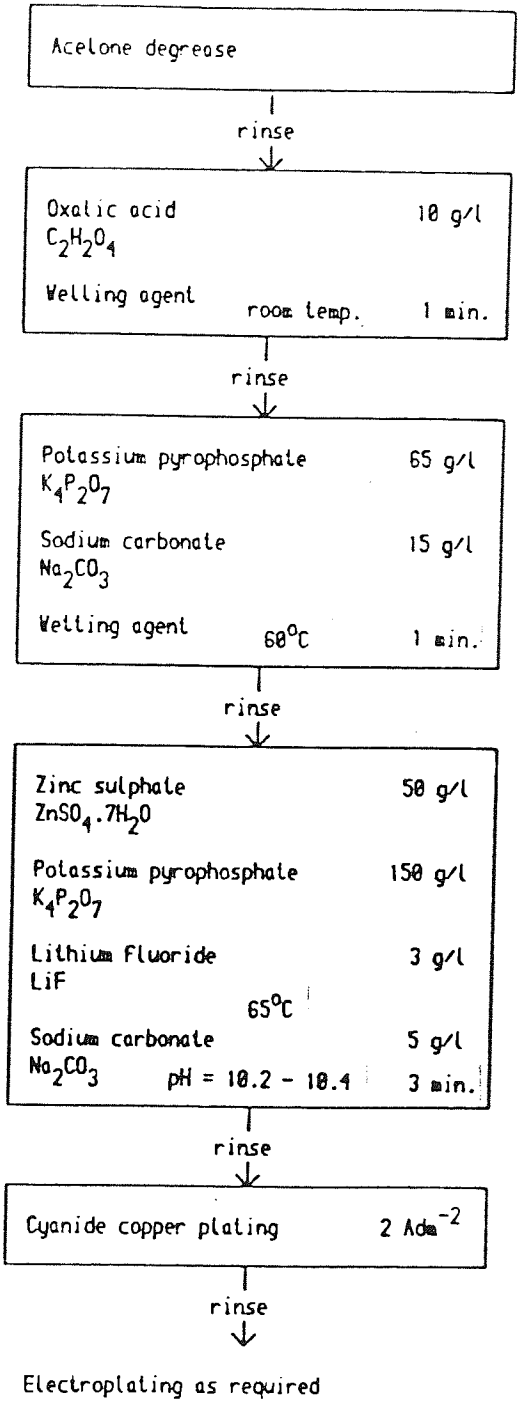


Fig.10 Flow chart for the Norsk Hydro process.

### 1.5.2.1 ACTIVATION IN OXALIC ACID

In the first step of the activating of magnesium alloys, an aqueous solution of 0.2 to 1% oxalic acid is used at room temperature to pickle the surface of magnesium articles instead of other organic or inorganic acids recommended in the Dow patent. Oxide and non-metallic inclusions are dissolved and transformed. Reaction products formed on the surface are simply removed by rinsing in water. It was found that the reactivity increases in the subsequent treatment in the pyrophosphate bath.

### 1.5.2.2 ACTIVATION IN ALKALI METAL PYROPHOSPHATE

An aqueous solution of 10-200 g/l potassium or sodium pyrophosphate is used for the second activating step. The activation is based upon the ability of the pyrophosphate to dissolve metal oxides and hydroxides by the formation of a soluble complex according to the following principles:

$$2\,Mg(OH)_2 + XP_2O_7^{4-} \longrightarrow (Mg(P_2O_7)X)^{-2x} \text{ ------ (A)}$$

The formation of magnesium hydroxide proceeds continuously on the metal surface according to the following reaction:

$$Mg + 2H_2O \longrightarrow Mg(OH)_2 + H_2 \quad \text{(B)}$$

Up to 50 g/l of potassium or sodium carbonate is added in order to adjust the pH to between 10 and 11.5. Addition of a small amount of wetting agent in both activating baths is desirable since gas is generated in both activating processes.

Both reactions (A) and (B) should also take place during direct chemical zinc coating without previous activation because of the excess of pyrophosphate in the zincating bath. However, the direct zinc coating has the disadvantage of having an uneven surface. This is because the most active areas are coated first and it will take a longer time to cover the less active areas with zinc. It is suggested that the zincating process should not exceed 3 minutes with regard to the coating quality and the life of the bath. Moreover, the precipitation process may be upset by the generated hydrogen.

Olsen and Halvorsen (77) have claimed that:

1) Uniform zinc precipitation over the metal surface can be achieved by a two-step activation with negligible or no

gas generation in the precipitation process.

2) Since the pyrophosphate activation has the effect of increasing the reaction rate in the zinc coating process, it results in increased bath life and lower consumption of chemicals.

3) The secondary activation is carried out preferably with potassium pyrophosphate ($K_4P_2O_7$) at a concentration of from 50 to 75 g/l as alkali metal pyrophosphate in the bath, at 55-65 °C.

After carrying out several experimental tests with alloy AZ61 and AZ91, Olsen has shown that [28] :

1) AZ61 exhibited better electroplatability compared with AZ91 owing to less alloy segregation.

2) Hot chamber casting appeared to be better than the cold chamber process for achieving a cost effective polishing and plating sequence.

### 1.5.2.3 PROPERTIES OF MAGNESIUM ALLOY DIE CASTINGS ELECTROPLATED BY THE NORSK HYDRO PROCESS

ADHESION

It has been found[77] that the copper-nickel plated castings showed good brightness with no blister formation after thermal cycling by subjecting them to heating at 150 °C for 1 hour followed by quenching in water at 20 °C to 25 °C. In contrast, all the castings produced by the Dow process showed blister formation even prior to the heat test.

CORROSION RESISTANCE

Promising results from accelerated corrosion testing of plated magnesium pressure die castings were obtained by Olsen[33]. It is claimed that multi-layer plating systems including microporous chromium will provide adequate protection to exterior automative hardware in some locations.

## 1.6 ASSESSMENT OF PERFORMANCE

The most important methods of investigating the performance of the electroplated coating are adhesion and corrosion testing.

### 1.6.1 MEASUREMENT OF ADHESION AND ADHESION TESTS

The adhesion of electrodeposits to the basis metal plays a major role in the performance characteristics of the finished product. In order to assess the efficacy of changes in the process variables or of substrate preparations and to discriminate parts or products which have poor adhesion strength from those which are acceptable, the measurement of adhesion is important. Many methods have been suggested [79,80] to evaluate adhesion. However, the results obtained from one test cannot be compared directly to those obtained by another nor can their results be easily quantified.

Mittal [81] used the term "basic adhesion" to signify the summation of all interfacial intermolecular interactions which could be electrostatic, chemical or Van der Waals forces, and the term "practical adhesion" is used to

represent the forces or the work required for their disruption.

Experimentally, adhesion is measured in terms of forces or the work of detachment of the adhering phases. The separation may take place at the interface or in the bulk of the weaker adhering phase. Separation in the bulk is termed cohesive failure and is related to the cohesive strength of that bulk phase. The cohesive failure of a coating is unlikely to be the same as the cohesive failure of the same material in bulk form.

In real adhering systems, there can be many interphases in addition to the two bulk phases, and separation could be in any of the interphases. If the separation occurs in an interphase, Mittal suggested that the measured adhesion be labelled as "practical adhesion", unless the failure is deep in the bulk of the adhering phases. The forces required to disrupt the interphase can be applied in various forms (tensile, peel, shear, etc.).

Peel strength is measured in terms of force/width required to maintain the continuous detachment of a strip of adherate from an adherent at a specified detachment rate. Peel strength is also expressed in terms of work or energy per unit area.

Tensile strength is defined as the stress (force/area) required to remove a specific area of the adherate when the entire area of the adherate is pulled in a direction perpendicular to the adherent surface.

Basic adhesion is strictly an interfacial property and depends exclusively on the surface characteristics of adhering phases, i.e. it should be independent of the thickness of coating, specimen size and geometry, test rate, etc. However, the adhesion measurement techniques for determining practical adhesion are affected by all these factors.

Both Berdan[82] and Mittal[83,84] suggested a list of ideal features for adhesion tests but these are certainly not all satisfied by any test currently available. For example, one of Berdan's ideals was to have successful adhesion checks independent of cathode geometry. However, adhesion can rarely be determined unless a specimen is prepared which complies with certain dimensions and shapes. Consequently, an ideal test has not yet been developed. Choices can only be made with respect to the ideal feature.

### 1.6.1.1 QUALITATIVE ADHESION TESTS

Numerous qualitative tests have been used and listed in A.S.T.M. B571-79[85]. Some of the constraints of the tests are the geometry of the specimen, thickness of coating, initiative of the operator and the magnitude of the adhesion value. Tests included in this category are bending, twisting, burnishing, buffing, abrasing and cycling. All these qualitative adhesion tests were tabulated and commented on by Davies and Whittaker[79].

The bending and twisting tests are in common use since they are easily performed and the procedures can be standardised, particularly for strip or wire. Brittle coatings may crack, but ductile coatings do reduce stress by the very nature of their flow, thus preventing the coatings from being detached despite their poor adherence.

Burnishing, buffing and abrasion tests are based on severe local deformation. They can be applied on site to most production parts, and are considered by Davies and Whittaker as non-destructive tests where the adhesion process is acceptable. They are useful for thin coatings for which chiselling tests would not be satisfactory. This is because only thicker coatings facilitate chiselling at one point, followed by peeling with some type of grip. Most of the above-mentioned have been used to assess the bond strength

and performance of plated aluminium [86,87,88]. However, it was found that the most successful test was the temperature cycling test [89].

For complex-shaped components such as die castings, thermal cycling is particularly useful since the test is largely independent of the geometry of the part and may be non-destructive. Olsen and Halvosen [77] have tested their magnesium samples at 150 °C for one hour, followed by quenching in water at 20 °C to 25 °C. They were said to be satisfactory after this treatment.

### 1.6.1.2 QUANTITATIVE ADHESION TESTS

Tensile, shear and peel tests are the basis of many quantitative tests. They can be classified into three groups.

The first group of tests comprises the use of solders and adhesives and the Brenner nodule test [90]. Solders and adhesives are used to attach some form of grip to the coating through which the detaching force can be applied, while in the Brenner test, a nodule is electroformed on to the surface to serve as the grip. The primary limitation of

the test is the strength of the solder or adhesives and the strength of the nodule.

The second group comprises the Ollard Method[91] and its subsequent modifications[92,93,94] in which the detaching force is applied by gripping the coating itself and the stress is primarily tensile. Special test specimens must be prepared. Peel tests originate from Jacquet[95] and have a major advantage over tensile tests, in that a much thinner electrodeposited coating is required. The coating needs to be ductile and strong enough to permit continuous peeling of the deposit from the substrate. Otherwise a means of gripping the coating (the grip can be electroformed similar to the Brenner nodule) would be required. This type of test is very easy to carry out in the case of systems for which the adhesive value is relatively low. Such and Wyszynski[96], and Golby[97] have used this technique for dull nickel on aluminium.

Mathematical analysis of the peel test for determining the adhesion of electrodeposits to plastics by Saubestre et al[98] has indicated that the resulting numerical reading is not a true measure of adhesion. It was claimed to be a measure of a multiplicity of complex factors including the thickness of the electrodeposited metal, the Young's moduli and tensile strength of the substrate and coating. Details of the analysis are shown in Appendix II. Using the limited evidence available, it is believed that this study also

applied to the peeling of electrodeposits from metal substrates.

The third group covers a variety of specialised techniques where the primary mode of stressing is in shear [99,100]. Ultracentrifuge techniques are suggested to be the most capable for detaching coatings from substrates. The disadvantages of the method are the complexity of the necessary apparatus and the fact that the test cannot be carried out on actual components but only on a special test-piece.

Of all the above quantitative tests studied, the peel test was chosen in this project to determine adhesion. The major reason was that the results obtained can be directly compared with those achieved by using aluminium and its alloys which have been widely studied [96,97].

### 1.6.2 CORROSION TESTS

As well as service trials of plated specimens in the actual environment in which they will be exposed, two types of tests can be used to evaluate the corrosion resistance of coatings, namely accelerated and outdoor exposure corrosion tests.

Various accelerated corrosion tests are specified for the assessment of nickel and chromium electroplated coatings. They are listed in BS 1224:1970[101]. Two of these accelerated tests will be considered:

(a) Acetic acid salt spray test

(b) Copper accelerated salt spray test (CASS test)

### 1.6.2.1 ACETIC ACID SALT SPRAY TEST

This test is carried out in a non-corrodible cabinet at 35 °C. 50g/l of sodium chloride is used as spray solution with its pH adjusted to 3.2 by glacial acetic acid. The spray rate is controlled so that its collection rate over an area of 800 $mm^2$ is between 1-2 ml/hr. The collected spray solution must have a concentration of 5 ± 1 % NaCl and its pH must remain the same. A very detailed procedure is also listed in A.S.T.M. B287-74[102].

Fintschenko and Groshart[103] have carried out the salt spray test on magnesium panels which had been pretreated using Norsk Hydro sequence and plated with different coating systems including electroless nickel. They found that all plating exhibited porosity after 6 hours of exposure. Total thicknesses of coatings on all panels were 25 μm.

1.6.2.2 CASS TEST

This test is very similar to the acetic acid salt spray test except that 0.26 g/l of cupric chloride is added to the salt spray solution, and the temperature is raised to 50 °C. The cabinet is similar to that used for the previous test, but a larger humidifying unit is required so that the compressed air supplied to the jet is sufficiently humid to prevent evaporation of the sprayed liquid. This is in fact a more accelerated test than the acetic acid salt spray test. Detailed procedures are listed in A.S.T.M. B368-68 (104).

Of the two accelerated tests for corrosion, the CASS test was employed because it is a more severe test and also is known to give good correlation with some industrial environments.

Both accelerated tests were employed by Olsen (33) to test magnesium alloy die castings with different coating systems and thicknesses. *Samples* were electroplated by the Norsk Hydro sequences. It is claimed that multi-layer plating systems including microdiscontinuous chromium will provide adequate protection to exterior automative hardware in some locations.

The choice of test method is influenced by the particular requirement. Dennis and Such [105,106] tabulated the order of merit of various coating systems when subjected to different corrosion tests, and showed that it could be misleading to use a single test without knowing the limitation of the test.

### 1.6.3 METHODS OF EVALUATION OF CORROSION RESULTS

The British standard and the A.S.T.M. standard include the systems used most frequently for evaluating nickel plus chromium coatings.

The method recommended in British Standard BS 374S:1970 [107] demands less skill and experience on the part of the assessor than the A.S.T.M. B380-65 [108] and A.S.T.M. B537-70 [109].

However, it is a severe rating system because a small number of corrosion spots results in a low rating number. It differs from the A.S.T.M. system in that it only takes into consideration sites at which visible penetration of the coating to the substrate has occurred. Surface staining or discolouration is not assessed. The ASTM method was used in the present project since it is preferable for evaluation of research results.

# CHAPTER 2 EXPERIMENTAL PROCEDURES

## 2.1 MAGNESIUM ALLOY SAMPLES FOR PLATING TRAILS

A number of commercial magnesium alloy die castings were supplied by the Norsk Hydro company in the vibratory finished condition. Information on the alloys' composition is given in Table 4. The alloys were:

(1) AZ91, cold chamber pressure die casting test panels 40 X 100 X 5 mm.

(2) AZ61, cold chamber pressure die casting test panels 50 X 100 X 5 mm.

(3) AZ91, hot chamber pressure die casting loud speaker parts 113 X 80 X 2.5 mm.

(4) AZ71, hot chamber pressure die casting paper knives.

Three sets of AZ91 alloy door handles were provided by Promagco Ltd. of Worcester, England. They are hot chamber pressure die castings in the as cast condition. The samples were made with different materials from three companies, and they were cast at temperatures ranging from 610 $^{o}$C to 660 $^{o}$C. The object of this was to compare the surface quality and consequently the platability of each casting made by different materials at different temperatures.

Table 4 COMPOSITION OF MAGNESIUM ALLOY SAMPLES

| Alloy | Al | Zn | Mn | Si | Fe | Cu | Ni | Be ppm |
|---|---|---|---|---|---|---|---|---|
| AZ91* cold chamber | 9.1 | 0.75 | 0.20 | 0.04 | 0.011 | 0.006 | 0.001 | 3 |
| AZ61* cold chamber | 6.8 | 0.56 | 0.22 | 0.05 | 0.010 | 0.007 | 0.001 | 7 |
| AZ91* hot chamber | 9.2 | 0.66 | 0.17 | 0.04 | 0.005 | 0.001 | 0.001 | 5 |
| AZ71 hot chamber | 7.4 | 0.70 | 0.12 | 0.04 | 0.005 | 0.001 | 0.001 | 5 |

*Data obtained from the Norsk Hydro a.s.

All the plating processes employed in the test programme involved the zincate immersion technique.

## 2.2 PRELIMINARY METALLOGRAPHIC EXAMINATION

Ease of cutting and grinding makes the preparation of the magnesium alloy specimens for micro-examination a simple matter. Little difficulty arises when a scratch-free preparation is desired for examination in the polished and unetched condition e.g. for the use of the Electron Probe Micro Analysis (EPMA).

The samples were cut and mounted in conductive bakelite, ground with various grades of emery paper and finally polished with 1 $\mu$m diamond on a wheel. Glycol (1 ml of conc. $HNO_3$ + 75 ml of ethylene glycol + 24 ml of $H_2O$) was used as a metallographic etchant to illustrate the grain boundaries and the constituents.

## 2.3 COMPOSITION ANALYSIS

EPMA was firstly used to obtain qualitative information on the constituents present in the surface of the alloys.

However, the percentage of aluminium obtained from the EPMA was rather low since it was expected to be about 9% for AZ91 alloys and 6% for AZ61 alloys. The highly reactive nature of magnesium and consequently its affinity for oxygen, causes the formation of the oxide film on the surface, which may well be one of the reasons for the low reading of the percentage of aluminium obtained. Therefore, an atomic absorption spectrophotometer was used to obtain quantitative information on the constituents present in the alloys.

### 2.3.1 ATOMIC ABSORPTION SPECTROPHOTOMETER

An Atomic Absorption Spectrophotometer (AAS), which can be used to measure the concentration of metallic element in a variety of matrices [110,111], was chosen to find out the amount of aluminium, zinc and manganese in the magnesium alloys.

The sample solution, blank solution and standard solution for each sample were made up according to the standard conditions for aluminium, zinc and manganese. The readings were integrated over a period of 5 seconds.

## 2.4 SURFACE EXAMINATION

The alloy surfaces were examined at various stages in the test programme using scanning electron microscopy and electron-probe micro-analysis (EPMA). A scanning electron microscope fitted with an energy dispersive X-ray micro-analysis attachment was also used to identify elements present on the surface.

## 2.5 DEVELOPMENT OF THE ELECTROPLATING PROCEDURES

A series of experiments on several pretreatment sequences was carried out. All of the sequences involved the zincate immersion step.

### 2.5.1 THE STANDARD DOW PRETREATMENT SEQUENCE

The standard practice for 'preparation of magnesium and magnesium alloys for electroplating' recommended by A.S.T.M. based on the the Dow process was followed (64).

Step 1 Acetone degrease.

Step 2 Water rinse.

Step 3 Cathodic alkali clean at 8 $Adm^{-2}$ and 80 °C for 60 seconds. (30 g/l of Minco cleaner* was used owing to its low alkalinity and its freedom from silicates. It was originally formulated to provide a clean film free surface on aluminium (71).

Step 4 Water rinse.

Step 5 Ferric nitrate pickle for 2 min. at room temp.

| | |
|---|---|
| Chromic acid | 180 g/l |
| Ferric nitrate | 40 g/l |
| Potassium fluoride | 3.5 g/l |

Step 6 Water rinse.

Step 7 Activate in the following solution for 2 min. at room temp.

| | |
|---|---|
| Phosphoric acid | 200 ml/l |
| Ammonium bifluoride | 105 g/l |

Step 8 Water rinse.

Step 9 Zincate in the following solution for 10 min. at 80 °C.

| | |
|---|---|
| Zinc sulphate | 30 g/l |
| Tetrasodium pyrophosphate | 120 g/l |
| Lithium fluoride | 3 g/l |
| Sodium carbonate | 5 g/l |
| pH | 10.2-10.4 |

Step 10 Water rinse.

Step 11 Copper plating in alkaline/cyanide bath.

| | |
|---|---|
| Cuprax high efficiency copper salt | 210 g/l |

*Minco cleaner is one of W. Canning's formulations.

| | |
|---|---|
| Current density | 2 $Adm^{-2}$ |
| Time | 6 min. |
| Temperature | 60 °C |

Step 12 Water rinse.

Electroplating as required.

### 2.5.1.1 VARIATIONS OF THE CLEANING AND ACTIVATION STAGES IN THE PRETREATMENT SEQUENCES

Attempts have been made to improve the Dow process by using different chemical agents in the cleaning stages in order to achieve a more evenly etched surface, better adhesion and brightness. Two sequences have been attempted. They are referred to later as the first and second modification of the Dow process.

Sequence 1 (The first modification of the Dow Process)

Step 1 Acetone degrease.

Step 2 Water rinse.

Step 3 Activate in oxalic acid solution at room temp.

| | |
|---|---|
| Oxalic acid | 10 g/l |
| Wetting agent | 0.5 g/l |
| Treatment time | 1 min. |

Step 4 Water rinse.

Step 5 Alkaline clean in Kelco solution in order to clean and activate the aluminium rich areas on the surface of the alloys.*

| | |
|---|---|
| Kelco cleaner | 25 g/l |
| Temperature | 65-80 °C |
| Time | 1-2 min. |

Step 6 Water rinse.

Step 7 onwards are the same as the Dow pretreatment sequence, i.e. activate in amonium bifluoride $NH_4HF$ solution followed by chemical zincating.

Sequence 2 (The second modification of the Dow process)

This sequence is very similar to sequence 1 except that 2% HF solution was used to clean and activate the magnesium alloy surface in Step 7 rather than using ammonium bifluoride solution. It is assumed that magnesium and aluminium oxides are highly soluble in HF solution and that a fluoride film is formed which may be dissolved and washed away during the subsequent rinsing step, leaving the surface free of oxide or hydroxide film.

* Kelco cleaner is specially formulated by W. Canning Ltd. to be used for the cleaning and light etching of aluminium.

THE FIRST MODIFICATION OF THE DOW PROCESS

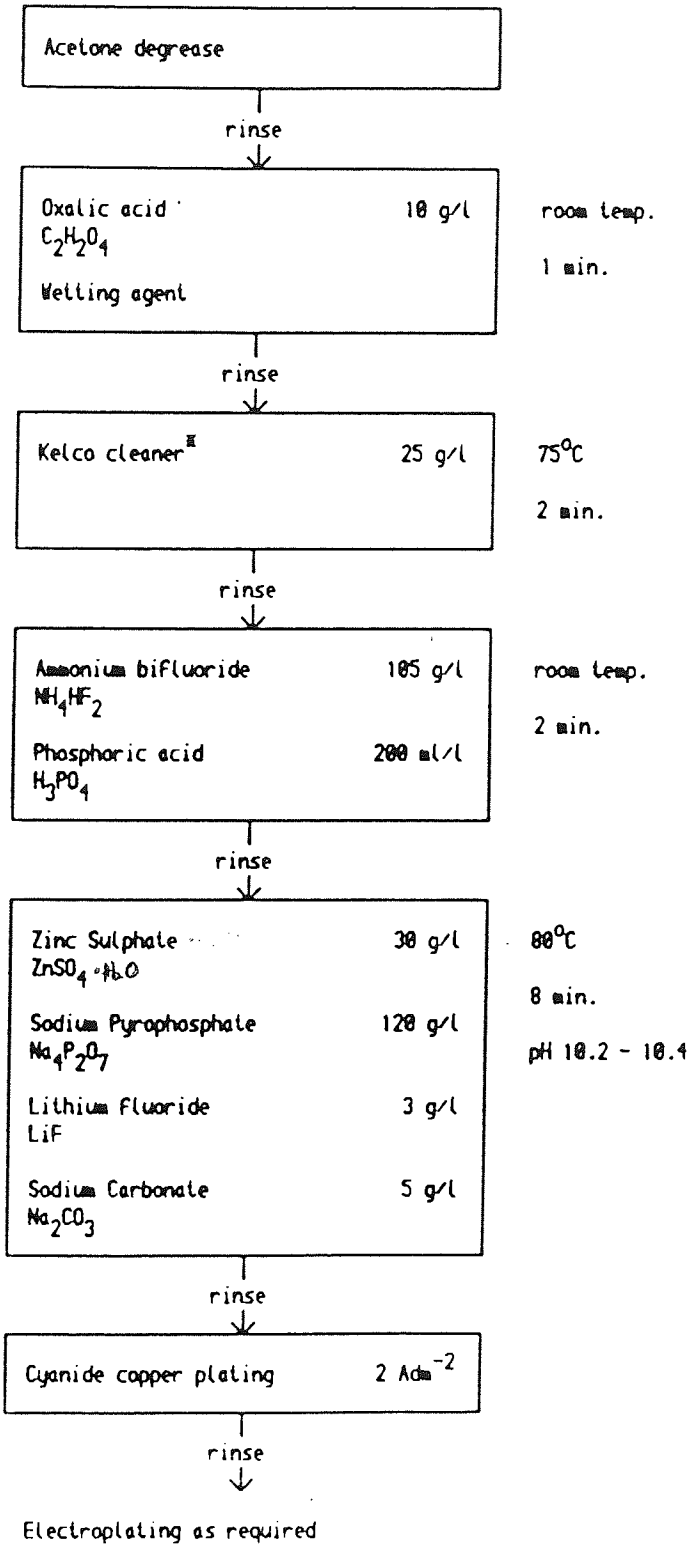


* Kelco cleaner is one of W.Canning Ltd's formulations.

Fig.11 Flow chart showing the first sequence employed to modify the Dow process

THE SECOND MODIFICATION OF THE DOW PROCESS

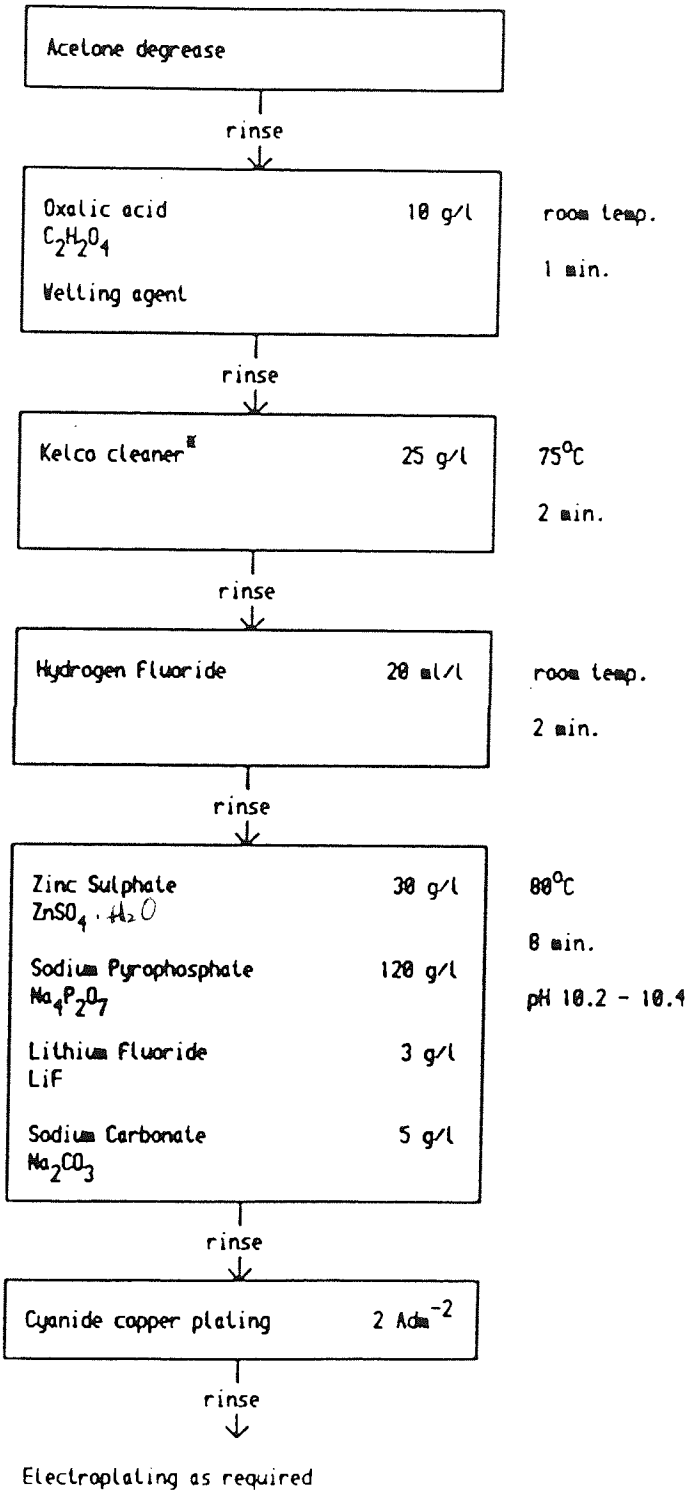


* Kelco cleaner is one of W.Canning Ltd's Formulations.

Fig.12 Flow chart showing the second sequence employed to modify the Dow process

## 2.5.2 THE STANDARD NORSK HYDRO PRETREATMENT SEQUENCE

The pretreatment sequence for electroplating magnesium alloys, invented by Olsen & Halvorsen (77) of Norsk Hydro a.s. was followed. The treatment involves two activation steps followed by chemical zincating which is similar to the Dow immersion zincating step except that a higher concentration of alkali pyrophosphate at lower temperature and shorter immersion time is employed.

| | | |
|---|---|---|
| Step 1 | Acetone degrease. | |
| Step 2 | Water rinse. | |
| Step 3 | Activate in oxalic acid solution at room temp. | |
| | Oxalic acid | 2-10 g/l |
| | Wetting agent (FT248) | 0.5 g/l |
| | Time | 60 sec. |
| Step 4 | Water rinse. | |
| Step 5 | Activate in pyrophosphate bath. | |
| | Potassium or sodium pyrophosphate | 50-75 g/l |
| | Sodium carbonate | 15 g/l |
| | Wetting agent | 0.5 g/l |
| | Temperature | 55-65 °C |
| | pH | 10.0-11.5 |
| | Time | 2 min. |
| Step 6 | Water rinse. | |
| Step 7 | Chemical zincating. | |
| | Zinc sulphate | 50 g/l |
| | Potassium pyrophosphate | 150 g/l |

| | |
|---|---|
| Potassium fluoride | 7 g/l |
| Sodium carbonate | 5 g/l |
| Temperature | 60-65 °C |
| pH | 10.2-10.5 |
| Time | 3 min. |

Step 8 Water rinse.

Step 9 Copper plating in alkaline/cyanide bath similar to the Dow process.

Step 10 Water rinse.

Electroplating as required.

2.5.2.1 VARIATION OF THE SECONDARY ACTIVATION STEP IN THE NORSK HYDRO SEQUENCE

Initially the secondary activation was carried out with potassium pyrophosphate ($K_4P_2O_7$) at a concentration of 50-75 g/l at 50-55 °C as recommended by Norsk Hydro. However, to improve adhesion it was operated

(a) in the temperature range of 50-80 °C and

(b) at a concentration from 10-200 g/l

## 2.5.3 THE CANNING PRETREATMENT SEQUENCE

This was one of the series of pretreatment sequences carried out in the laboratory of W.Canning Material Ltd. The attempt is to improve the standard Norsk Hydro process.

Step 1 to Step 4 are the same as the Norsk Hydro pretreatment sequence, i.e. using oxalic acid to clean and dissolve the oxide film on the magnesium alloy surfaces.

Step 5 Activate in Borax solution, which comprises:

| | |
|---|---|
| Sodium borax | 40 g/l |
| Tetrasodium pyrophosphate | 70 g/l |
| Sodium fluoride | 20 g/l |
| Temperature | 75 °C |
| Time | 2 min. |

This is in fact another activation solution recommended by DeLong [67,89] and it is said to be suitable where the work surface is free of chromate film.

Step 6 onwards are the same as the standard Norsk Hydro pretreatment sequence i.e. the work is rinsed in water and transferred immediately to the zinc immersion coating solution prior to cyanide copper plating.

THE CANNING PROCESS

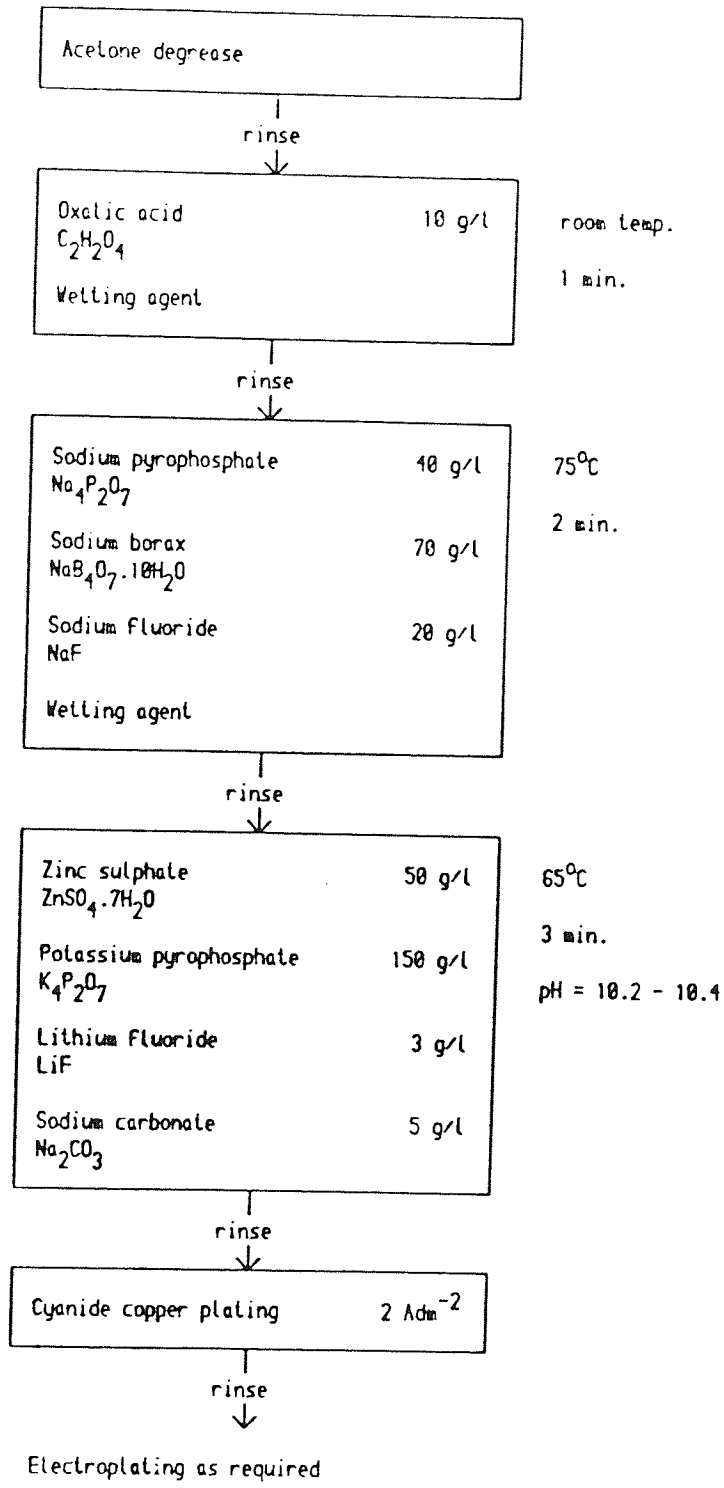


Fig.13 Flow chart for the Canning process.

## 2.5.4 PRETREATMENTS INCORPORATING THE DOUBLE ZINCATING TREATMENT

The use of a double dip treatment is known to be effective for plating onto some 'difficult' aluminium alloys and so it was considered worthwhile to adopt a similar procedure for the plating onto die cast magnesium alloys. The aim of the double dip method in the plating of aluminium is to deposit a thin adherent immersion film. The deposition and removal of the first film eliminates the most active sites from the surface. The second film is applied onto a more chemically uniform surface at a slower rate and a uniform thickness is obtained.

One of the double dip treatments applied to magnesium alloys seemed rather promising at first, but the adhesion levels obtained were virtually nil. The sequence employed was as follows:

Step 1
to
Step 7 are the same as the Canning pretreatment sequence.

Step 8 Water rinse.

Step 9 The zinc deposits were removed by

| | |
|---|---|
| Phosphoric acid | 200 ml/l |
| Ammonoum bifluoride | 105 g/l |

Step 10 Water rinse.

Step 11 2nd zincate treatment.

Step 12 Water rinse.

Electroplating as required.

### 2.5.5 PRETREATMENTS INCORPORATING USE OF ZINCATE SOLUTION OPERATED ELECTROLYTICALLY

A layer of zinc was applied on alloy AZ61CC electrolytically after the activation steps. One set of samples was activated with the Canning sequence, while another set was activated using the Norsk Hydro sequence. ~~The final set of samples was simply degreased in acetone with no other prior chemical treatment.~~ Different times and current densities were employed for different conditions.

## 2.6 STUDY OF DIFFERENT PRETREATMENT SEQUENCES PRIOR TO CYANIDE COPPER PLATING USING S.E.M.

The S.E.M. was used to investigate the surface response of the alloys to the different pretreatments prior to final cyanide copper plating. Specimens were pretreated, vacuum-coated with carbon and gold palladium and examined using the S.E.M. The surface was also analysed using the X-ray micro-analysis attachment previously described.

## 2.7 STUDY OF DIFFERENT PRETREATMENT SEQUENCES PRIOR TO CYANIDE COPPER PLATING USING AUGER ELECTRON SPECTROSCOPY

Auger analysis was used as an additional method of studying the composition of surface films after various stages in the pretreatment sequences. A.E.S. was chosen owing to its sensitivity over the sample surface since its wavelength is small $10\ \text{A}^{\circ}$. The minimum detectable is typically larger than that for many other techniques (112). Samples were cut into less than $10 \times 10\ \text{cm}^2$ in size and pretreated accordingly. Kinetic energies-Auger lines excited by electron bombardment were recorded respectively for each stage.

## 2.8 STUDY OF DIFFERENT PRETREATMENT SEQUENCES USING POTENTIAL TIME MEASUREMENTS

Apart from using the S.E.M. and A.E.S. to study the surface response to the different pretreatment stages, and the variation of surface potential with time during cleaning, activation and zincating steps of the Norsk Hydro and the Canning process were also measured by reference to a saturated KCL Calomel electrode and continuously monitored with a fast response chart recorder. The Calomel electrode was connected to the positive terminal of the recorder.

Potential-time results were used to compare the relative nobility of a number of metals and magnesium alloys when immersed in the same solution under identical conditions. Products formed on the surfaces of alloys during immersion were then dried and collected for X-ray diffraction examination.

## 2.9 STUDY OF ZINCATE FILM MORPHOLOGY

The morphology and growth characteristics of the zincate deposits were investigated using the S.E.M. and the X-ray micro-analysis attachment. Speciments for S.E.M. examination were prepared as described in Section 2.6. The

inference of pretreatment, the pH of the zincate solution, its composition and the duration of immersion were monitored.

## 2.10 DETERMINATION OF ZINCATE FILM WEIGHT

For each alloy type a set of two carefully machined and measured test samples were prepared. Two sets of samples were zincated after the Norsk Hydro and the Canning pretreatment respectively. One set of samples was just degreased and zincated without any prior chemical treatment. All the samples were zincated in the same zincate solution under the same conditions but for different immersion times.

The samples were then dried and weighed. The zincate film of each sample was subsequently stripped in 5% HF solution. The weight of the film for each sample was therefore determined by the final reweighing.

## 2.11 ELECTRODEPOSITION

The test samples were polished and plated using proprietary solutions and standard conditions. Solutions and operating conditions are listed in Table 5. All coatings were plated directly on to the cyanide copper layer.

### 2.11.1 PLATING FOR ADHESION TESTING

A 20 μm acid copper layer followed by 20 μm bright nickel deposit was used to determine performance during thermal cycling tests.

Details of the peel test are given in section 2.12.2. A 250 μm thick pyrophosphate copper deposit was used to support the peeling load involved during peel tests.

### 2.11.2 PLATING FOR CORROSION TESTING

Studies [96,113] have shown that the corrosion resistance of aluminium (plated using the modified alloy zincate process) is dependent upon thickness and nature of coating system.

Table 5 OPERATING CONDITION OF THE PLATING SOLUTIONS

| Plating solution | Current density A $dm^{-2}$ | pH | Temp. $^{o}C$ | Agitation |
|---|---|---|---|---|
| Pyrophosphate copper | 4 | - | 55 | air |
| acid copper | 4 | - | 18 | air |
| Bright nickel | 4 | 4.5 | 55 | air |
| Watts nickel | 4 | 4.0 | 60 | air |
| Nickel seal | 4 | 3.5 | 55 | air |
| Bright decorative Chromium | 10 | 1.0 | 35 | none |

They have also confirmed the superior corrosion resistance of the duplex nickel and microcracked chromium system. These were recommended for severe conditions, capable of meeting the requirements of B.S. 1224:1970 [101]. For normal indoor service however, the bright nickel-decorative chromium system was satisfactory. All magnesium test samples were initially plated with 15 μm of acid copper, and hence four coating systems were employed.

1. Decorative chromium

   30 μm bright nickel

   0.3 μm decorative chromium

2. Microporous chromium

   30 μm bright nickel

   2.5 μm nickel seal

   0.3 μm decorative chromium

3. Duplex-double layer nickel

   20 μm semi-bright nickel

   10 μm bright nickel

   0.3 μm decorative chromium

4. Semi-bright nickel with microporous chromium

   30 μm semi-bright nickel

   2.5 μm nickel seal

   0.3 μm decorative chromium

Microporous chromium deposits were obtained using the following procedure: after deposition of the bright or duplex nickel layer, a special nickel layer of about 1 μm was deposited from a solution containing silica particles, which were approximately 0.02 μm diameter. The inert particles were kept in suspension by vigourous air agitation and co-deposited with the nickel. A chromium layer was then deposited using a conventional decorative chromium plating solution. Deposition of the chromium was arrested at the silica particles which resulted in a microdiscontinuous chromium top coat.

The microporosity of the nickel solution was examined by immersing a microporous nickel plated sample in an acid copper sulphate solution at room temperature and plating for about 3 minutes at a current density of 0.3 A $dm^{-2}$. After plating, the sample was rinsed, dried and finally examined under high magnification. Since copper would only be plated on nickel, the number of copper particles per $cm^2$ was counted and the microporosity of the nickel solution was therefore determined. This is known as the Dubpernell test [74,114].

After electroplating the samples were washed, dried and stored in a dry atmosphere until ready for corrosion testing.

## 2.12 ADHESION TESTINGS

### 2.12.1 THERMAL CYCLING TESTING

The samples for thermal cycling tests were plated with 20 μm of copper and 20 μm of bright nickel. They were then stored for 3 days before the test.

The samples were heated at 250 °C for 1 hour followed by quenching in water at 20-25 °C. Each sample was subjected to one cycle.

### 2.12.2 PEEL TESTING

The panels for peel testing were plated with 250 μm (± 20 μm) of pyrophosphate copper. Peel adhesion was measured using an " Instron " tensile testing machine fitted with a peel test attachment. Specimens were screwed to the movable trolley of the peel testing attachment. The trolley moved in such a way as to ensure that the angle of the peel strip was maintained perpendicular to the specimen surface. The width of the peeled deposit, standardized at 2.54 cm, was achieved by milling two parallel slits through the

coating into the substrate. A tab of deposit was then lifted from the substrate using a pair of pliers. The fluctuation of the adhesive force monitored by the Instron load cell were displayed on a chart recorder. The rate of peel and the chart speed were standardized at 5 cm/min. The peel adhesion per panel was determined by measuring the area under the peel curve using a planimeter. This gave a measure of the work expanded in detaching the plating from the substrate (Plate 28).

### 2.12.3 EXAMINATION OF PEEL ADHESION TESTED PANELS

After peel testing, samples of failure surfaces on the alloy substrate and the back of the peeled foil were cut from the test panels. Samples were vacuum-coated with carbon or gold-palladium alloy and examined using the S.E.M. The X-ray micro-analysis attachment linked to the S.E.M. was also used to qualitatively assess the amount of substrate detached.

## 2.13 CORROSION TESTING

The alloys used in this study were AZ91 and AZ61 cold chamber and AZ71 hot chamber die castings. These were processed using two different pretreatment sequences. The standard Norsk Hydro pretreatment sequence and the Canning pretreatment sequence. However, in order to achieve higher adhesion values, another set of samples was plated using the Norsk Hydro pretreatment sequence but the secondary activation step was operated at a higher temperature and concentration than recommended i.e. at 80 °C and a $K_4P_2O_7$ concentration of 210 g/l. The four coating systems applied are described in section 2.11.2. A programme of accelerated corrosion testing using the C.A.S.S. test was undertaken. A C.A.S.S. cycle time of 16 hours is equivalent to approximately one year of service outdoors. All panels were exposed to a total of 3 C.A.S.S. cycles. Hence the results of this severe test would indicate the corrosion resistance of the plated magnesium alloys under extreme conditions.

## 2.14 ASSESSMENT OF CORROSION BEHAVIOUR

All corroded samples were assessed visually using the A.S.T.M. specification B537-70 [109] rating method. This was based on comparing the corroded test samples with standard

photographs. Corrosion products were removed prior to rating by careful swabbing in warm water.

### 2.14.1 ANALYSIS OF VARIANCE

After the corroded samples had been assessed visually and rated, the information was tabulated and fed into the computer system for variance analysis. Since the corrosion testing involved four coating systems, three different alloys and pretreatment under three different conditions, the results could therefore be analysed by this programme.

The programme can accommodate up to 5 factors and up to 1000 individual results. (The results were duplicated in this case). The programme provides an analysis of variance table and the means of each factor at each level and therefore is useful for plotting summary graphs [115].

### 2.14.2 EXAMINATION OF CORROSION TESTED SAMPLES

Apart from visual assessment, corrosion sites on the corroded samples were studied using projection and scanning electron microscopy. The X-ray micro-analysis attachment on

the S.E.M. was used to identify elements present in the corrosion products. Dennis and Fuggle[116] described the use of the S.E.M. for the investigation of the morphology of corrosion pits in decorative nickel and chromium coatings. A similar procedure was adopted in this case.

# CHAPTER 3 RESULTS

## 3.1 SURFACE EXAMINATION OF MAGNESIUM ALLOY SAMPLES FOR PLATING TRIALS

All the castings supplied by the Norsk Hydro company including paper knives produced in AZ71 by the hot chamber process were in the vibratory finished condition. Because the latter samples were supplied part way through the programme, they were used only for the corrosion tests. The surface condition of the castings was variable as illustrated by visual examination and by optical and electron microscopy.

The AZ71 hot chamber paper knives had the smoothest surface finish of all the castings, whereas the AZ91 hot chamber loudspeaker parts were the most difficult alloy samples on which to achieve good adhesion because of their comparatively rough surfaces. Under the microscope, it was also apparent that the AZ91 hot chamber castings had undulating surfaces. Even with the naked eye, the crack lines on the surface were quite obvious at corners and at indented areas e.g. round the punch holes. The surfaces on AZ61 and AZ91 cold chamber panels appeared to be smoother than the hot chamber ones.

Each sample was checked and selected before plating. In the case of AZ91 hot chamber castings, only those which appeared to have the best surface characteristics were taken into the plating programme. However, imperfections in the surface were revealed under the S.E.M. (Plates 1a, b and c).

The surfaces of AZ91 hot chamber alloy car handle castings provided by Promagco Ltd. in Worcester were rough and porous even after polishing. Flow lines and roughness were visible to the naked eye. Plate 1d shows the polished surface of an AZ91 door handle casting under the scanning electron microscope at a magnification of X1000. The topography resembled pits and valleys.

It was difficult to polish magnesium die castings, since any penetration of the surface layer caused the underlying porosity to be revealed, and it was impossible to polish away the crack lines. Castings which had complicated shapes i.e. narrow access, indentation marks e.g. AZ71 paper knives, had polishing products embedded in the pattern in the handles. Therefore, the surface conditions were very much dependent on the quality of castings in their as-cast conditions.

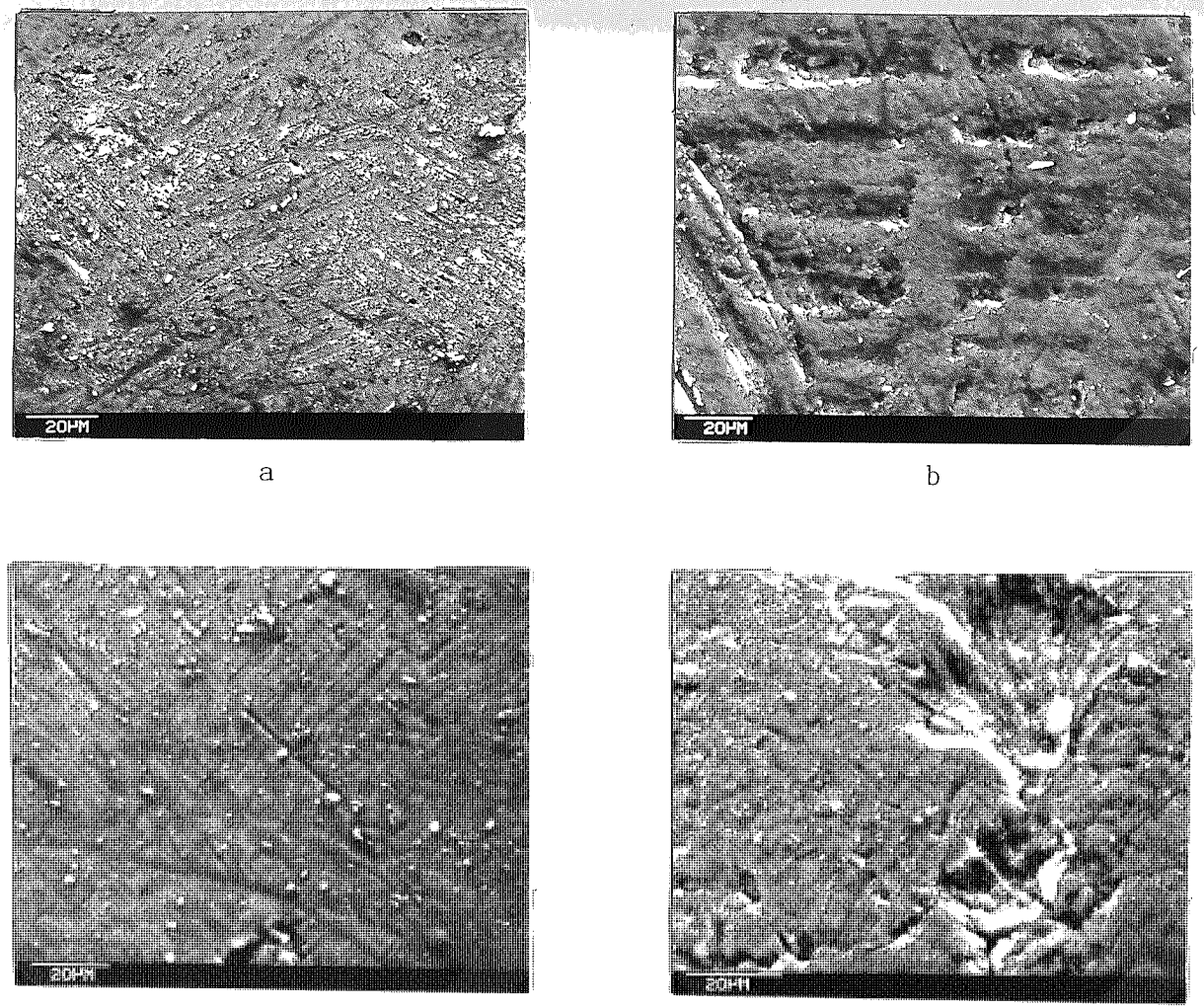


a b

c d

Plate 1 Scanning electromicrographs showing the surface appearance of as cast magnesium alloy samples.

a) AZ91 cold chamber panel.
b) AZ91 hot chamber panel.
c) AZ71 hot chamber knife blade.
d) AZ91 hot chamber car door handle.

## 3.2 PRELIMINARY METALLOGRAHIC EXAMINATION

All castings shown in Plate 2 exhibited fine structures. Since the cooling during pressure die casting took place so rapidly, no opportunity was given for directional solidification.

Because $\beta$ phase was present ($Mg_{17}Al_{12}$), the casting alloys were not homogeneous in microstructure. The hot chamber die castings appeared to have finer structures than cold chamber ones except that the dendrites of $\alpha$-phase were larger and more isolated. According to the Mg-Al phase diagram shown in Fig. 1, at temperatures below 650 $^{o}$C, magnesium starts to solidify ($\alpha$ + L). Since the casting temperature of magnesium aluminium alloys ranges from 600 $^{o}$C to 700 $^{o}$C, it is therefore believed that some of the liquid phase (magnesium rich phase) was solidified before the fluid reached its eutectic state ($\alpha + \beta$). Presence of porosity is one of the characteristics in die castings due to entrapped air.

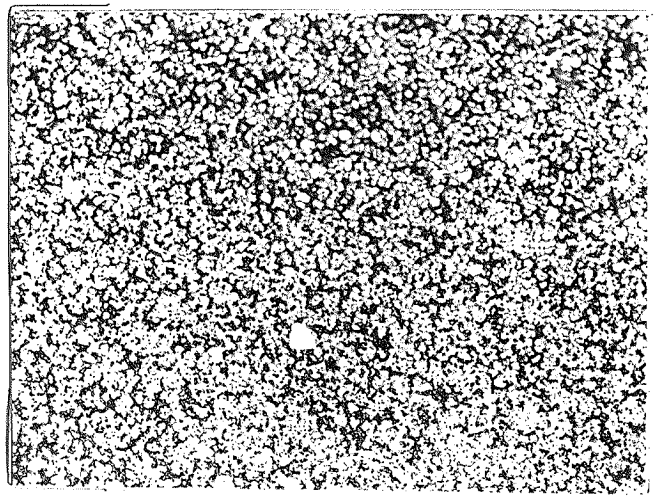

a

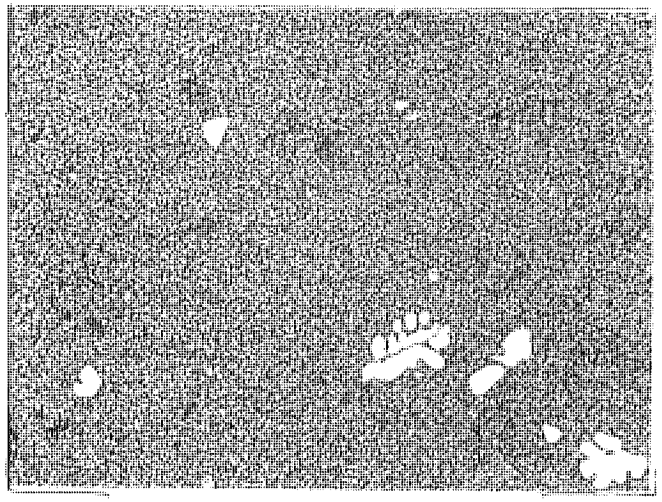

b

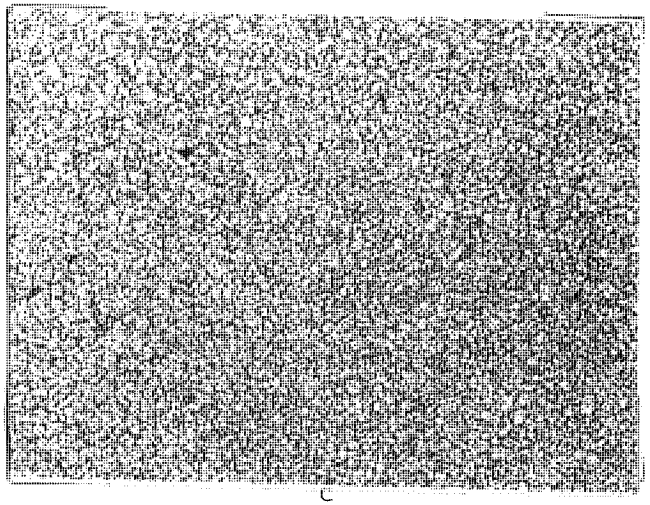

c

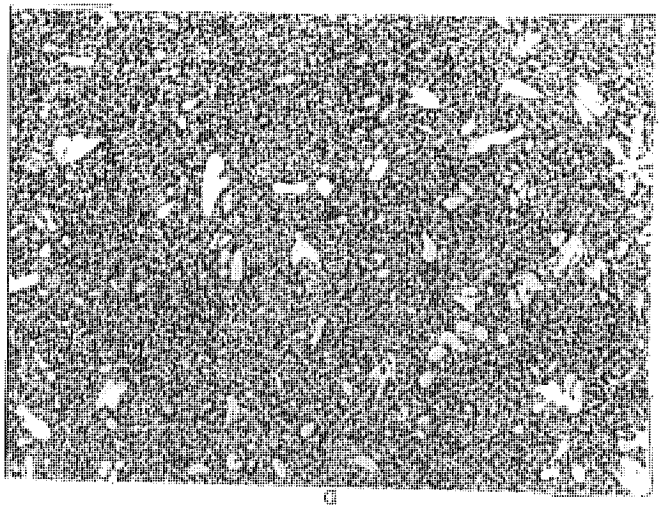

d

Plate 2 Optical photomicrographs showing the structure of:

a) AZ91 cold chamber panel (X150).
b) AZ91 hot chamber panel (X100).
c) AZ61 cold chamber parel (X100).
d) AZ71 hot chamber knife (X150).

## 3.3 COMPOSITION ANALYSIS

E.P.M.A. was used to obtain qualitative information about the constituents present in the surface of the castings. The average results were as follows:

| | AZ91 CC panels | AZ61 CC panels | AZ91 HC speaker parts | AZ71 HC knives | AZ91 HC handles |
|---|---|---|---|---|---|
| % Mg | 91.50 | 91.10 | 90.30 | 88.30 | 88.80 |
| % Al | 3.96 | 3.30 | 5.05 | 3.56 | 4.30 |
| % Zn | 0.54 | 0.54 | 0.60 | 0.50 | 0.53 |
| % Mn | 0.10 | 0.10 | 0.10 | 0.10 | 0.10 |

The highly reactive nature of magnesium (and consequently its affinity for oxygen) resulted in the formation of the oxide film on the surface. This may be one of the reasons for the low percentage values of aluminium obtained. However it should be borne in mind that since the alloys were not homogeneous in microstructure, it was difficult to obtain the exact percentage of alloying elements present by this technique.

The atomic absorption spectrophotometer AAS was therefore used to determine the concentration of metallic elements in the specimens. The average results of 5 readings were as follows:

| | AZ91 CC panels | AZ61 CC panels | AZ91 HC speaker parts | AZ71 HC knives | AZ91 HC handles |
|---|---|---|---|---|---|
| % Al | 8.84 | 6.80 | 8.98 | 7.35 | 7.92 |
| % Zn | 0.56 | 0.56 | 0.75 | 0.70 | 0.64 |
| % Mn | 0.20 | 0.22 | 0.17 | 0.12 | 0.22 |

Since the AAS results were not affected significantly either by the surface oxide film or by the microstructure, it was thus deduced that these AAS results provided much more accurate overall average composition values.

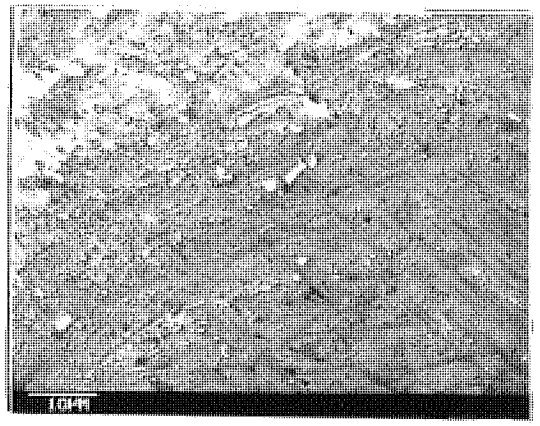

a

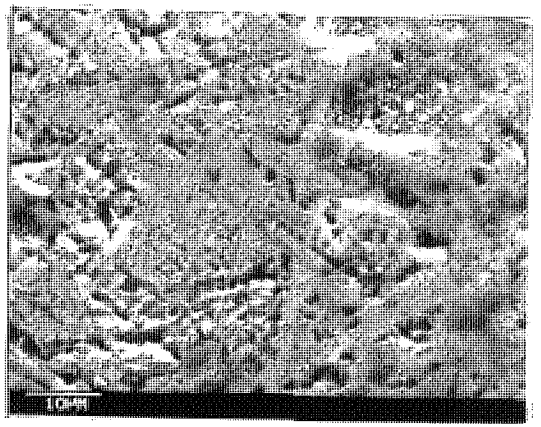

b

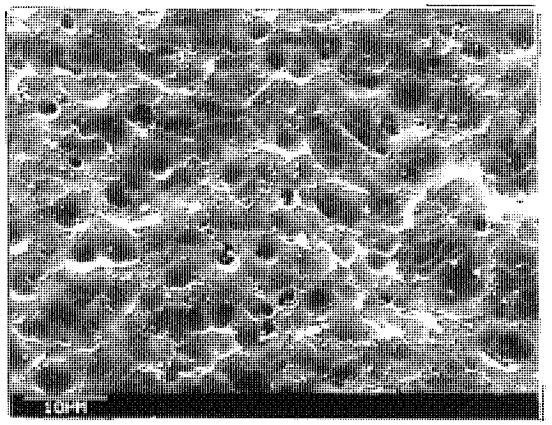

c

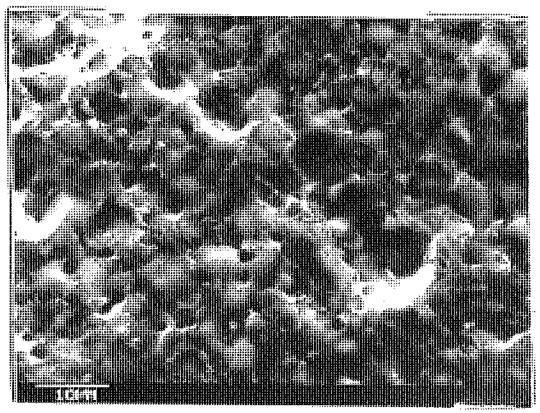

d

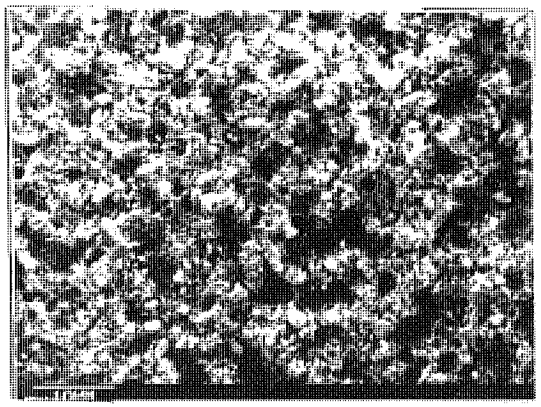

e

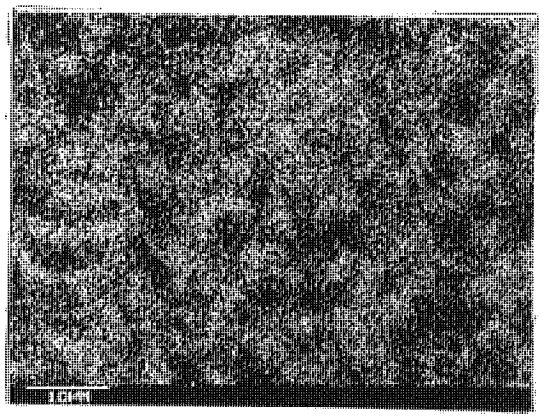

f

Plate 3 Effect of the Dow pretreatment prior to cyanide copper plating, on AZ91CC.

a) not pretreated.
b) After Minco cleaner.
c) After chromic acid pickle.
d) After ferric nitrate activation.
e) After immersion zinc deposition.
f) X-ray map showing distribution of zinc in 3e.

Magnesium dissolved into the zinc-pyrophosphate solution and zinc was deposited in situ. As shown in Plate 3e, more pits formed, indicating the dissolution of magnesium ions in the bath. The immersion zinc coating was porous and the distribution of zinc on the surface is shown by the X-ray map in Plate 3f which was taken with the aid of the energy dispersion X-ray micro-analysis attachment. These photographs also show a marked increase in surface roughness at each stage of the pretreatment.

### 3.4.1 EFFECT OF THE VARIATION OF THE CLEANING AND ACTIVATION STAGES IN THE STANDARD DOW PRETREATMENT

The surface response of AZ91 alloy cold chamber panel die castings in each modification of the cleaning and activating stages was revealed by S.E.M. and is shown in Plates 4 and 5.

The 1% oxalic acid pickling had a very different effect from the Dow pickle. Compounds formed on the surface of the magnesium alloy during the oxalic acid dip were washed off at the rinsing stage. As can be seen on Plate 4a, the oxalic acid seemed to have preferentially attacked the magnesium-rich phases, leaving the aluminium-rich phases in relief. The two phases were detected with the aid of the X-ray micro-analysis attachment.

On preliminary inspection, Plate 4b offers little information about the effect of Kelco cleaning, but on closer examination it revealed a greater concentration of aluminium-rich particles. When the alloy was dipped in ammonium bifluoride + phosphoric acid for 2 minutes, the surface characteristics changed completely (see Plate 4c). The activated surface indicated that all the aluminium-rich phases had now dissolved, leaving the surface uniform and featureless.

The zinc coating deposited with this sequence was again porous (Plate 4d). Pit formation is clearly indicated together with the distribution of zinc deposits.

In the second modification, 2% HF was used as the activating solution instead of ammonium hydrogen fluoride ($NH_4HF_2$) and phosphoric acid solution. Plate 5 shows the same alloy (AZ91) when activated by 2% HF, which resulted in irregular patches, indicating a preferential attack on parts of the surface. In contrast, activation by $NH_4HF_2$ solution demonstrated a more even reaction on the surface (see Plate 4c).

The presence of HF was common to both modifications of the Dow pretreatment sequence. The purpose of the second modification was to investigate the role HF played in this part of the pretreatment. It was found that it did remove

the oxide film very rapidly; the attack was almost instantaneous once the sample was immersed in the solution. However, the rate of attack slowed down appreciably after a few seconds, suggesting the formation of a passivating film.

In order to clarify the sequences adopted, the flow charts for the first and second modifications of the Dow process are shown in Figs. 11 and 12 respectively.

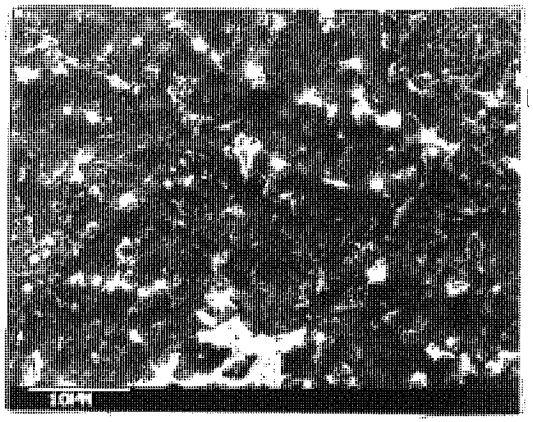

a

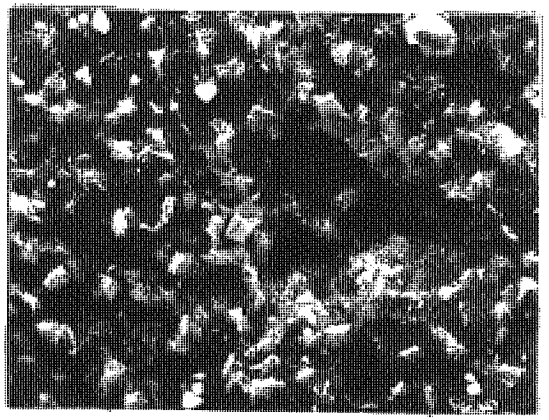

b

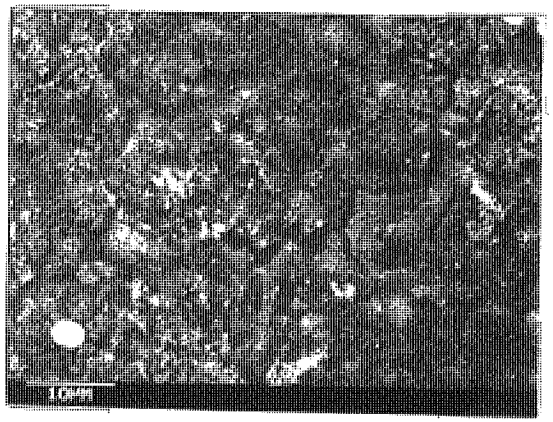

c

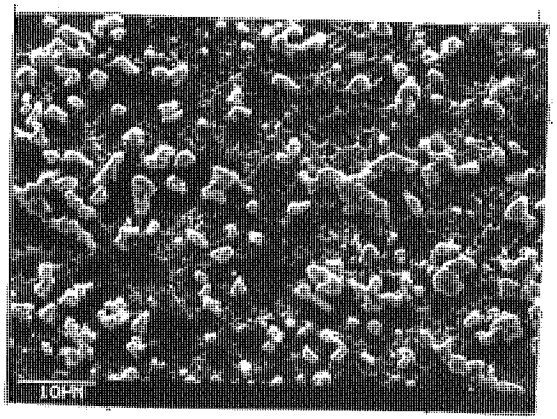

d

Plate 4 Surface response of alloy AZ91CC to the first modification of the Dow pretreatment.

a) After oxalic acid.
b) After Kelco cleaner.
c) After ammonium bifluoride activated
d) After immersion zinc deposition.

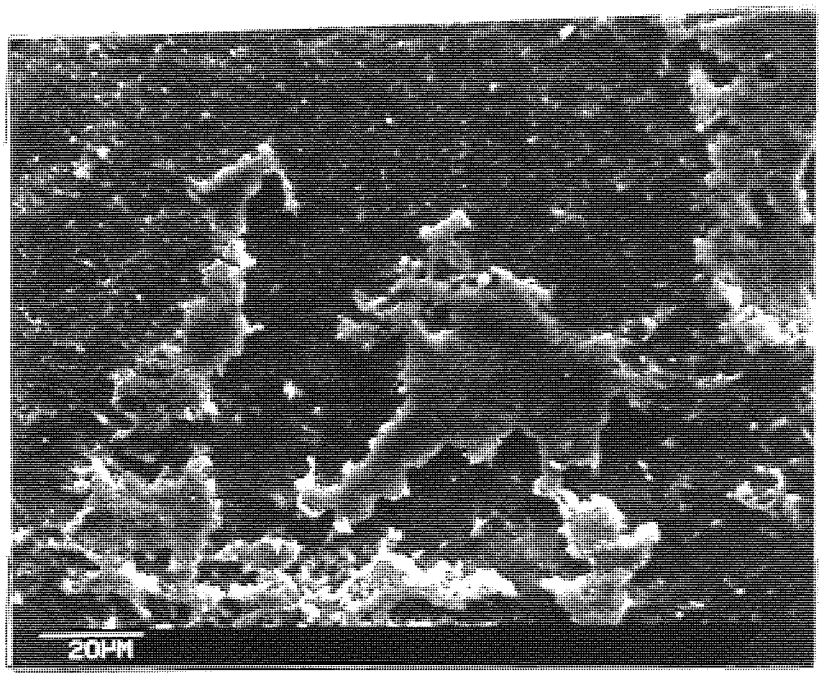


Plate 5 Surface response of alloy AZ91CC to the 2% HF solution, used in the second modification of the Dow pretreatment.

## 3.5 EFFECT OF THE STANDARD NORSK HYDRO PRETREATMENT PRIOR TO FINAL COPPER PLATING

The surface response of AZ91 alloy cold chamber die casting panel in each pretreatment stage was revealed by S.E.M. (see Plate 6).

In each pretreatment stage, the alloy surface behaved rather differently compared with the standard Dow pretreatment. The 1% oxalic acid pickling had a very different effect from the Dow pickle (Plate 6a). In order to highlight the contours in the sample surface, the same sample was tilted at $45^{o}$ (Plate 6d). When the alloy was dipped for only one minute in a warm solution of potassium pyrophosphate, further etching occurred, with crack lines clearly visible in Plates 6b and 6e. Some angular-shaped aluminium-rich particles were exposed and detected by the X-ray micro-analysis attachment.

As would be expected Plate 6c shows that the amount of zinc deposited onto the alloy surface after a 3-minute zinc immersion process was less than that in Dow pretreatment sequences in which an 8-10 minute zinc immersion was said to be necessary. The shapes of the zinc deposits resulting from the two pretreatment sequences seemed to be different as well. In the Dow pretreatment, the distribution of zinc

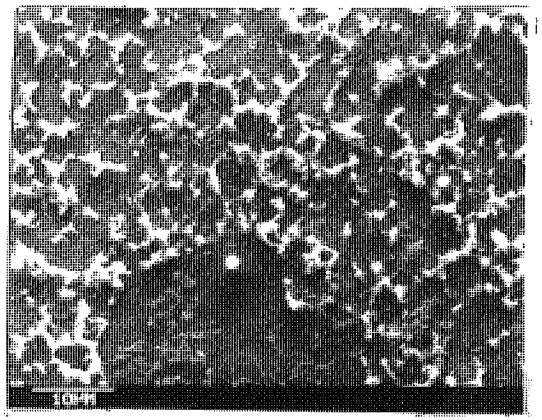

a

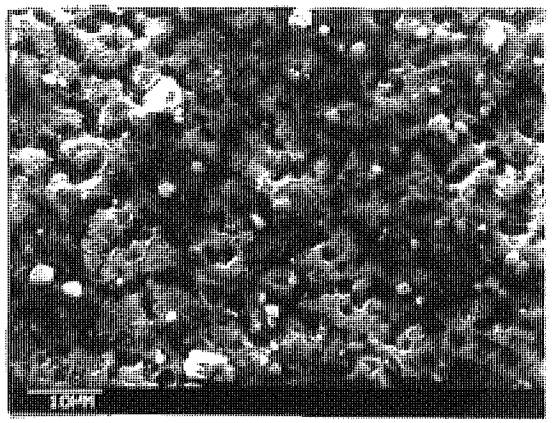

b

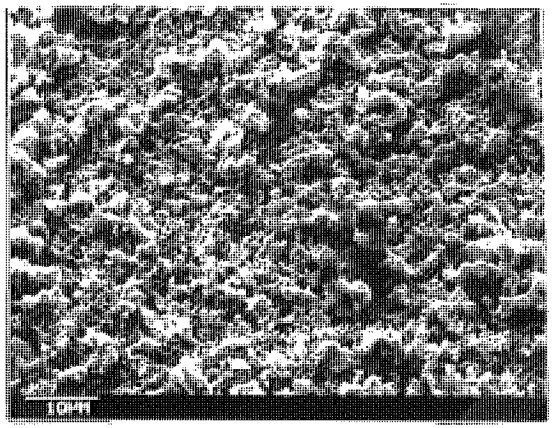

c

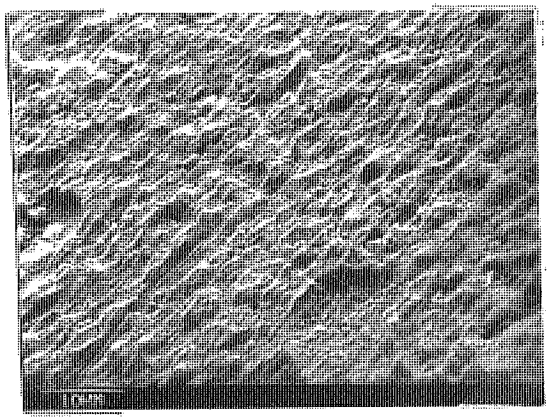

d

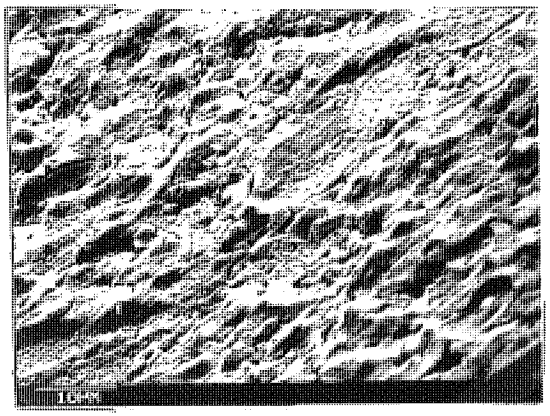

e

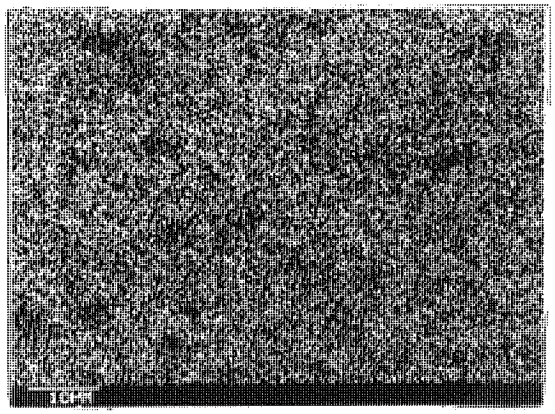

f

Plate 6 Effect of the Norsk Hydro pretreatment prior to cyanide copper plating, on AZ91CC.

a) After oxalic acid etch.

b) After pyrophosphate activation.

c) After immersion zinc deposition.

d) After oxalic acid etch, sample tilted at 45° in SEM.

e) After pyrophosphate activation, sample tilted at 45° in SEM.

f) X-ray map showing distribution of zinc in 6c.

was visually fairly even, whereas in the Norsk Hydro method, the zinc was fine and distributed irregularly in small patches over the surface. Apart from the difference in immersion time, the temperature for zincating was comparatively low, 60–65 °C, in the Norsk Hydro process.

### 3.5.1 EFFECT OF THE VARIATION OF THE SECONDARY ACTIVATION STEP IN THE STANDARD NORSK HYDRO PRETREATMENT

A higher concentration (210 g/l) of $K_4P_2O_7$ at a temperature of 75 °C was employed as the secondary activation step of the Norsk Hydro pretreatment. Also, the zincation stage was operated at a higher temperature in this variation.

The activated AZ91 cold chamber alloy die cast panel surface shown in Plate 7d seemed to be similar to surfaces activated at a lower temperature and concentration as in the standard Norsk Hydro sequence. Further etching occurred together with cavity formation.

After pyrophosphate activation, the alloy was dipped into the zincate solution for 4 min. at 75 °C. The micrograph in Plate 8a shows that a finely divided and massive layer of zinc was deposited on the surface of AZ91CC. The

distribution of zinc deposits is shown in Plate 8d with the aid of the X-ray micro analysis attachment.

### 3.5.2 COMPARISON OF ALLOY SAMPLES BY S.E.M.

This section deals with the comparison of three alloy samples by S.E.M. with respect to the Norsk Hydro pretreatment sequence but operated at a higher temperature in both activation and zincation stages (75 °C).

The three alloy samples were AZ91 cold chamber die cast panels, AZ61 cold chamber die cast panels and AZ91 hot chamber die cast loudspeaker parts. The samples were polished and degreased, but none of the three alloy surfaces was smooth, especially the AZ91 hot chamber ones. Cracks were present together with pits.

Micrographs 7a, b and c showed the surface response to the 1% oxalic acid dip. The AZ91 and AZ61 cold chamber panels (7a and 7b respectively) showed similar surface characteristics. The surface relief was rugged. The magnesium-rich phases were clearly seen but the phases in the hot chamber samples were more dispersed and consequently could not be captured in micrograph 7c.

Referring to micrographs (d), (e) and (f) of Plate 7, it can be seen that AZ91 and AZ61 cold chamber panels exhibited similar surface response. All the alloys having gone through pyrophosphate activation at 75 °C, the cold chamber panel plates 7d and 7e showed surface cavities indicating that further etching occurred. However the AZ91 hot chamber part, micrograph 7f, displayed particles of aluminium scattered on a finely pitted surface.

After pyrophosphate activation, the alloys were dipped into the zincate solution for 4 min. at 75 °C. The micrographs in Plate 8a, b and c showed that a finely divided and massive layer of zinc was deposited on the surface of each of the three alloys. In order to reveal the distribution of zinc deposits, the X-ray micro analysis attachment was used. The corresponding X-ray map of zinc is shown in Plates 8d, e and f.

It seemed that the zinc deposits did cover most of the alloy surfaces, but the distribution was again uneven. There are areas with much thicker zinc deposits than others. Preferential growth of zinc on the alloy surfaces was therefore believed to have taken place during the zincate process.

Both cold chamber and hot chamber castings indicated severely etched surfaces after the zincate process,

especially where the zinc deposits were thin. (see micrographs a, b and c of Plate 8).

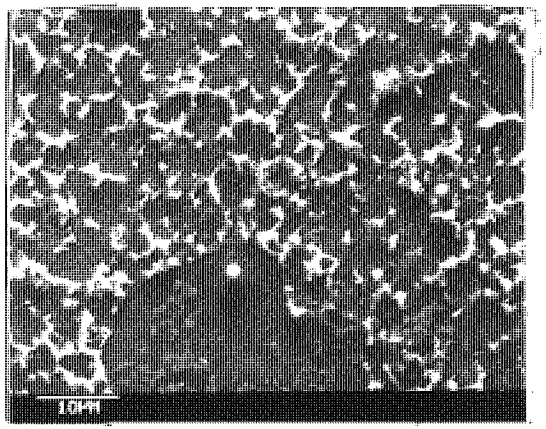

a

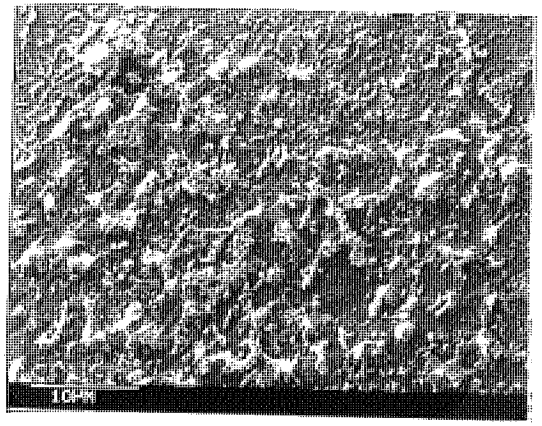

b

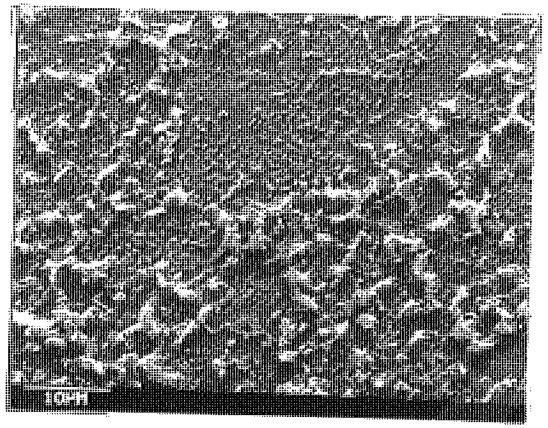

c

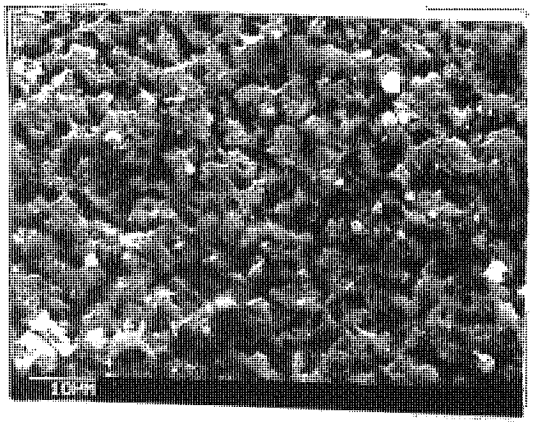

d

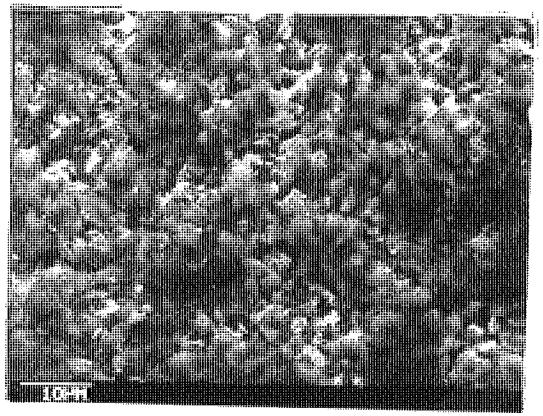

e

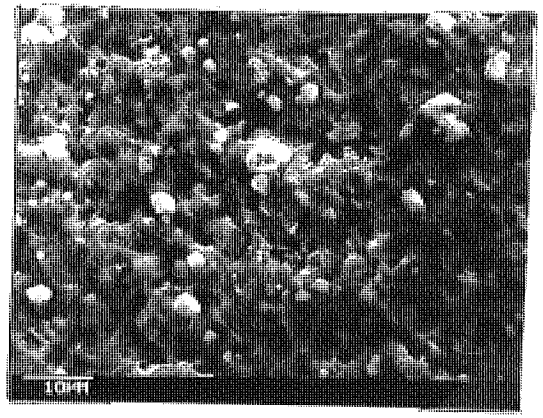

f

Plate 7 Alloys (AZ91CC, AZ61CC & AZ91HC) when pretreated using Norsk Hydro sequence operated at a higher temperature and concentration in the secondary activation stage.

a) AZ91CC after oxalic acid activation.
b) AZ61CC after oxalic acid activation.
c) AZ91HC after oxalic acid activation.
d) AZ91CC after secondary activation.
e) AZ61CC after secondary activation.
f) AZ91HC after secondary activation.

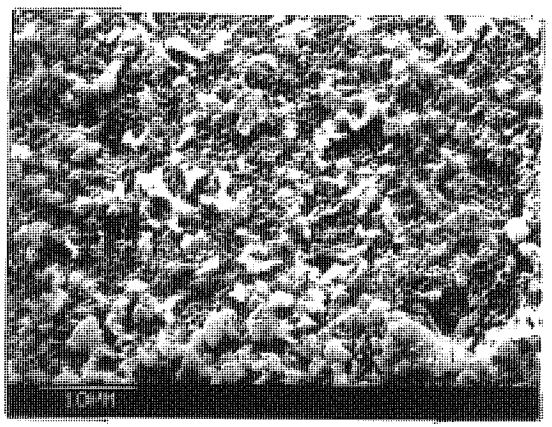

a

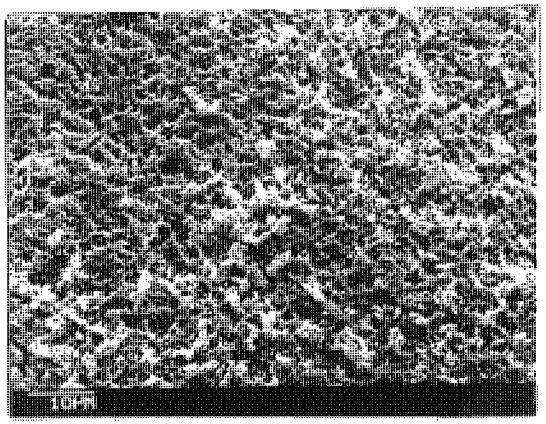

b

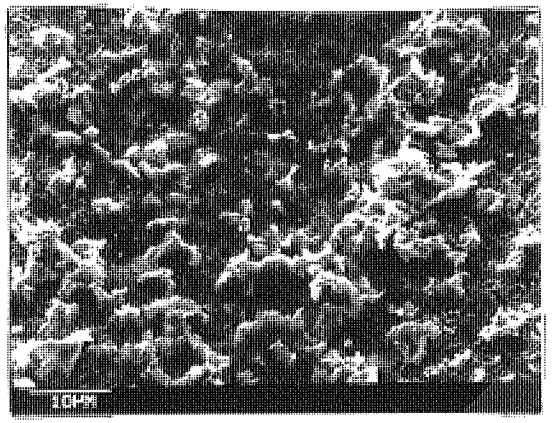

c

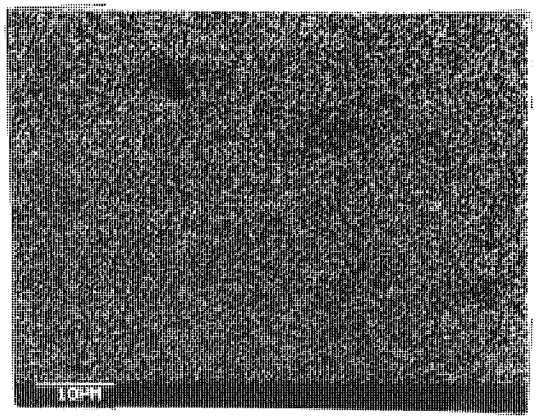

d

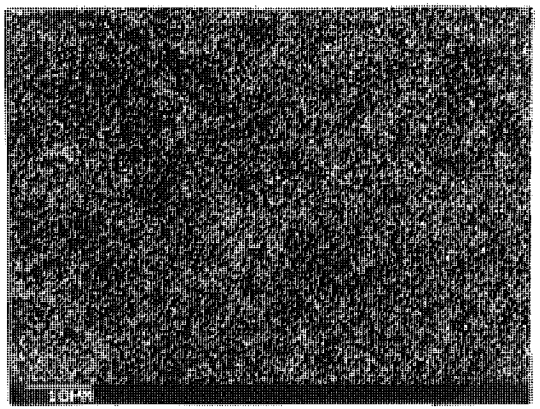

e

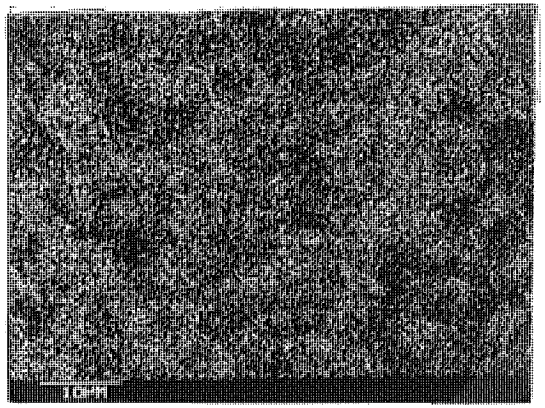

f

Plate 8 Alloys (AZ91CC, AZ61CC & AZ91HC) when pretreated using Norsk Hydro sequence operated at a higher temperature and concentration in the secondary activation step.

a) AZ91CC after immersion zinc deposition.
b) AZ61CC after immersion zinc deposition.
c) AZ91HC after immersion zinc deposition.
d) X-ray map showing distribution of zinc in 8a.
e) X-ray map showing distribution of zinc in 8b.
f) X-ray map showing distribution of zinc in 8c.

## 3.6 EFFECT OF THE CANNING PRETREATMENT PRIOR TO FINAL COPPER PLATING

In the pretreatment sequence termed the 'Canning process', different chemical agents were employed in the secondary activation step compared with the Norsk Hydro pretreatment sequence. The activation solution is one of the solutions recommended by DeLong[61] and is said to be suitable where the work surface is free of chromate film. The flow chart of the Canning sequence is shown in Fig. 13.

After rinsing off the loosely attached compounds which formed on the surface of AZ91 alloy cold chamber casting panel resulting from the 1% oxalic acid dip, the work was transferred to the warm solution of sodium borax with sodium pyrophosphate and sodium fluoride, under the conditions previously described. The alloy surface was brightened visually after the 2-minute immersion in this solution. Dissolution of magnesium ions was indicated by pit formation (see Plate 9a). The etching effect at this stage was clearly milder than the corresponding stage in the standard Norsk Hydro process, even though the temperature employed was higher at 75 °C as compared with 65 °C in the standard Norsk Hydro process. Again, in order to highlight the surface roughness at this stage, the sample was tilted at 45 °C (shown in Plate 9c).

Visually, a uniform zinc coating was deposited on the sample surface after the zinc immersion step as described in the Norsk Hydro sequence. Micrographs 9b and the X-ray map of zinc 9d revealed that the zinc deposits were spread finely over the surface despite the presence of cathodic, aluminium-rich regions after the earlier pretreatment stages.

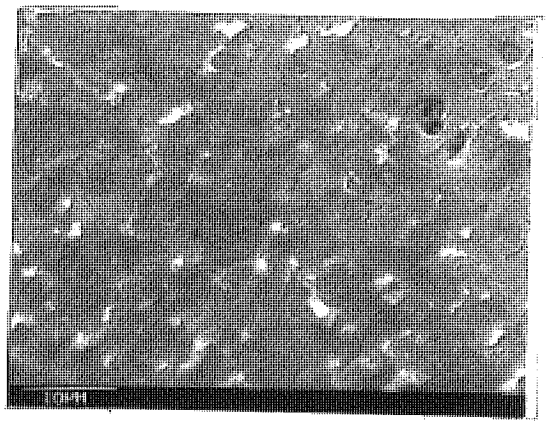

a

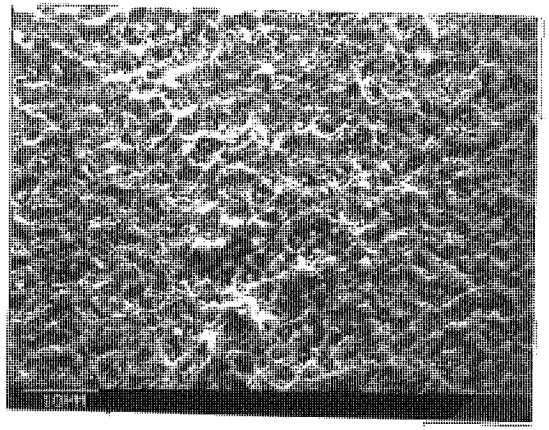

b

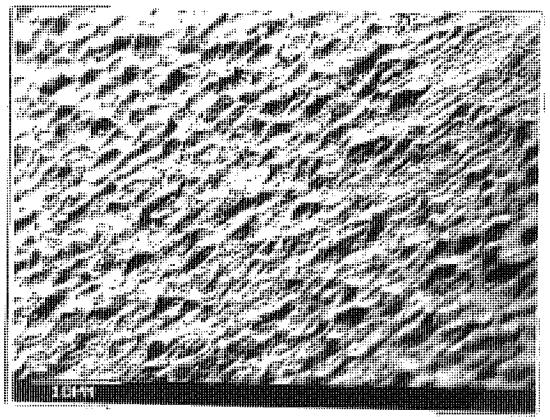

c

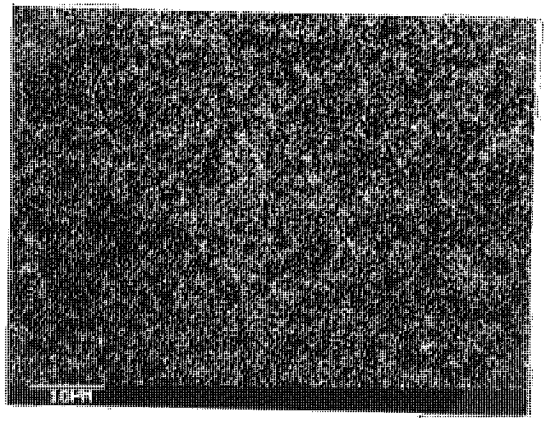

d

Plate 9 Effect of the Canning pretreatment prior to copper plating, on AZ91CC.

a) After pyrophosphate/fluoride second stage solution.

b) After immersion zinc deposition.

c) After pyrophosphate/fluoride second stage solution, sample tilted at $45^{o}$ in SEM.

d) X-ray map showing distribution of zinc in 9b.

## 3.7 POTENTIAL MEASUREMENTS

The changes in potential with time during each pretreatment stage in the Norsk Hydro sequence and the Canning sequence were monitored. The potential-time curves for each pretreatment step for different alloys were then compared with the appropriate details of surface response discussed previously.

### 3.7.1 POTENTIAL MEASUREMENTS OF THE OXALIC ACID ACTIVATION STEP

Oxalic acid activation is common to both the Norsk Hydro and Canning sequences. Fig. 14 indicates the potential-time curves recorded for the three alloy samples AZ91 cold chamber casting panels, AZ61 cold chamber casting panels and AZ91 hot chamber castings during the oxalic acid activation stage. Three virtually identical curves were obtained on the alloy samples, indicating that the alloys behaved similarly to one another.

The initial potential value shown in Fig. 14 is -1.7 V and the potential rises gradually in a shallow parabolic manner, moving to a more noble value. (Since the rise in potential indicates a decrease in activity or an increase in nobility,

the reactivity therefore seemed to be decreasing with time.) Layers of compounds were evidently building up on the surfaces of the samples during the acid dip. When the dissolution or removal of the surface layers of compound is slower than the diffusion of the acid onto the magnesium alloy surface, the rate of attack will decrease as the thickness of the compound layer increases. By using the strip and re-weigh technique, the rate of attack during the 1% oxalic acid immersion for alloy AZ61CC was recorded (see Fig. 15).

The compound formed on the surface of the magnesium is likely to be magnesium oxalate, since

$$Mg + C_2H_2O_4 \longrightarrow MgC_2O_4 + H_2 .$$

Magnesium oxalate is relatively insoluble in water. The solubility is about 0.7 g/l at 16 °C, according to the C.R.C. Handbook (108). In order to ascertain the compound formed on the surface of magnesium alloy samples during the acid immersion, the compound was taken for X-ray diffraction examination.

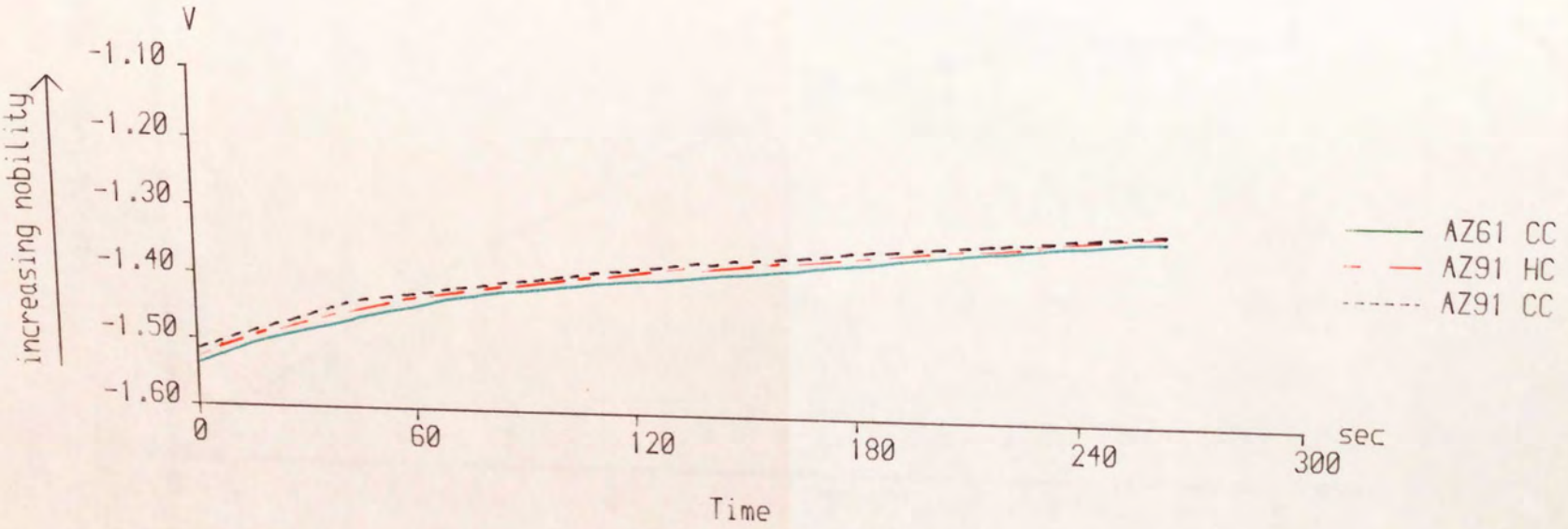


Fig.14 Potential-time curves recorded for three alloy samples during the oxalic acid activation.

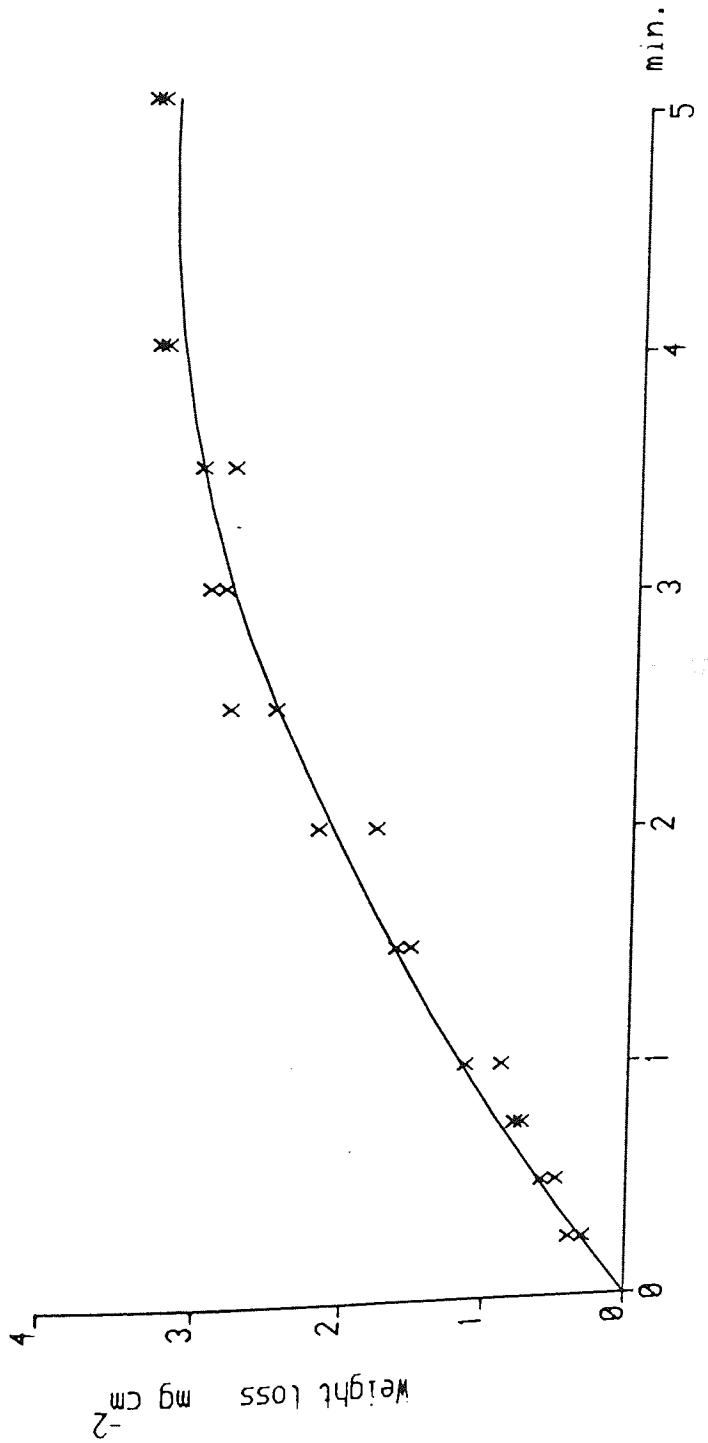


Fig.15 Rate of attack during 1% oxalic acid immersion for alloy AZ61CC.

### 3.7.1.1 X-RAY DIFFRACTION EXAMINATION

The surface compound formed on the surface of the magnesium alloy during the 1% oxalic acid dip was expected to be magnesium oxalate as previously mentioned. In order to test the above assumption, a piece of magnesium alloy was immersed into a 1% oxalic acid for about 2 hours. When the surface compound layer formed during the immersion had grown to a moderate thickness, the magnesium sample was dried. The compound formed on the surface was then scratched off for X-ray diffraction examination. The result is shown in Table 6 and Fig. 16.

### 3.7.2 POTENTIAL MEASUREMENT DURING THE SECOND STAGE ACTIVATION OF THE STANDARD NORSK HYDRO SEQUENCE

A characteristic curve was obtained when any of the samples of AZ61CC, AZ91CC and AZ91HC was immersed into the secondary solution of the Norsk hydro sequence. The solution is composed of 65 g/l potassium pyrophosphate, with about 15 g of sodium carbonate added in order to adjust the pH to about 11. The results are shown in Fig. 17 for sample AZ61CC. The initial rapid fall in potential, region A-B, indicates the removal of the surface film, leaving the surface in a much more active condition (-1.7 V). From B to C, the potential rises shallowly but remains at a fairly base

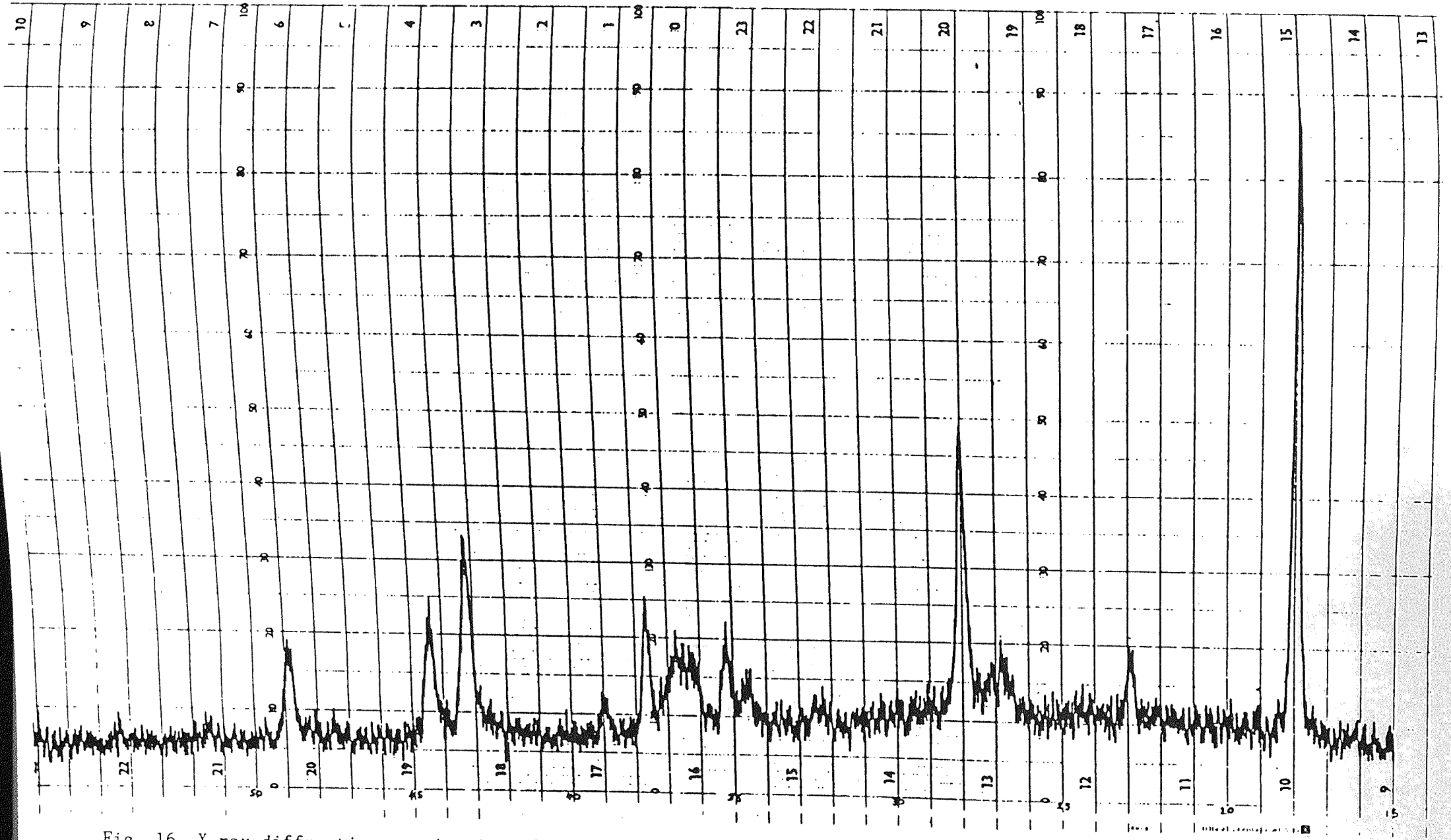

Fig. 16 X-ray diffraction examination of surface film formed on magnesium during 1% oxalic acid dip.

Table 6 X-RAY DIFFRACTION EXAMINATION CORRESPONDING TO FIG.16.

| $2\theta$ | I | d | $\beta C_2MgO_4.2H_2O$ | (AlMg) - $\beta$ | Mg |
|---|---|---|---|---|---|
| 18.0 | 90 | 4.92 | 4.89 | | |
| 28.1 | 50 | 3.17 | 3.17 | | |
| 32.4 | 5 | 2.76 | | 2.76 | |
| 34.5 | 15 | 2.60 | | | 2.61 |
| 35.3 | 20 | 2.54 | | | |
| 36.3 | 20 | 2.49 | | 2.5 | |
| 36.7 | 20 | 2.45 | | 2.46 | |
| 37.7 | 25 | 2.38 | 2.38 | | |
| 39.0 | 10 | 2.31 | | 2.33 | |
| 43.3 | 35 | 2.09 | 2.09 | | |
| 44.4 | 25 | 2.02 | 2.04 | | |
| 48.8 | 20 | 1.83 | 1.86 | | |

$$d = \frac{\lambda}{2 \sin \theta} \qquad \lambda = 1.5406$$

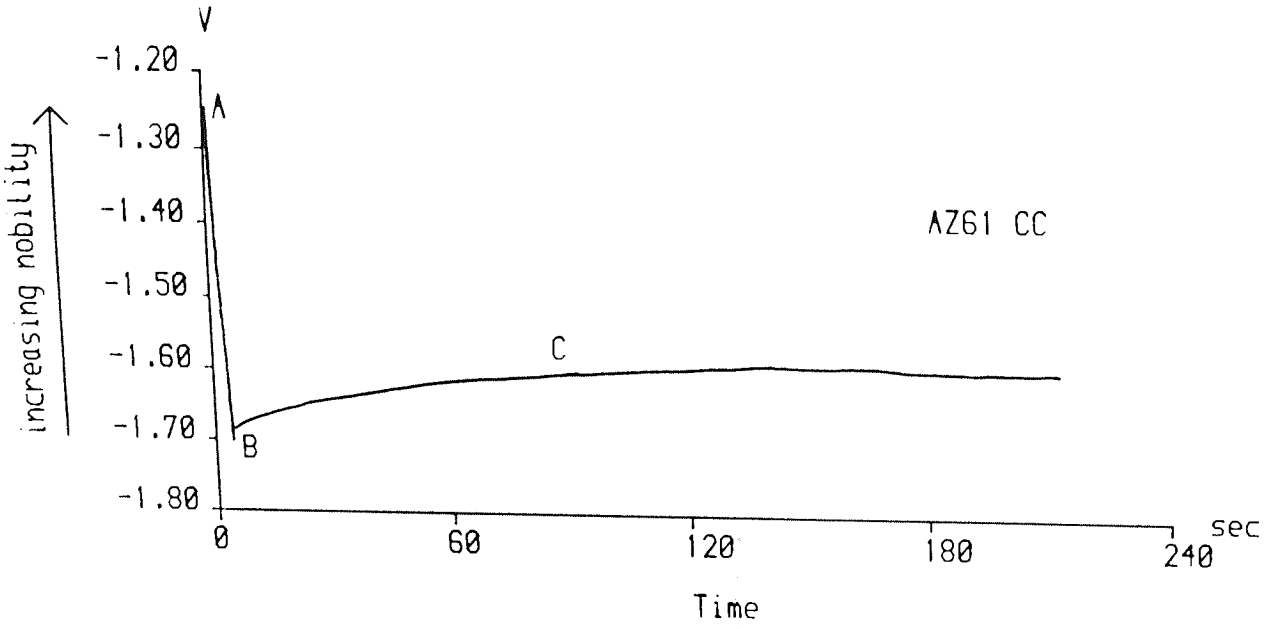


Fig.17 Potential-time curve recorded for alloy AZ61CC during the standard Norsk Hydro secondary activation.

value. Magnesium hydroxide is very likely to form at pH > 10. However, at the same time, pyrophosphate forms soluble complexes with the hydroxide film and this is likely to be the reason for the potential remaining at such a base value.

### 3.7.3 POTENTIAL MEASUREMENTS DURING THE SECOND STAGE ACTIVATION OF THE CANNING SEQUENCE

Fig. 18 shows the potential-time curves recorded for the three alloy samples during the secondary activation step after rinsing from the oxalic acid dip. The activation solution was composed of 40 g/l of sodium borax, 70 g/l of sodium pyrophosphate and 20 g/l of sodium fluoride. Again, three virtually identical curves were obtained on the alloy samples, indicating that the alloys behaved similarly to one another. First there was a slight increase in the positive direction indicating an enobling effect, then a change in the opposite direction occurred suggesting the removal of the protective film. After about 20 seconds, a constant potential was attained. In order to ascertain the role of each reagent in the activation solution, potential-time curves were recorded for each of the reagents when added successively to the solution.

Sample AZ61CC was transferred to a solution of 70 g/l of sodium borax after the rinsing from the oxalic acid dip. As

shown in Fig. 19 an immediate fall in potential value suggested that the alloy surface was being cleaned of its oxide and/or surface contaminants that were picked up during the previous treatment step. Subsequently, the shallow rise in potential indicated that a layer of magnesium hydroxide was being built up. Sodium borax with its pH ranging from 10.5 to 11.5 seemed to be working as a buffer.

When 40 g/l of sodium pyrophosphate was added into the solution and a freshly rinsed AZ61CC sample immersed in it a similar potential-time curve was obtained (but at a lower value than in the case above). Addition of pyrophosphate ion has certainly made the surface of the sample more active by forming soluble complexes with the surface hydroxide film.

$$2\,Mg(OH)_2 + X\,P_2O_2^{4-} \longrightarrow (Mg_2(P_2O_7)_X)^{-2X}$$

A potential-time curve similar to that shown in Fig. 18 resulted when the final chemical ingredient, 20 g/l of sodium fluoride was added into the solution. It is apparent that the addition of fluoride ions caused passivation of the magnesium alloy surface since the potential time curve remained at a relatively noble value of -1.5 V. Formation of fluoride film is thought to be the cause of passivity.

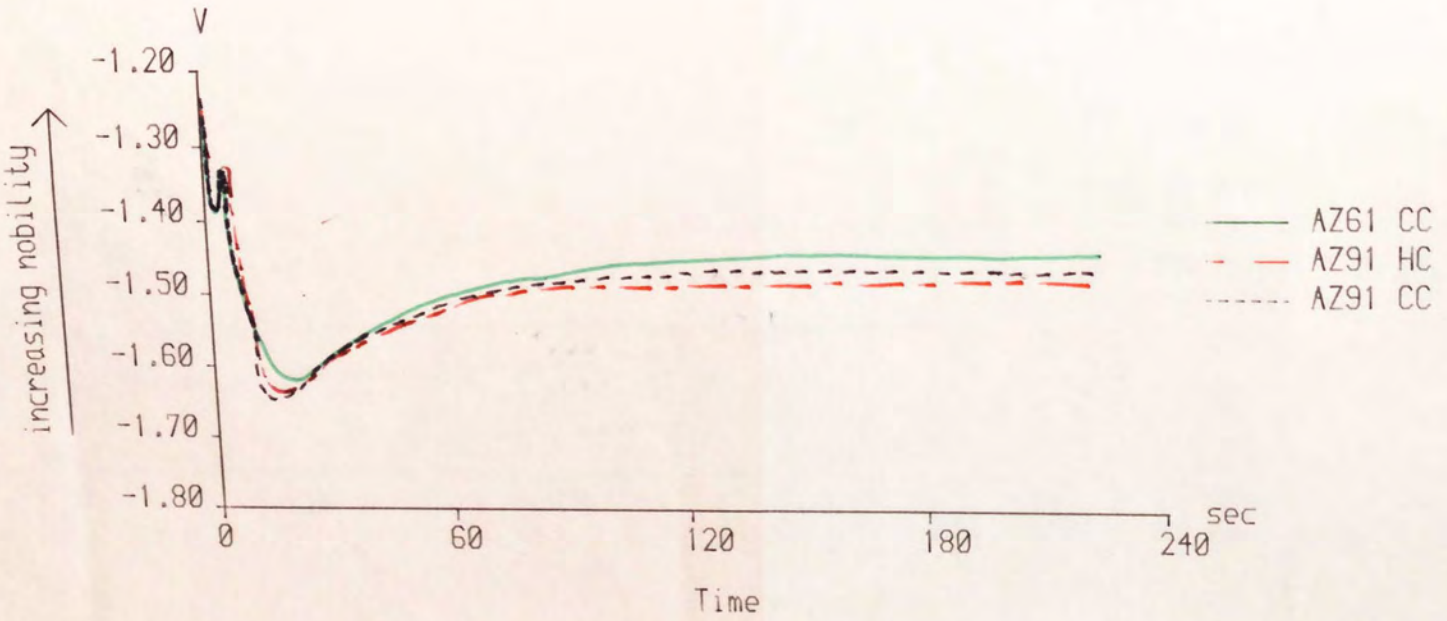


Fig.18 Potential-time curves recorded for three alloys during the Canning secondary activation.

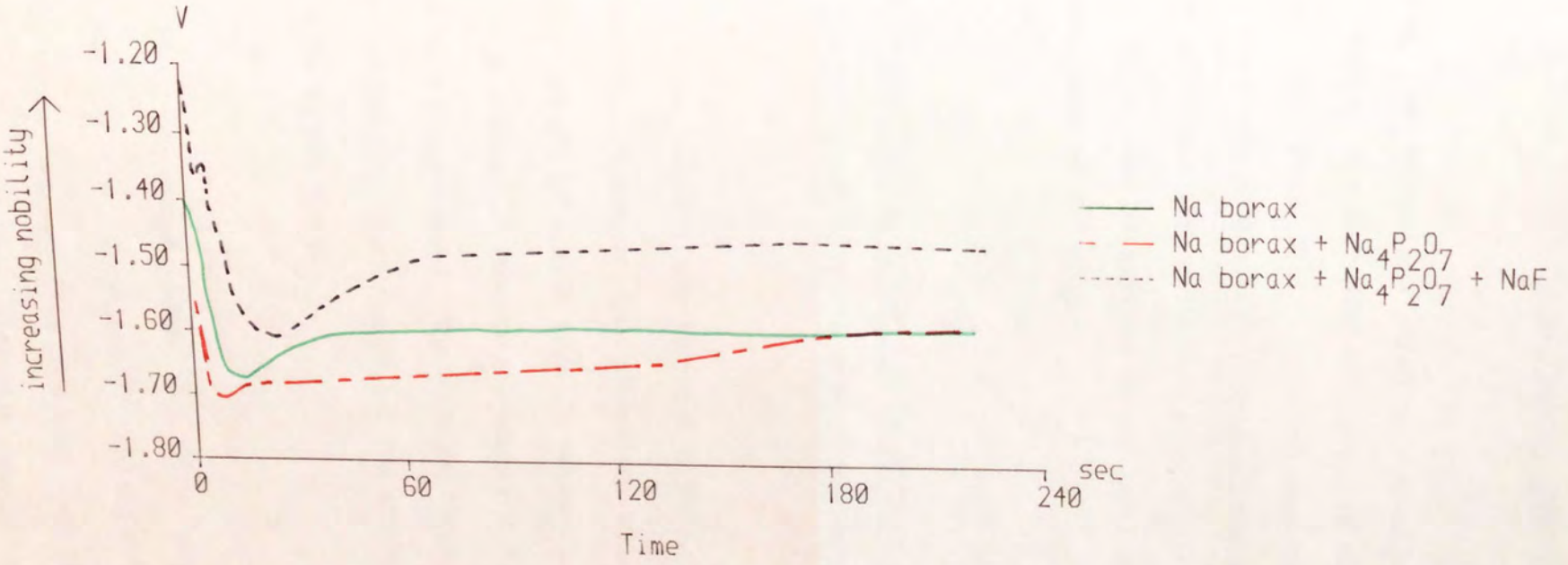


Fig.19 Potential-time curves recorded for alloy AZ61CC during 70 g/l sodium borax immersion, sodium borax + 40 g/l sodium pyrophosphate immersion and sodium borax + sodium pyrophosphate + 20 g/l sodium fluoride immersion.

### 3.7.3.1 RATE OF ATTACK DURING CANNING SECONDARY ACTIVATION

By using the strip and re-weigh technique, the rate of attack during the secondary activation of alloy AZ61CC was recorded (see Fig. 20). It can be seen that weight loss during the second activation stage is almost negligible compared with that lost during the oxalic acid dip. After 2 minutes there was no apparent weight loss, as shown by the horizontal part of the graph.

### 3.7.3.2 INVESTIGATION OF THE ROLE OF FLUORIDE IN THE SECOND STAGE SOLUTION OF THE CANNING SEQUENCE

Potential-time results are recorded in Figs. 21 and 22 for alloy AZ61CC, magnesium and aluminium in an electrolyte containing 20 g/l of sodium fluoride present in the Canning second stage solution. Results are quoted at two pH values, 5.5 and 11.0 respectively. The solution contained only the fluoride containing salt except for the addition of sodium carbonate to adjust the pH.

At the lower pH value (Fig. 21), aluminium passivated rapidly due to the formation of aluminium fluoride and aluminium oxide but at high pH a more base potential was attained since an aluminium oxide film cannot form.

In the case of magnesium, passivation occurred at both pH values but more rapidly at pH 11.0. As anticipated, the behaviour of the alloy was intermediate between the two individual metals.

### 3.7.4 POTENTIAL MEASUREMENTS DURING THE ZINCATE IMMERSION OF THE NORSK HYDRO SEQUENCE

Fig. 23 shows the potential-time curve recorded for the pretreated alloy AZ61CC during the zincate immersion. The initial part of the curve represents the sample surface being cleaned of its oxide film. After about 40 seconds a surface film had built up as indicated by the rise in potential value. The grey surface film betrayed the presence of magnesium hydroxide and/or zinc deposit. After about 1 minute, a fairly stable potential value of -1.3 V was attained. At this stage, the whole sample was thought to be covered with a surface film of zinc.

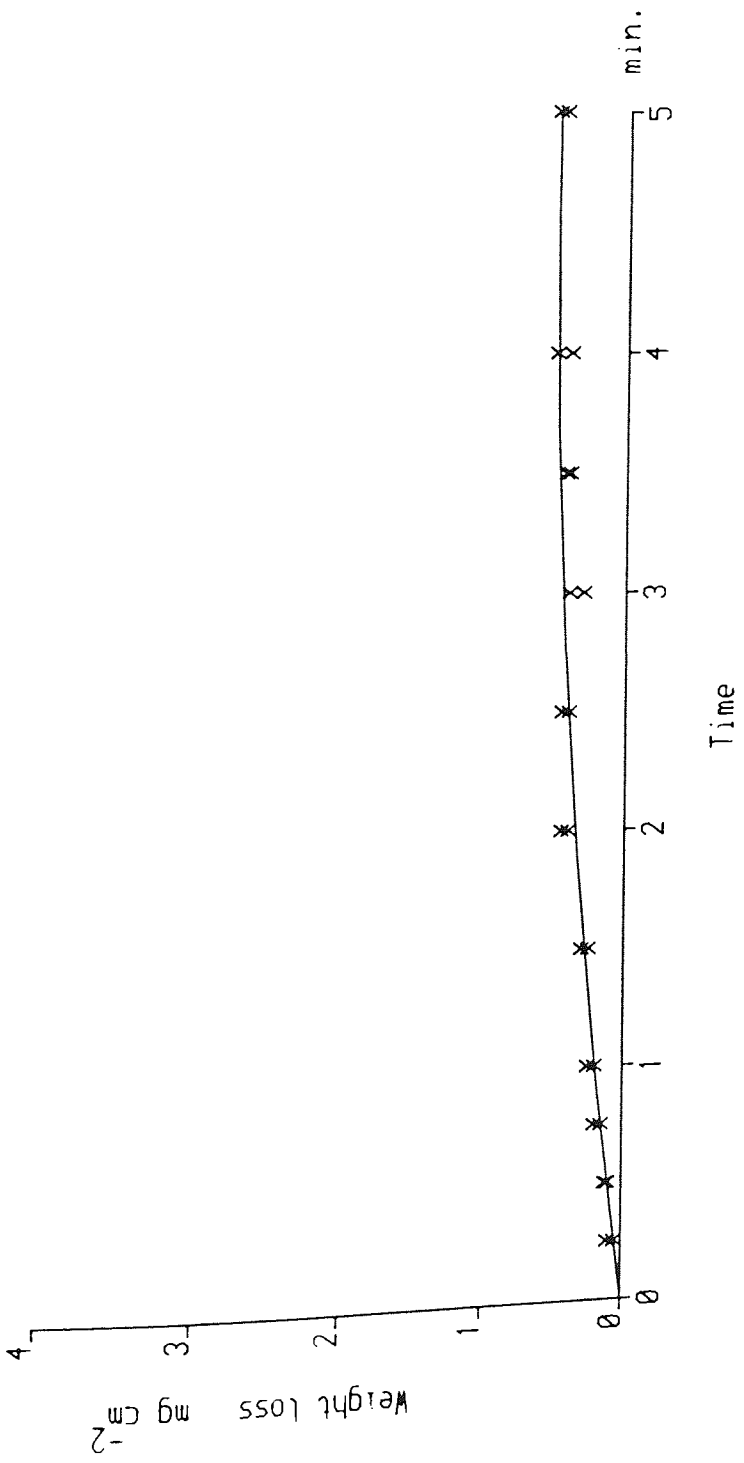


Fig.20 Rate of attack during Canning secondary activation.

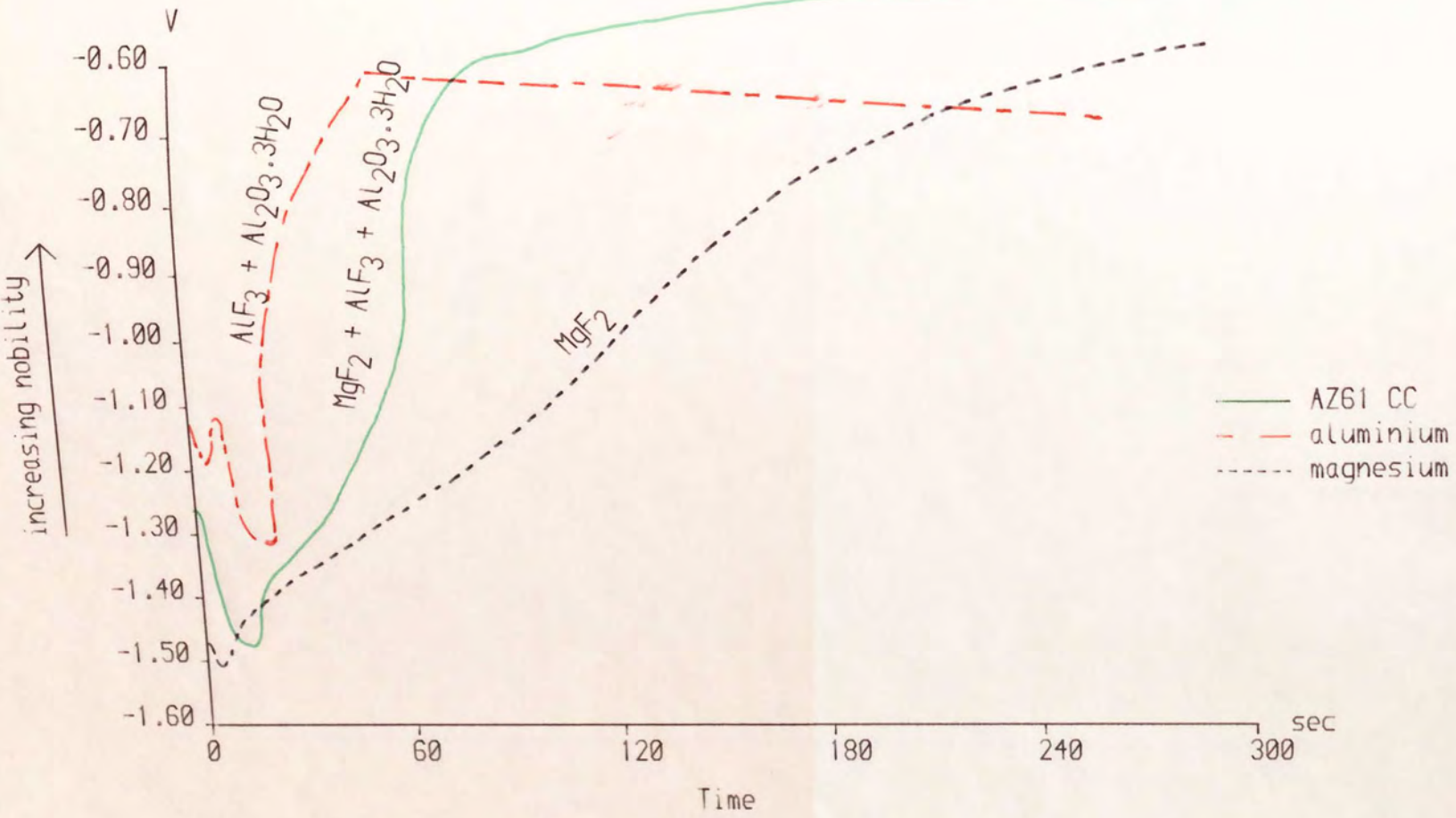


Fig.21 Potential-time curves recorded for magnesium, aluminium and alloy AZ61CC during 20 g/l sodium fluoride immersion at pH = 5.5.

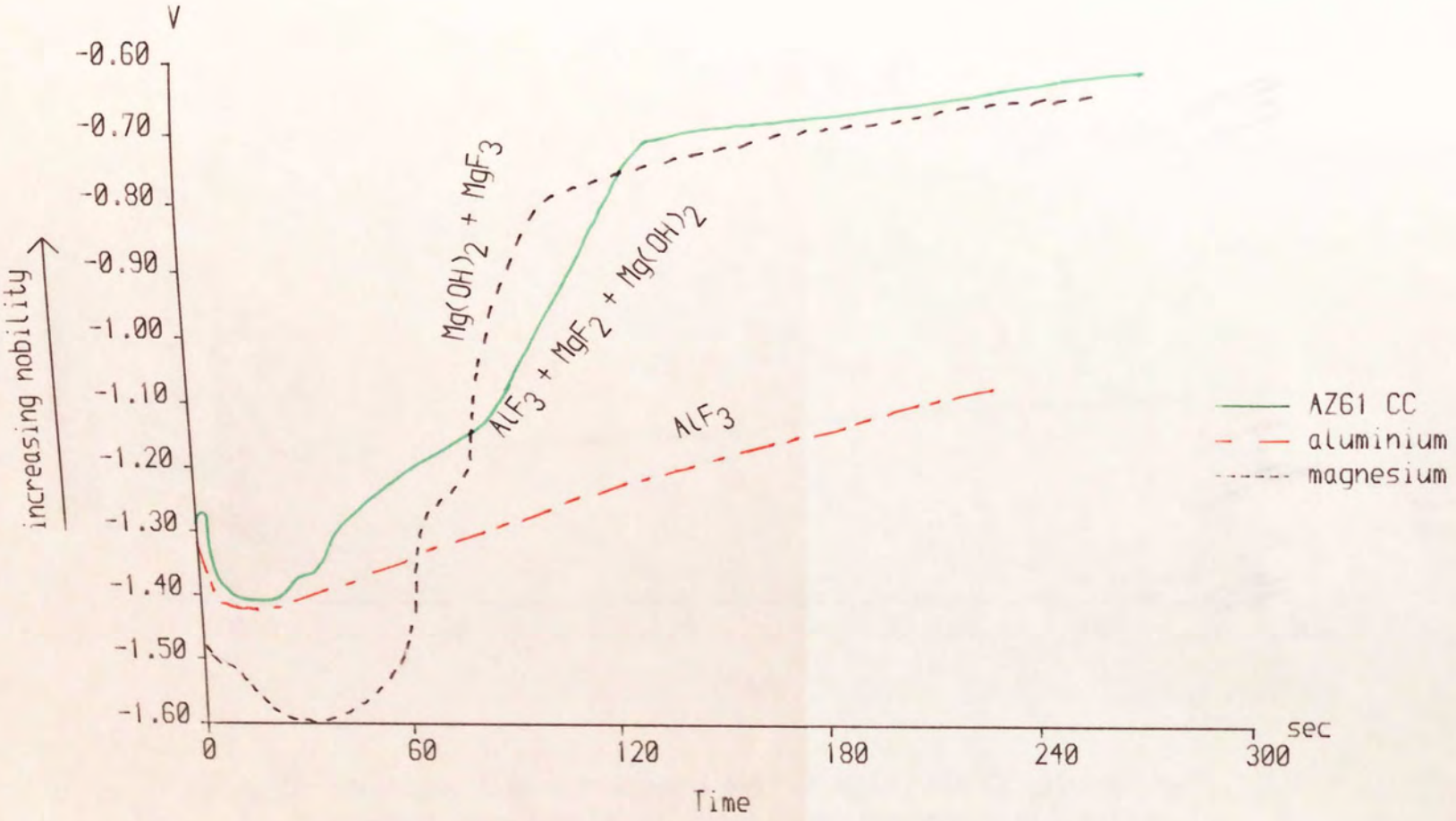


Fig.22 Potential-time curves recorded for magnesium, aluminium and alloy AZ61CC during 20 g/l sodium fluoride immersion at pH = 11.0.

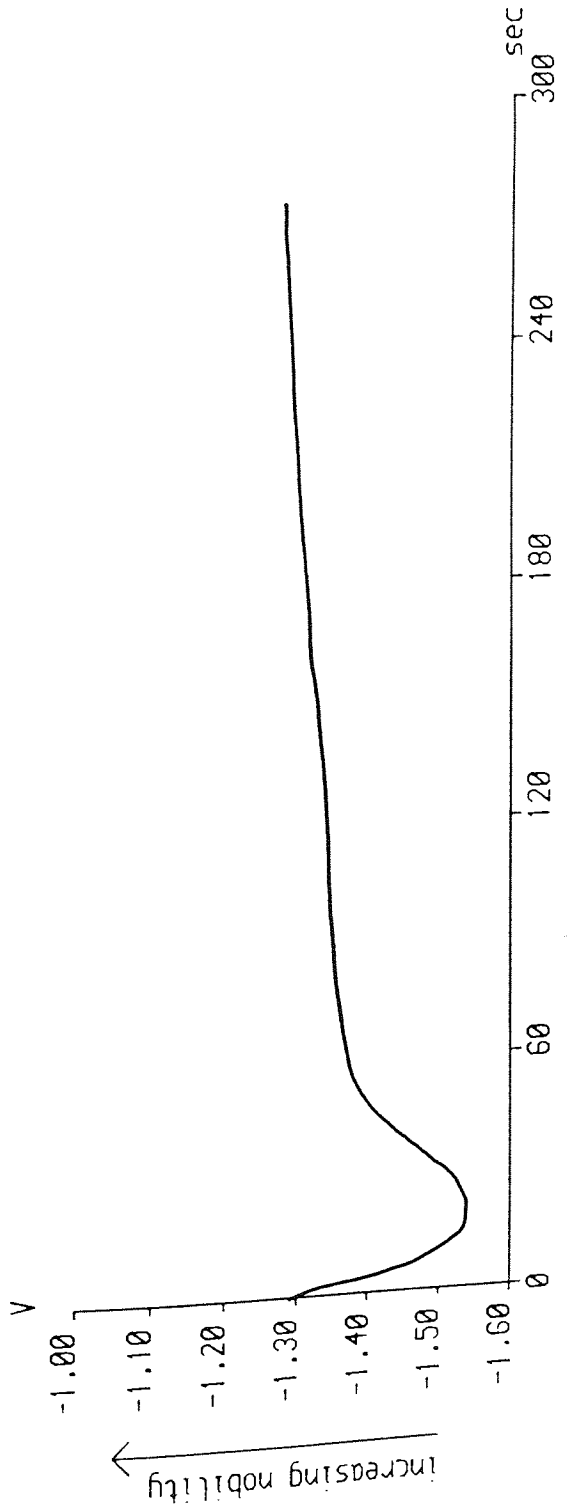


Fig.23 Potential-time curve recorded for alloy AZ61CC during the zincate immersion after Norsk Hydro secondary activation.

### 3.7.5 POTENTIAL MEASUREMENTS DURING THE ZINCATE IMMERSION OF THE CANNING SEQUENCE

The change in potential with time during the zincate immersion stage of the Canning sequence was monitored for the three alloys that were mentioned in 3.7.1. The solution formulation was 50 g/l zinc sulphate, 150 g/l potassium pyrophosphate, 3 g/l lithium fluoride and 5 g/l sodium carbonate. The pH of the solution was 10.30. Again, three virtually identical curves were obtained on the alloy samples indicating that the alloys behaved similarly to one another (Fig. 24). After 2-3 seconds of surface cleaning by the alkaline solution, a surface film started to build up which was likely to be the immersion zinc coating. A sudden change in potential occurred after about 60 seconds. Then it finally became constant, at which stage it was thought that the surface was completely covered by a coherent film of zinc.

In order to investigate the mechanism of surface film formation during zincate immersion, the potential time curves were studied in conjunction with scanning electromicrographs, taken after specific immersion times, denoted by A, B and C on Fig. 24.

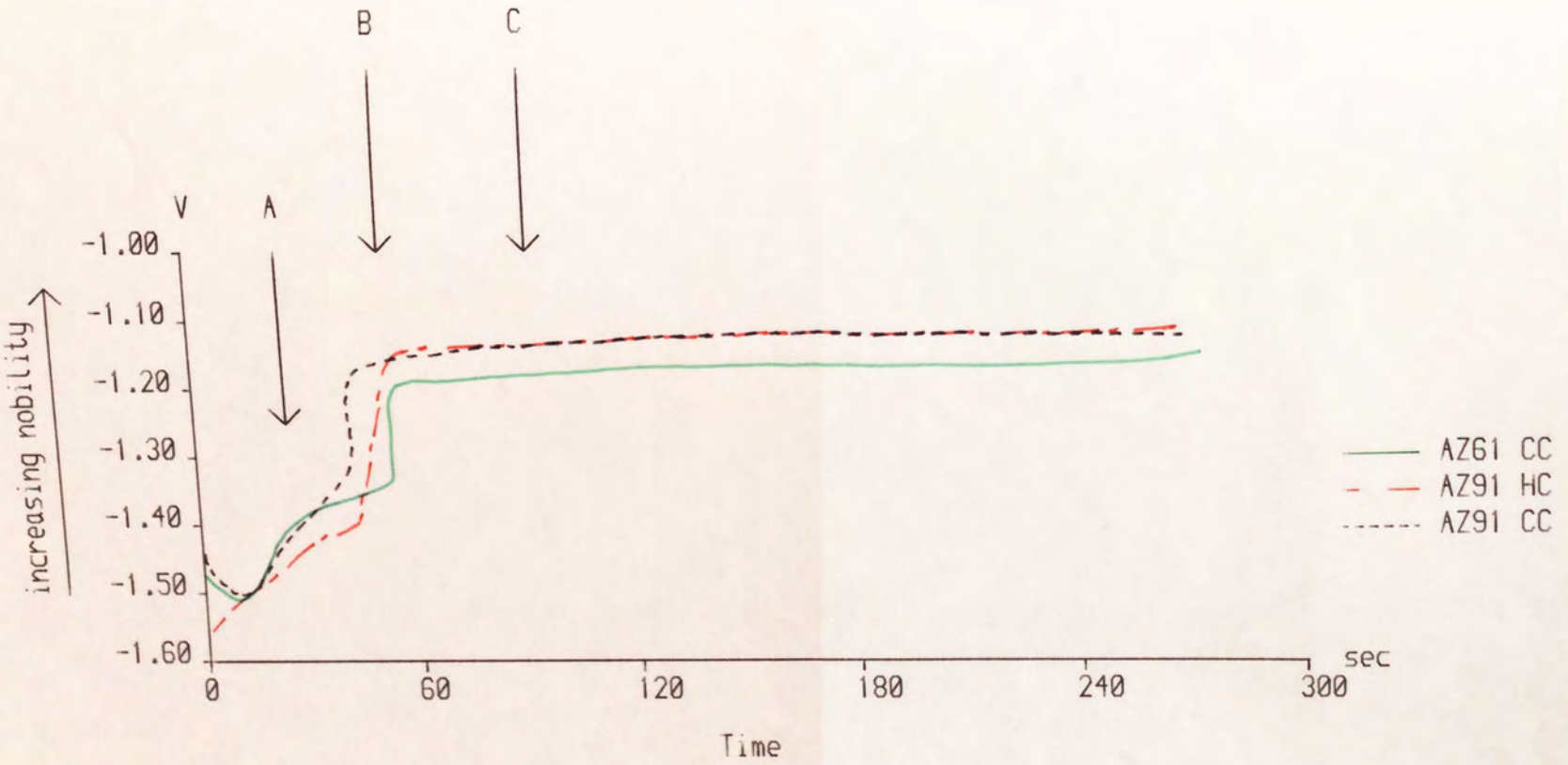


Fig.24 Potential-time curves recorded for the three alloy samples during the zincate immersion after Canning secondary activation.

### 3.7.5.1 STUDY OF THE SURFACE EFFECT DURING ZINCATE S.E.M. EXAMINATION AFTER DIFFERENT IMMERSION TIMES IN THE ZINCATE SOLUTION

Experiments were carried out using a series of pretreated AZ91 cold chamber alloy panels by dipping them into the zincate solution. Once the desired stage, as indicated by the potential-time recorder, was reached, the samples were immediately withdrawn from the solution. Tests were carried out on a succession of samples after various times of immersion. The surface effects at stages A, B and C were revealed by S.E.M. as shown on Plate 10. With the aid of the X-ray analysis attachment, corresponding X-ray maps of zinc distribution were obtained.

At stage A, the sample was immersed for only about 30 seconds, when it was apparent that a layer of zinc had already deposited onto the surface as shown on Plates 10a and 10b. At stage B, the sample surface seemed to have become covered with a denser layer of zinc compared with stage A. It therefore suggested that the zinc deposit had thickened and/or spread during the further 30-second immersion from stage A to stage B (Plates 10c and 10d). The scanning electron micrograph did not reveal any apparent zinc growth from stage B to stage C (Plates 10e and 10f) together with the corresponding X-ray map of zinc. However, at this time, the corresponding potential-time curve suggested that some kind of equilibrium had been approached,

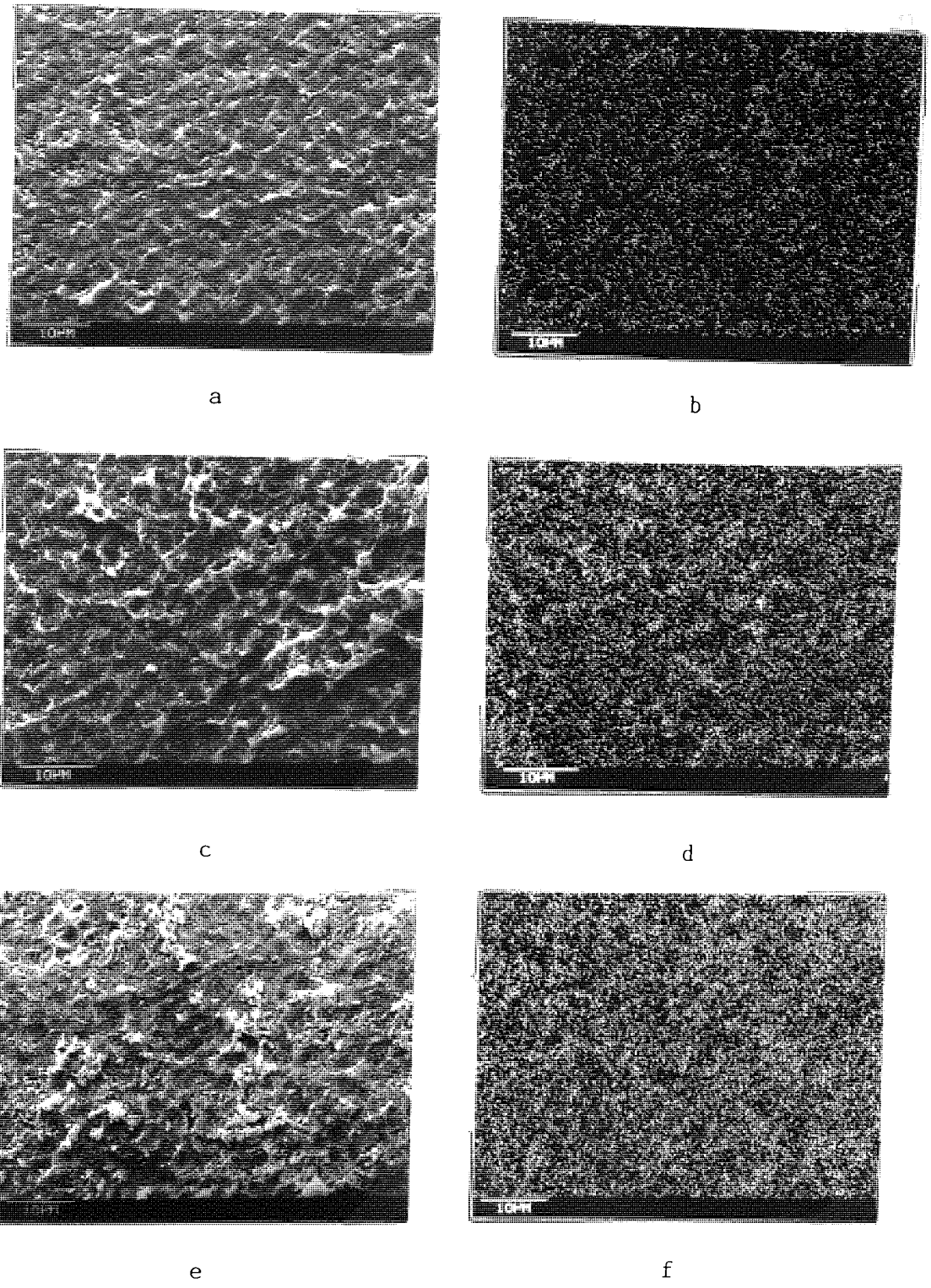

Plate 10 Appearance of the surface of alloy AZ91 cold chamber panel during zincate immersion at different stages. (as indicated by the potential-time curve in fig. 24.)

a) at stage A. b) X-ray map showing distribution of zinc in 10a.
c) at stage B. d) X-ray map showing distribution of zinc in 10c.
e) at stage C. f) X-ray map showing distribution of zinc in 10e.

i.e. the whole alloy surface could have become covered with a surface film. At this point, the zinc layer still contained porosity, and it does not therefore appear that the sharp step in the potential time curve is associated entirely with zinc coverage of the surface.

### 3.7.5.2 INFLUENCE OF pH ON THE ZINC IMMERSION STAGE

The pH of the zincate solution is critical as was mentioned previously in sections 1.3.2 and 1.5.1.2.3. It is therefore believed that changing the pH of the solution may change the characteristic or the shape of the potential-time curve and simultaneously alter the response of the surface to the solution. In order to ascertain the extent of the effect played by the pH of the solution, more experiments were carried out.

Pretreated AZ91 cold chamber alloy panels were immersed into the zincate solution at pH values from 9.02 to 11.01. A fresh zincate solution was used for each test and the desired pH was adjusted by the addition of sodium carbonate $Na_2CO_3$ or sulphuric acid $H_2SO_4$. Once stage C was reached (as indicated by the potential time recorder), the samples were withdrawn immediately from the solution. The surface appearance of each sample at stage C, from solutions of different pH, was revealed by S.E.M. and the X-ray analysis

attachment. The micrographs together with the X-ray maps for zinc from the same area are shown in Plates 11-22. Corresponding potential-time curves are illustrated in Figs. 25-35.

It is evident that the lower the pH of the zincate solution, the longer it took for the surface of the alloy to reach its equilibrium condition. When the pH of the zincate solutions was adjusted below 9.4, stage B of the curves could not be detected, even after 5 minutes immersion (Figs. 25,26), i.e. the step in the curve did not occur. The samples immersed into the zincate solution with pH = 9.02 and 9.20 respectively were withdrawn from the solution after 5 minutes. Dense layers of zinc deposits are shown on both samples after the 5 minute immersion. However, high stress seemed to have developed in the zinc deposits obtained by immersion into the zincate solution at pH 9.02. This was indicated by the cracking shown on Plate 11. On Plate 12 (pH 9.2), the alloy surface appeared to be well covered with zinc deposit.

When the pH of the solution was adjusted to 9.40, the sample surface reached its equilibrium after 3.25 minutes immersion (Fig. 27). Micrographs shown in Plates 13, 14, 15, 16 and 17 present the alloy topography after the immersion in the solutions of pH = 9.4, 9.6, 9.8, 10.01 and 10.25 respectively, until stage C was reached. The surface

characteristics shown are similar to one another: pit formation, porous zinc and preferential growth at areas which appeared to be $\alpha + \beta$ eutectic. The corresponding potential-time curves Figs. 27 to 31 show that as the pH of the zinc solution increases, the time taken to reach equilibrium decreases. In other words, less time is taken to reach stage C as pH increases.

With the pH of the zincate solution adjusted to 10.44 and above, it is apparent that the zinc deposit became more porous. The surface effect on the samples immersed in the zincate solution with pH = 10.44, 10.61, 10.77 and 11.01 are shown on Plates 18, 19, 20 and 21 respectively. The X-ray maps of zinc and the potential-time curves are also shown. The amount of zinc deposited decreases as the pH of the zincate solution increases. This may well be due to the shorter time of immersion since less time was required to reach stage C as the pH of the zincate solution increased (indicated by the corresponding potential-time curve). To investigate this point, another piece of pretreated AZ91 cold chamber alloy was immersed in the zincate solution with pH = 11.01 for 3 minutes. The surface characteristics of the sample shown on Plate 22 together with the corresponding X-ray map of zinc were then compared with Plate 14 and its corresponding X-ray map of zinc. Plate 14 shows the surface effect after 3 minutes of immersion into the solution with pH = 9.60. Thus, the surface effects are compared for the

same length of time of immersion but with different pH values. In Plate 22, the sample was immersed into the solution with pH = 11.01 for 3 minutes. The zinc deposited onto the surface of the sample that had been immersed in the zincate solution with pH = 9.2 appeared to be denser as shown by the X-ray map, though the same length of time of immersion had been employed.

Plate 23 a and b shows the surface appearance of AZ61CC which had no prior chemical treatment before being immersion zincated at pH 8.7 and 10.3 respectively. It is significant that the zinc coverage is apparently finer and more evenly spread at pH 10.3. The areas where zinc is absent are found to be magnesium-rich i.e. phases. Preferential growth of zinc deposits at areas which had higher aluminium content i.e. $\alpha + \beta$ phase is clearly shown in both micrographs.

A freshly activated sample of AZ61CC using the Canning sequence was immersed into the zincate solution at pH 8.70 for 2 minutes. Again large areas of magnesium-rich surface were left uncovered by zinc as shown in Plate 24. Plates 23 and 24 suggest that the passivation film that forms at pH 10.3 suppresses the rate of zinc deposition onto the aluminium rich surface.

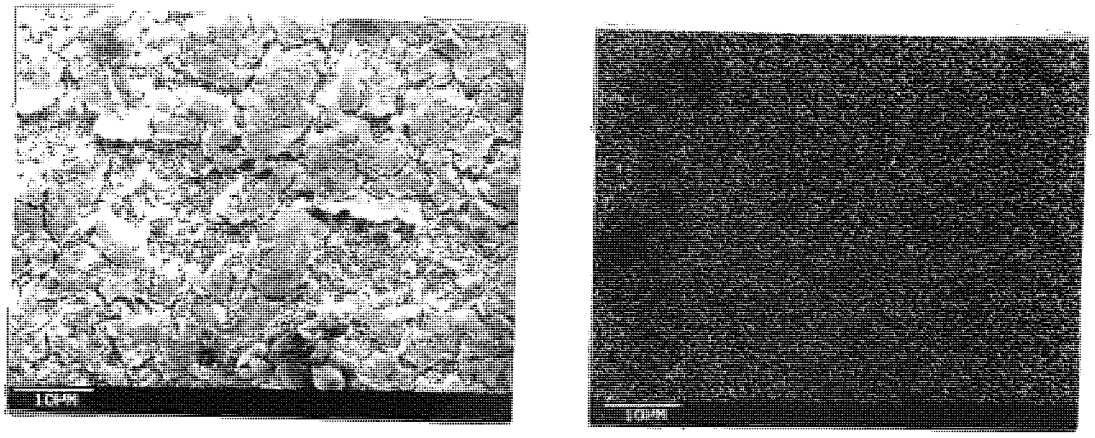

a b

Plate 11 a) Surface appearance of alloy AZ91CC after 4-minute zincate immersion with pH 9.02.
b) X-ray map showing distribution of zinc in plate 11a.

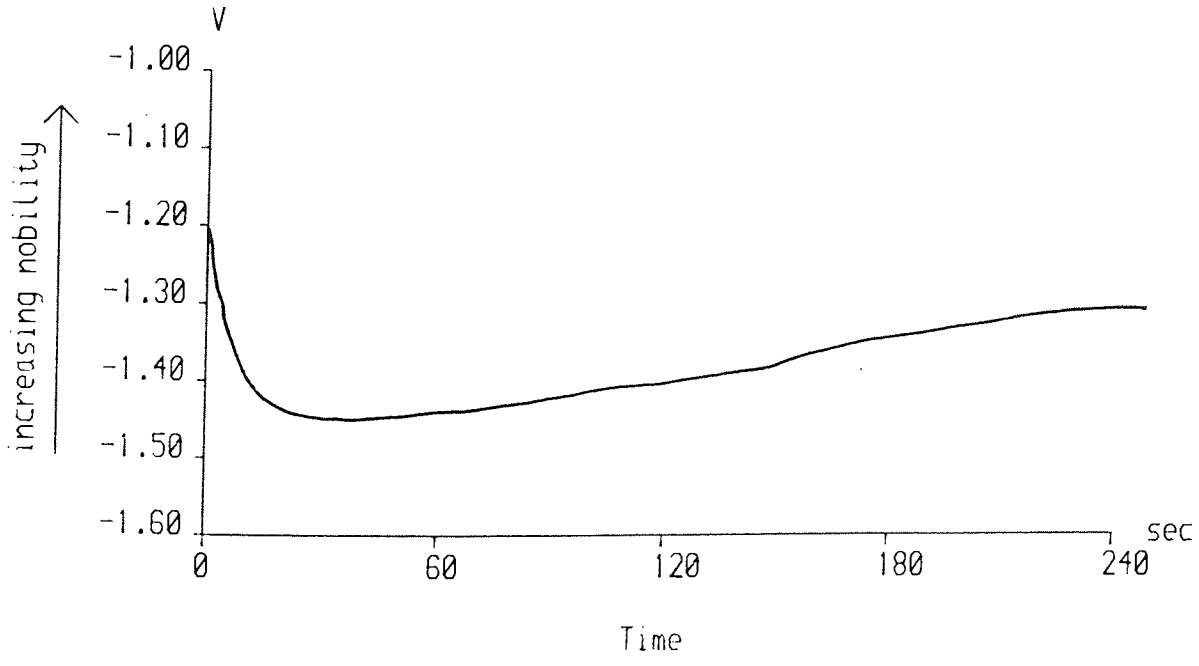


Fig.25 The corresponding potential-time curve, pH = 9.02.

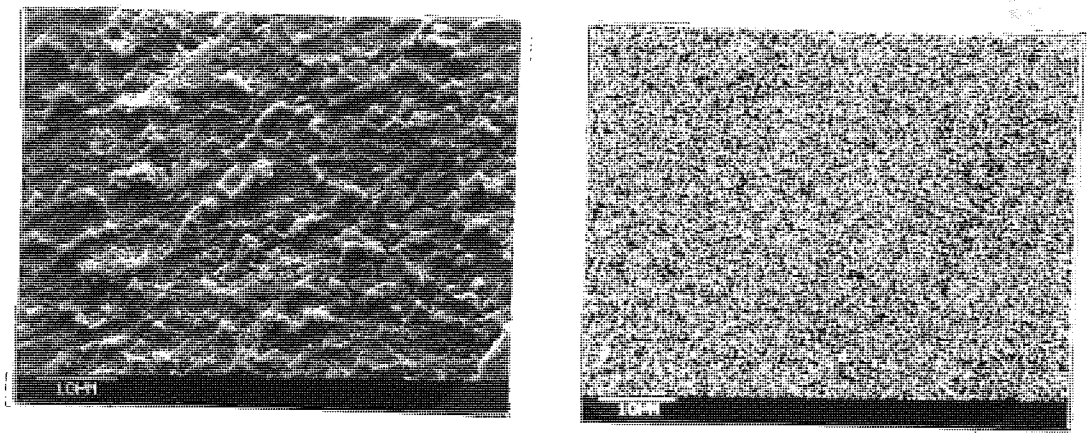

a b

Plate 12 a) Surface appearance of alloy AZ91CC after 4-minute zincate immersion with pH 9.20.
b) X-ray map showing distribution of zinc in plate 12a.

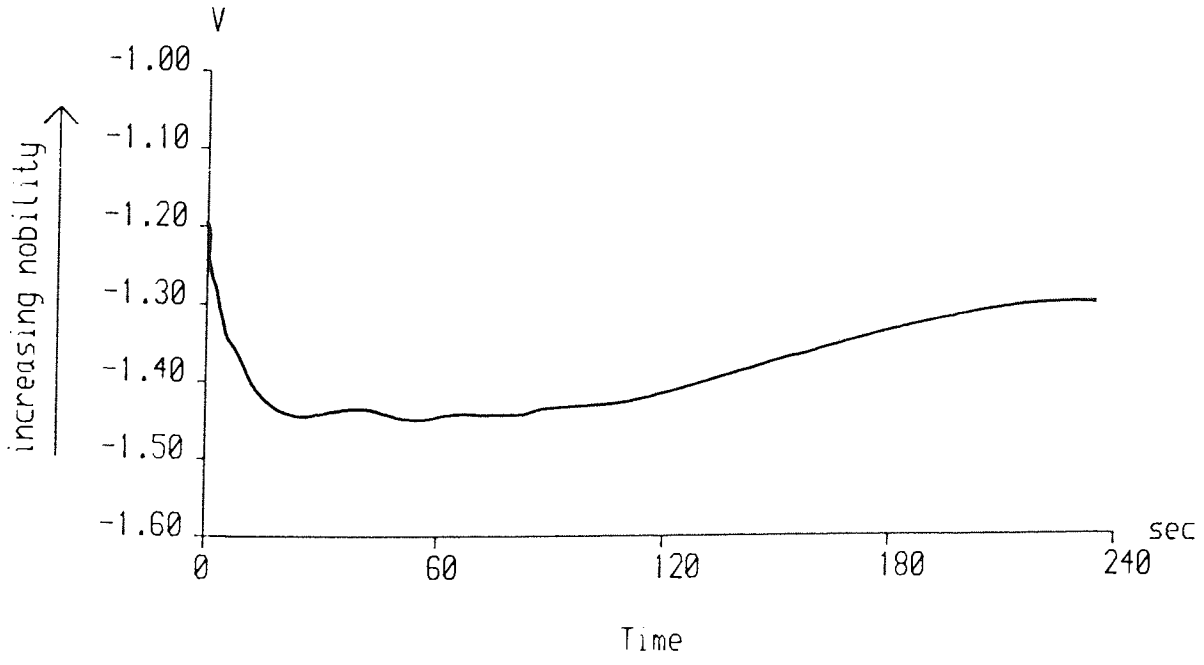


Fig.26 The corresponding potential-time curve, pH = 9.20.

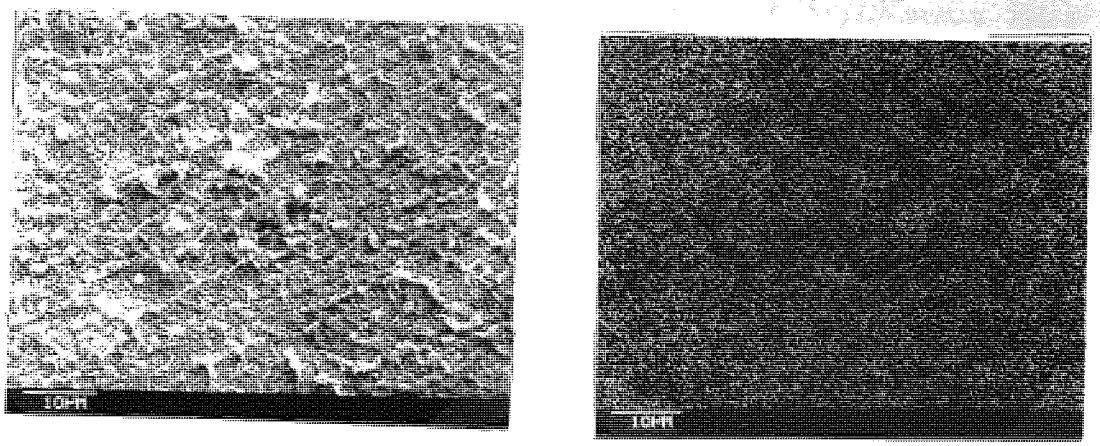

a b

Plate 13 a) Surface appearance of alloy AZ91CC after 3 min. 20 sec. zincate immersion with pH 9.40.
b) X-ray map showing distribution of zinc in plate 13a.

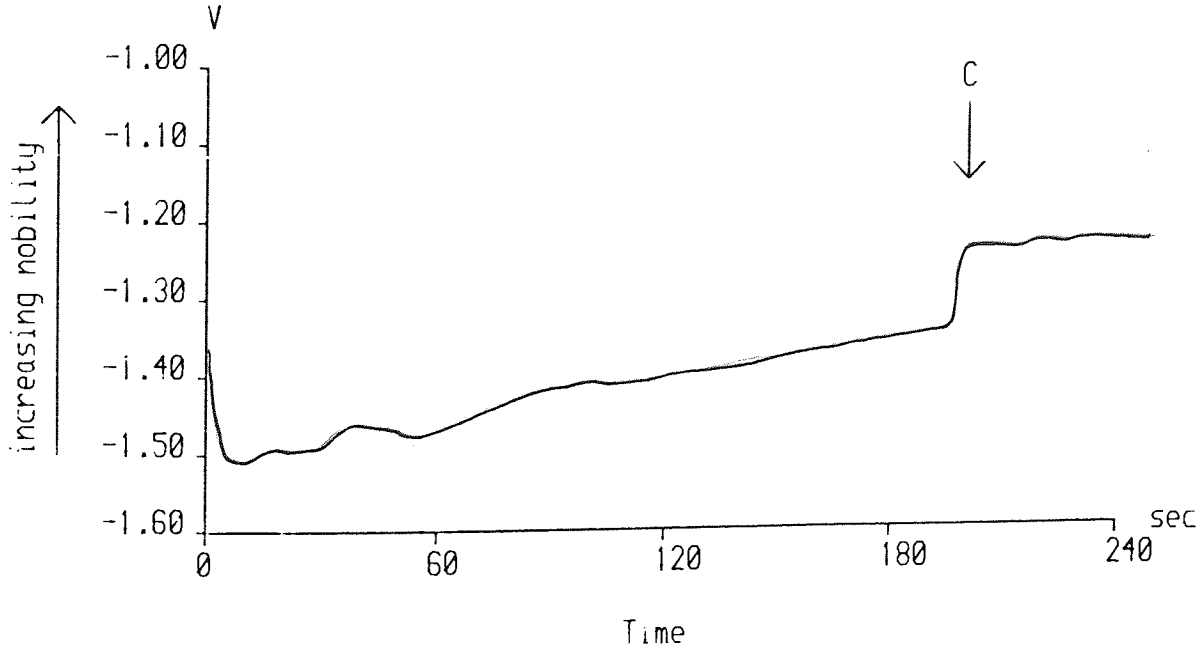


Fig.27 The corresponding potential-time curve, pH = 9.40.

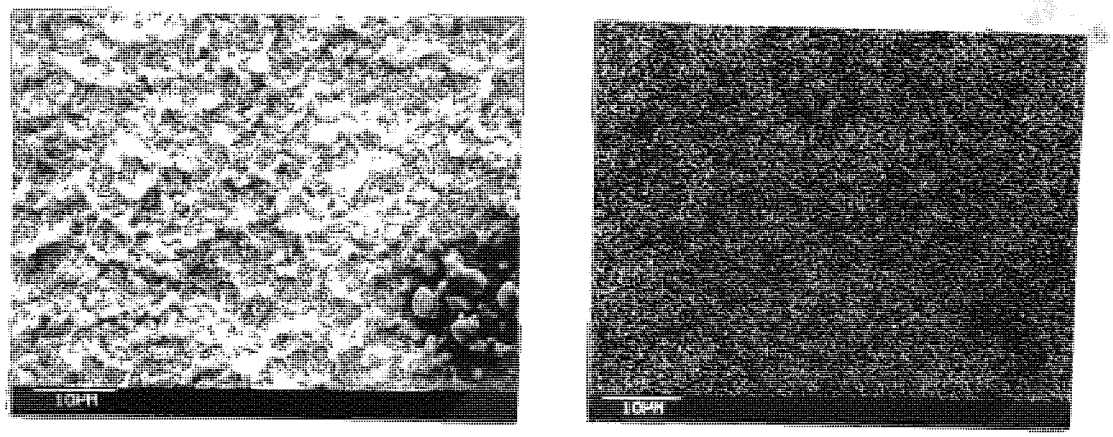

a b

Plate 14 a) Surface appearance of alloy AZ91CC after 3-minute zincate immersion with pH 9.60.
b) X-ray map showing distribution of zinc in plate 14a.

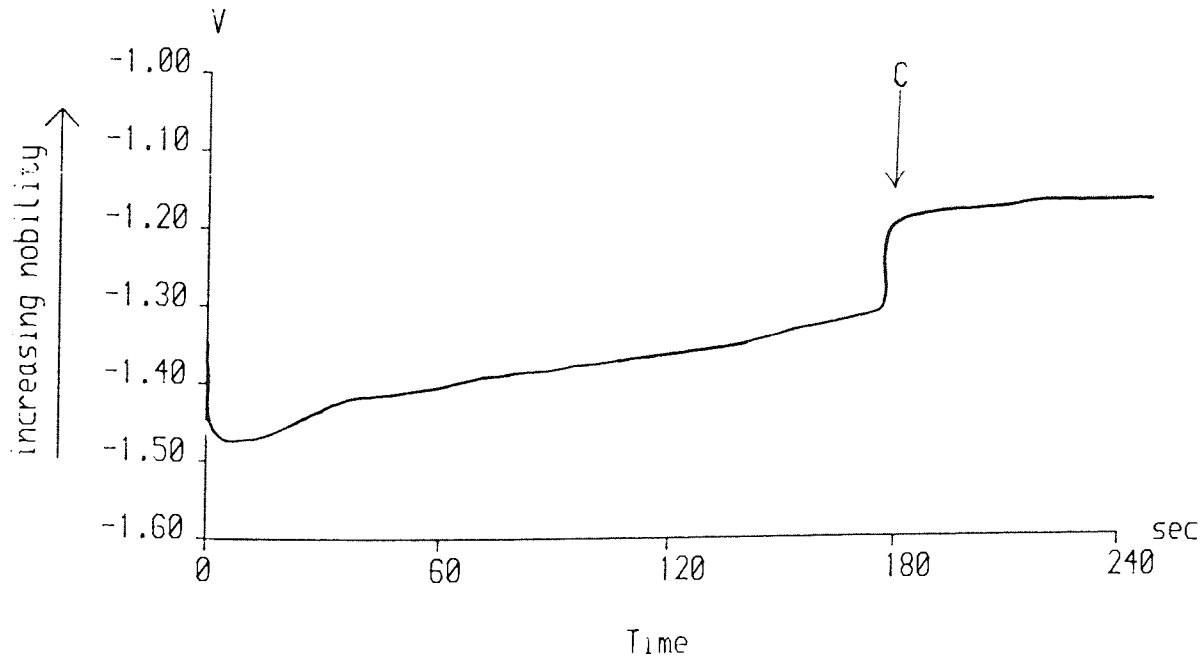


Fig.28 The corresponding potential-time curve, pH = 9.60.

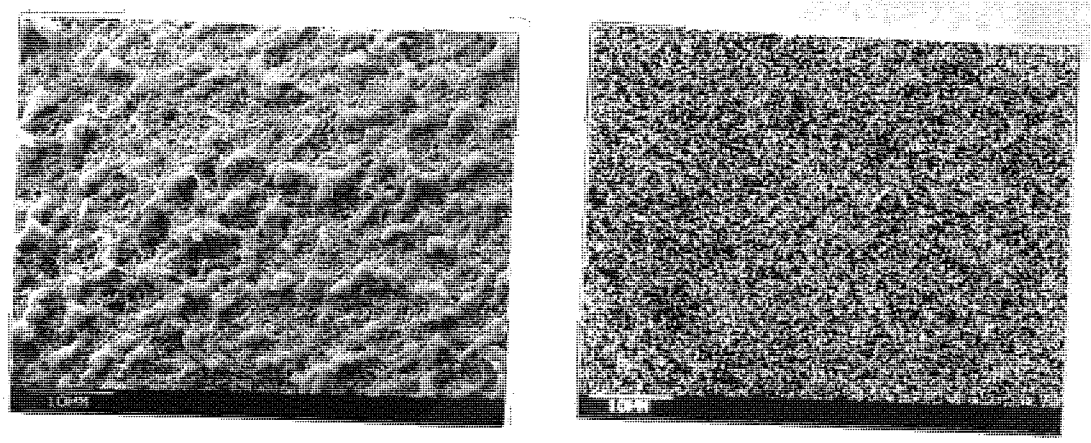

a b

Plate 15 a) Surface appearance of alloy AZ91CC after 2 min. 20 sec. zincate immersion with pH = 9.80.
b) X-ray map showing distribution of zinc in plate 15a.

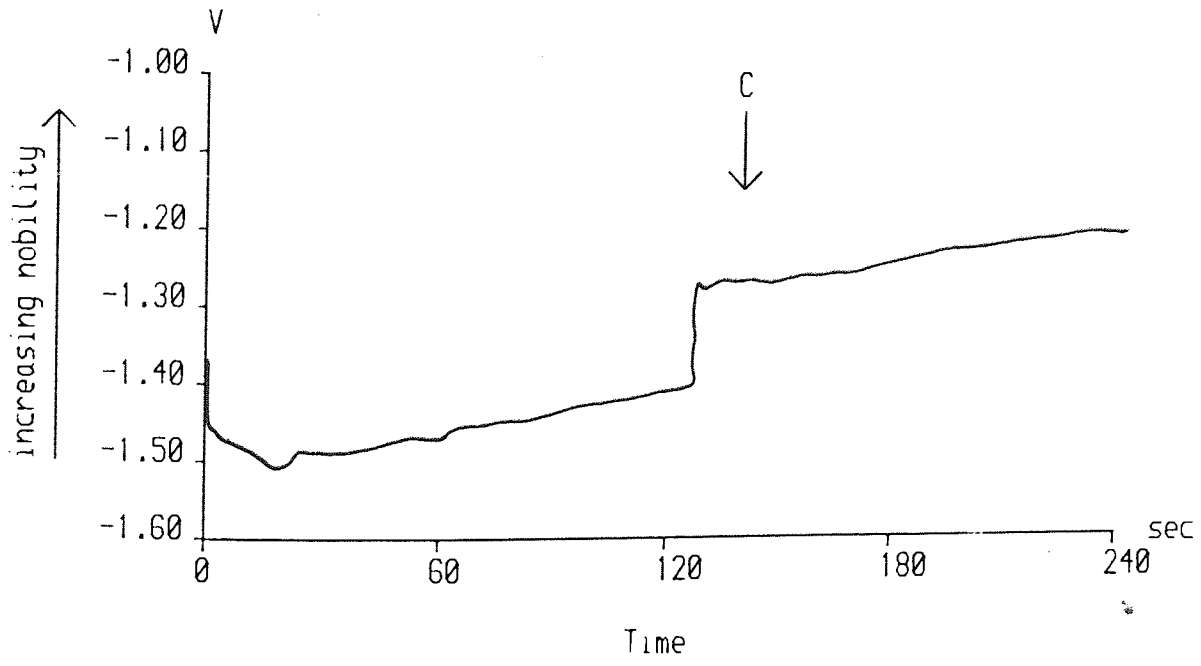


Fig.29 The corresponding potential-time curve, pH = 9.80.

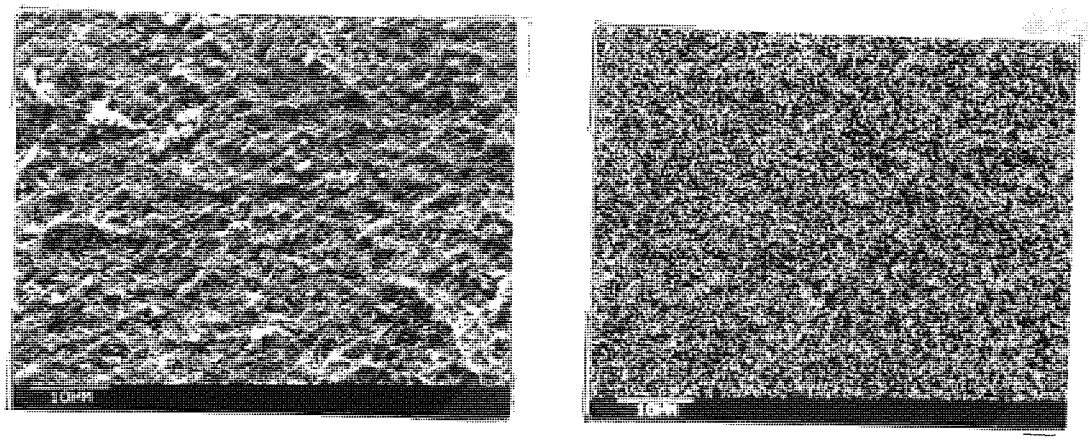

a b

Plate 16 a) Surface appearance of alloy AZ91CC after 2-minute zincate immersion with pH = 10.01.
b) X-ray map showing distribution of zinc in plate 16a.

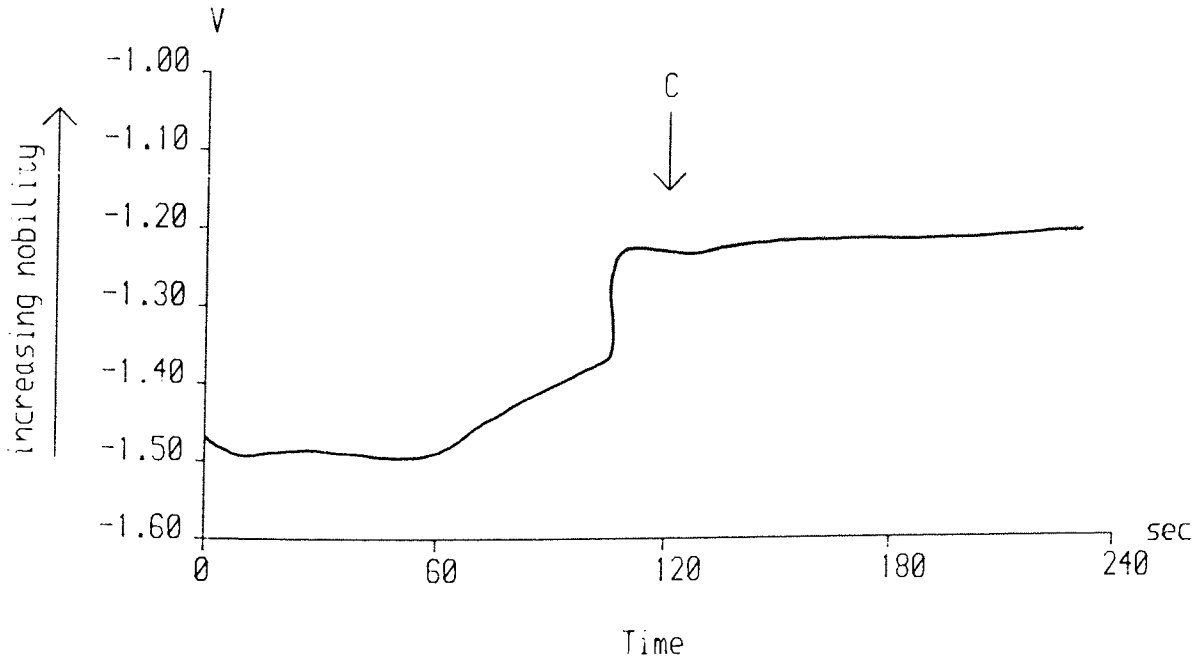


Fig.30 The corresponding potential-time curve, pH = 10.01.

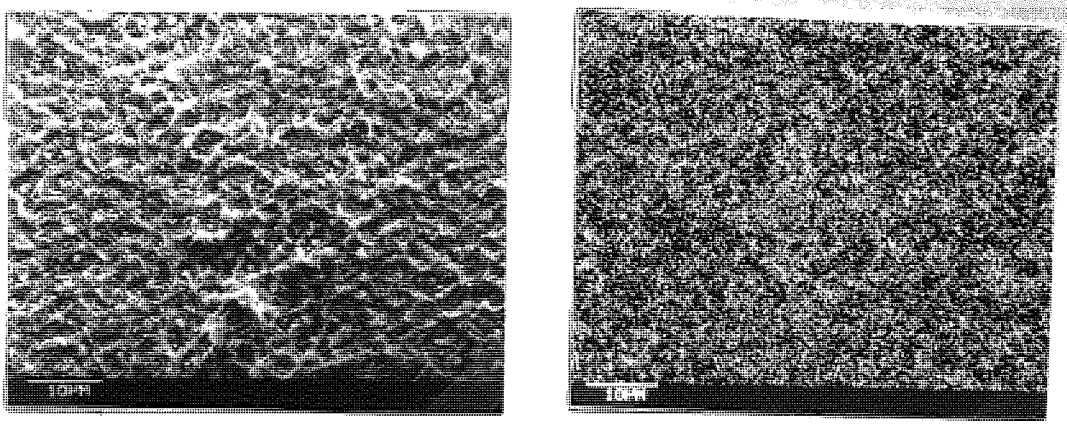

a b

Plate 17 a) Surface appearance of alloy AZ91CC after 1 min. 40 sec. zincate immersion with pH 10.25.
b) X-ray map showing distribution of zinc in plate 17a.

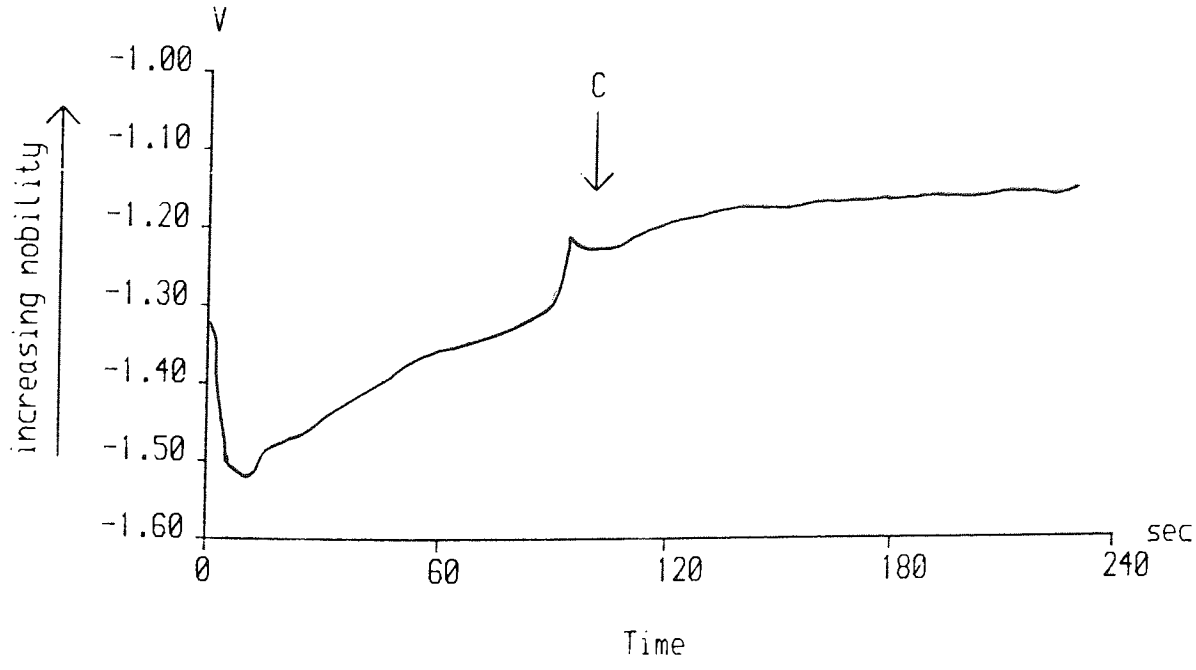


Fig.31 The corresponding potential-time curve, pH = 10.25.

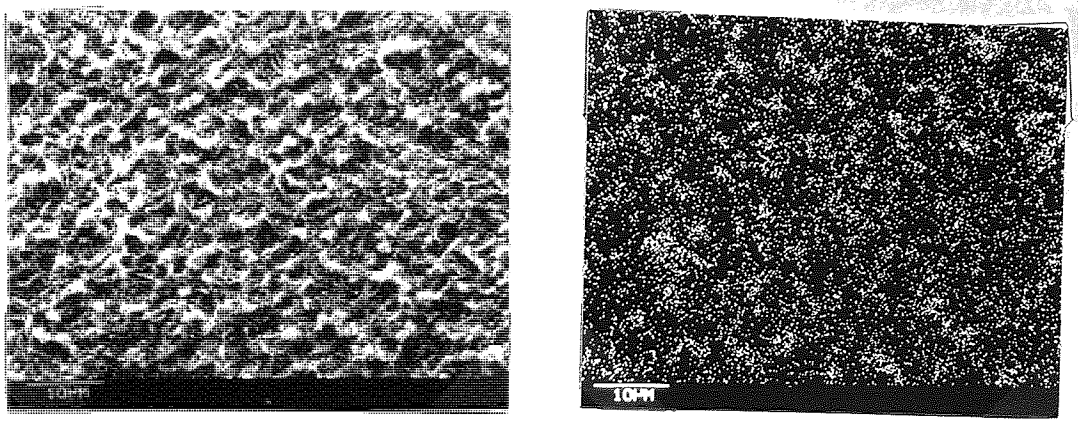


a b

Plate 18 a) Surface appearance of alloy AZ91CC after 1 min. 30 sec. zincate immersion with pH = 10.44.
b) X-ray map showing distribution of zinc in plate 18a.

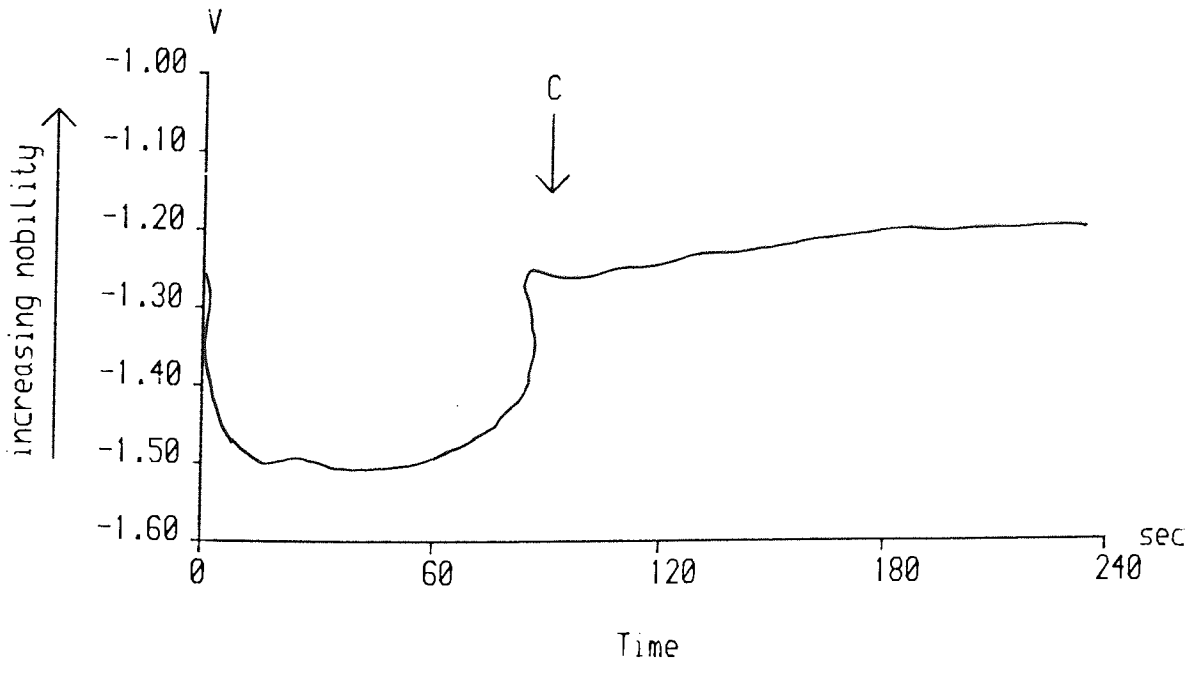


Fig.32 The corresponding potential-time curve, pH = 10.44.

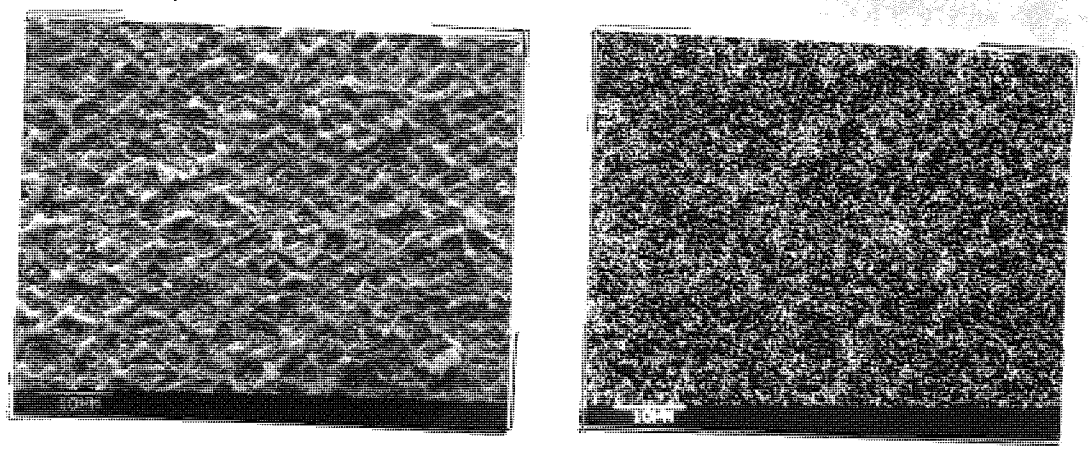

a b

Plate 19 a) Surface appearance of alloy AZ91CC after 1-minute zincate immersion with pH 10.61.
b) X-ray map showing distribution of zinc in plate 19a.

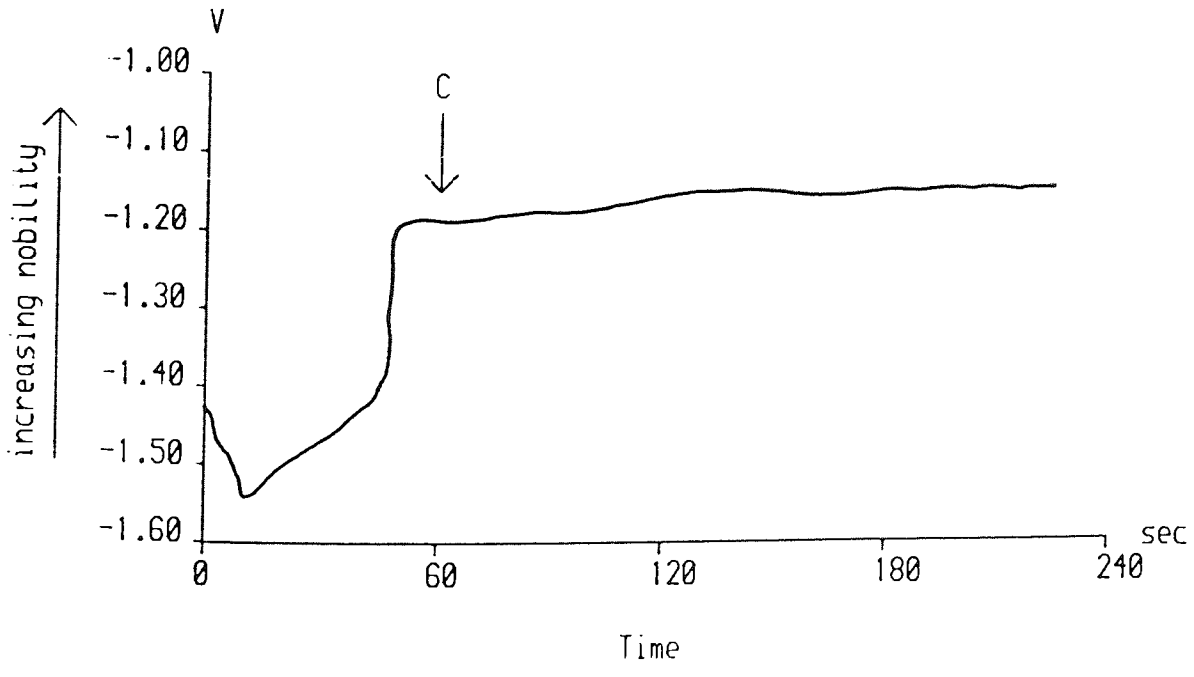


Fig.33 The corresponding potential-time curve, pH = 10.61.

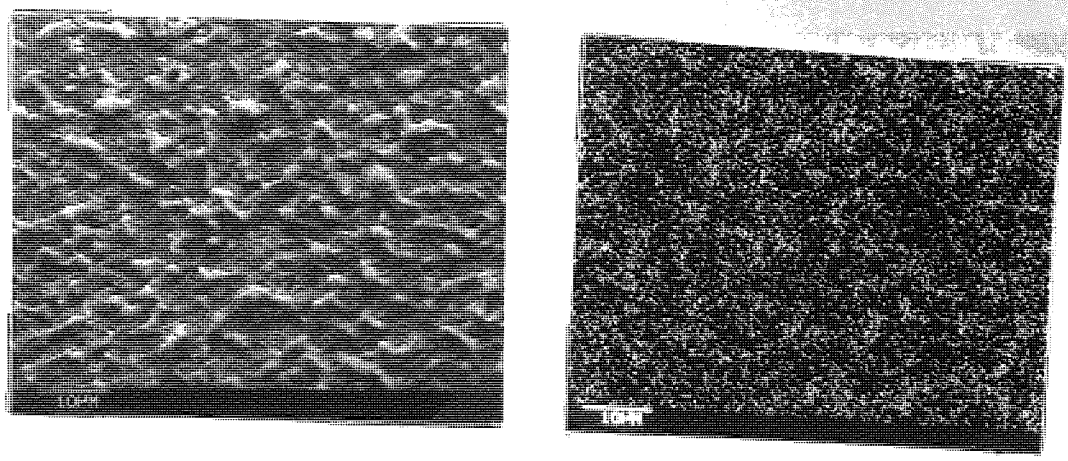

a b

Plate 20 a) Surface effect of alloy AZ91CC after 40-second zincate immersion with pH 10.77.
b) X-ray map showing distribution of zinc in plate 20a.

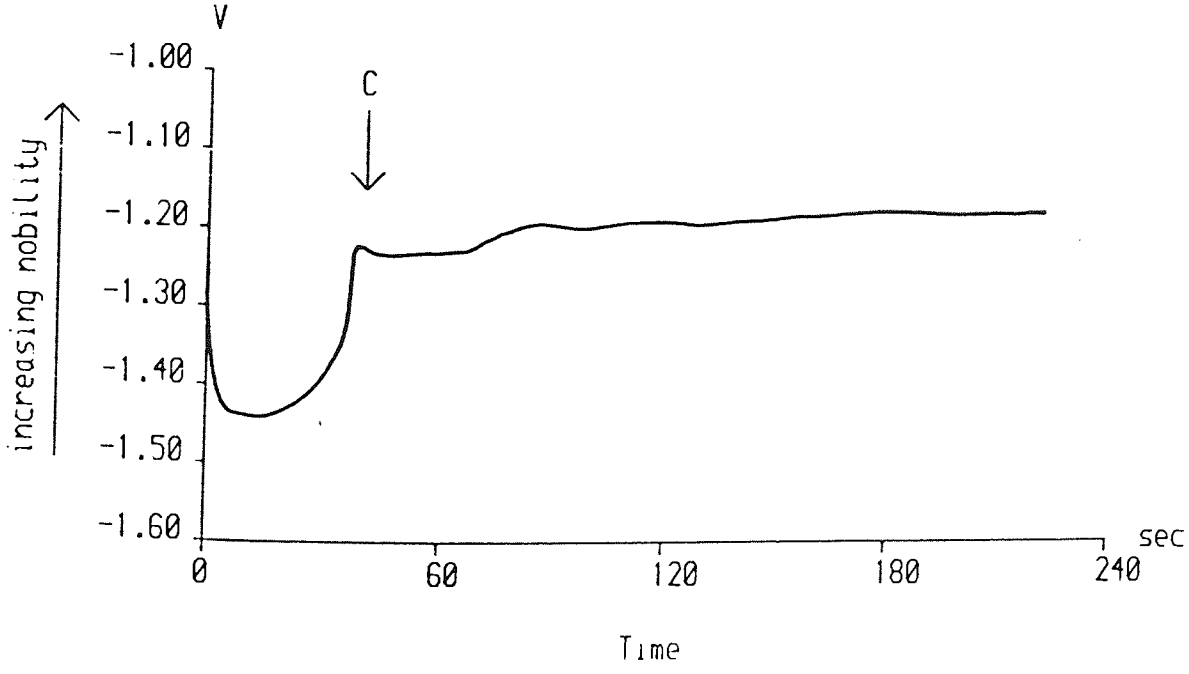


Fig.34 The corresponding potential-time curve, pH = 10.77.

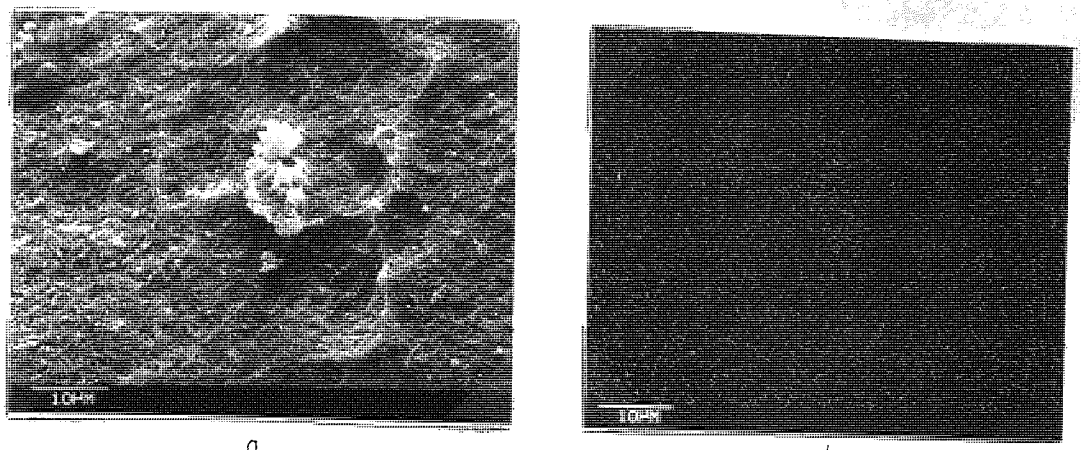

a b

Plate 21 a) Surface appearance of alloy AZ91CC after 30-second zincate immersion with pH 11.01.
b) X-ray map showing distribution of zinc in plate 21a.

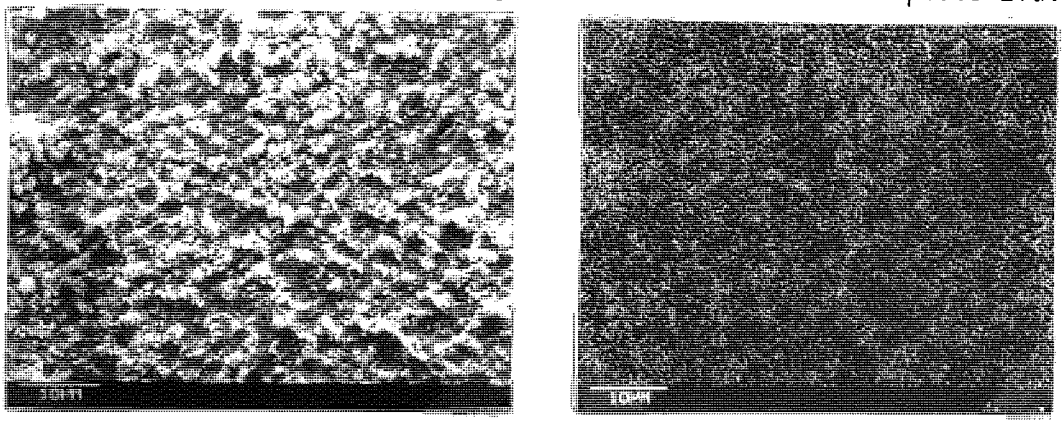

a b

Plate 22 a) Surface appearance of alloy AZ91CC after 3-minute zincate immersion with pH 11.01.
b) X-ray map showing distribution of zinc in plate 22a.

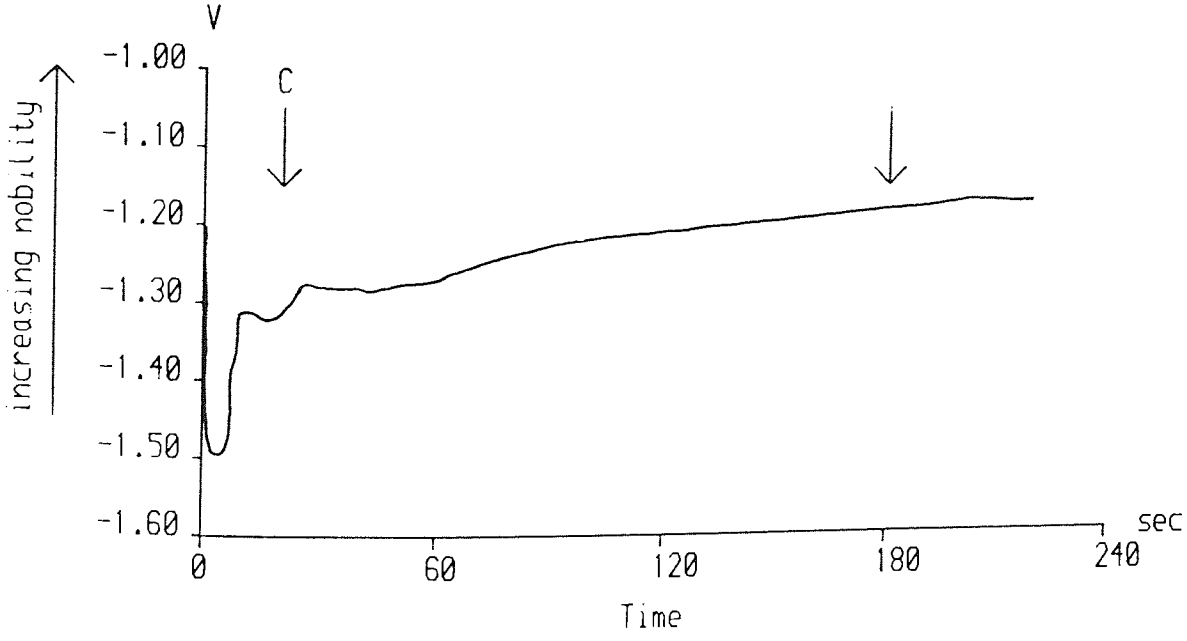


Fig.35 The corresponding potential-time curve, pH = 11.01.

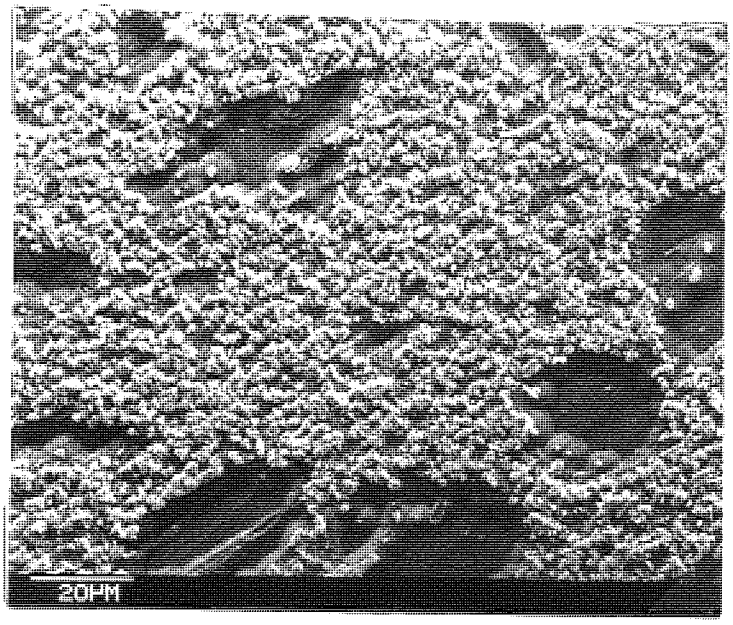


a

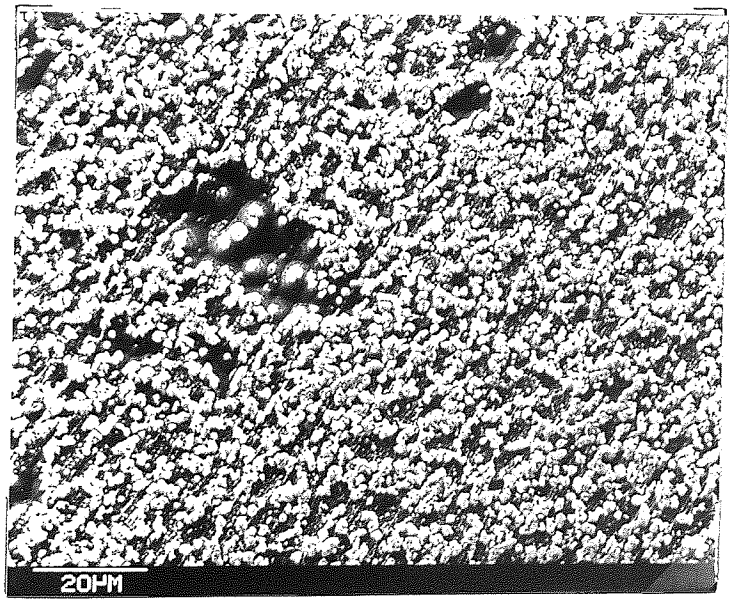


b

Plate 23 Surface appearance of alloy AZ61CC which has no prior chemical treatment but immersion zincate treatment at different pH.

a) After 3 minute immersion zinc deposition at pH 8.7.
b) After 3 minute immersion zinc deposition at pH 10.3.

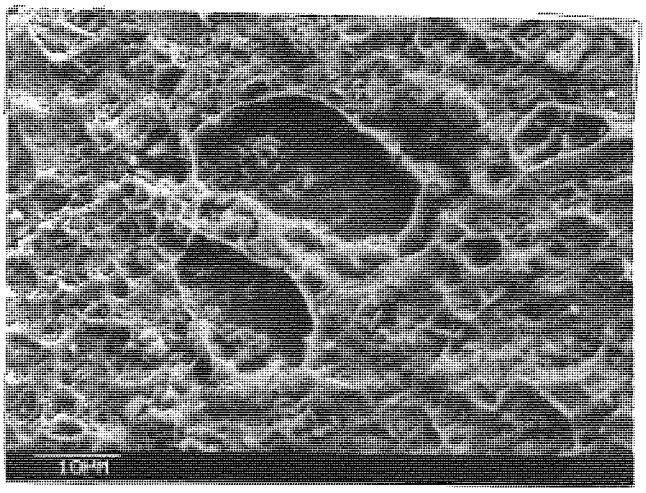

Plate 24 Surface appearance of alloy AZ61CC after immersion zinc deposition for 2 min. at pH 8.70, pretreated using Canning sequence.

## 3.8 DETERMINATION OF ZINCATE FILM WEIGHT

Fig. 36 shows the change in zincate film weight with immersion time in the zincate solution for the various alloys. The pH of the solution was 10.30. All the curves have a similar characteristic shape in that there is a high initial growth rate, but after one minute, the film weight increases more slowly and essentially linearly with time.

It can be seen that film growth was greatest on AZ91 cold chamber castings and least on AZ61 cold chamber castings. It is therefore suggested that the zinc film weight may increase with the aluminium content of the alloy.

AZ91 cold chamber castings and AZ91 hot chamber castings were very similar in film weight gain with time. Therefore it is difficult at this stage to determine whether the hot or cold chamber process would make any difference to the film weight gain.

It is clearly indicated in Fig. 36 that after a 60-second immersion, the film weight gain was essentially linear with time. This observation applied to all alloy samples. The time taken for the change in rate of deposition to occur is significant if reference is made to the polarisation/time

curves in Fig. 24. It more or less corresponded with the time at which equilibrium potential was reached.

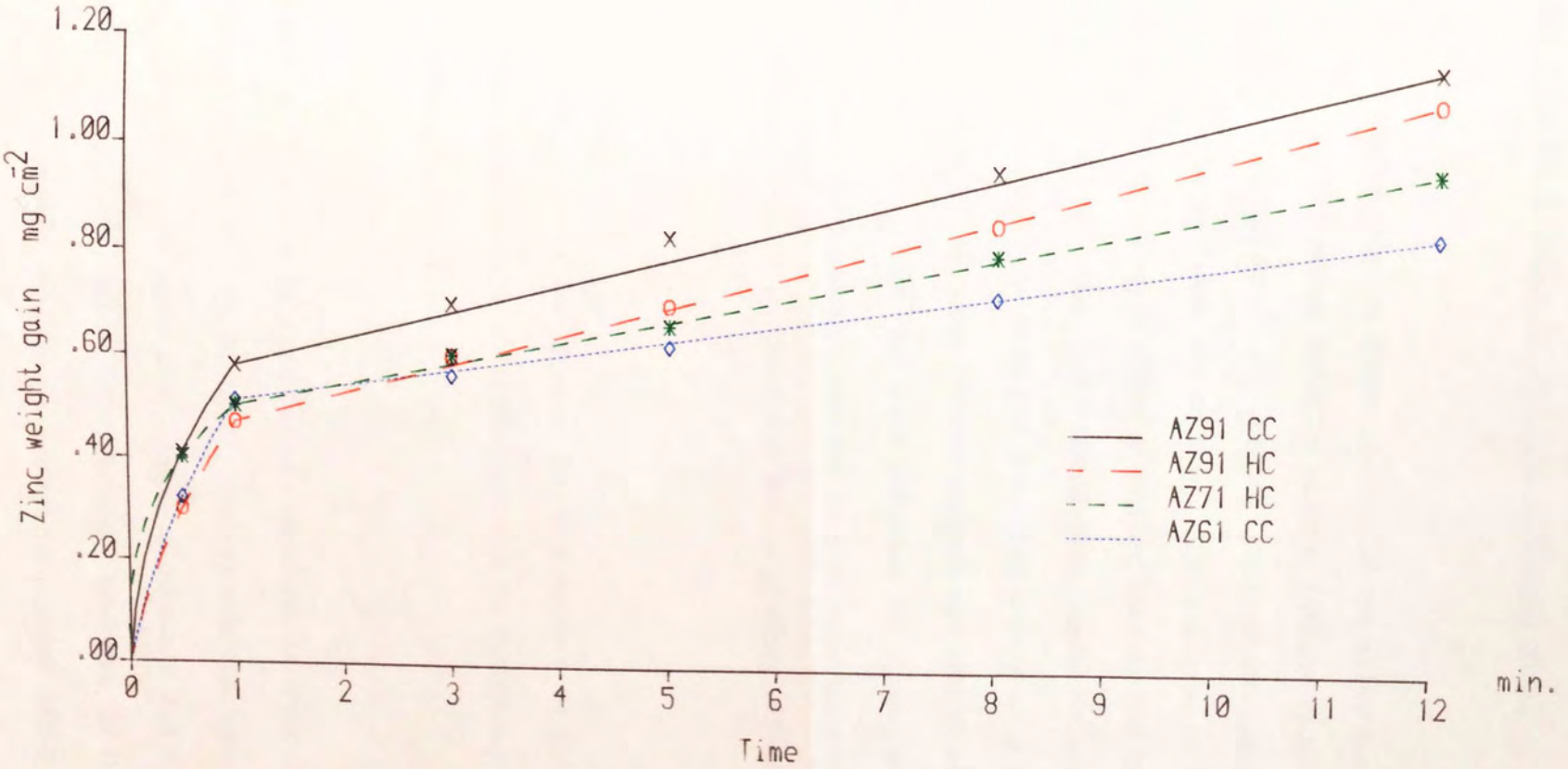


Fig.36 The change in zincate film weight with immersion time in the zincate solution.

## 3.9 THE ROLE OF FLUORIDE IN THE ZINC IMMERSION STAGE

Potential time curves are shown in Fig. 37 for alloy AZ61CC immersed in a zincating solution without lithium fluoride and sodium carbonate. An unusual oscillation effect occurred when pretreatment was omitted. The position of the step in the curve occurred after a shorter time in the case of the Canning sequence and oscillation was eliminated. Corresponding curves showing the zinc film growth rate are illustrated in Fig. 38. The Canning process had the slowest growth rate. A result is also included for a sample of magnesium (not pretreated) immersed in a zincate solution. A step still occurred in the curve but only after almost 4 minutes.

The study of zinc film growth on the surface of alloy AZ61CC, when the zincate solution contains no fluoride, is shown in Plate 25.

The effect of fluoride on zinc deposit coverage is shown in both Plates 23 and 25. In Plate 23, even though the sample had no prior chemical treatment, complete coverage did not occur when the solution contained fluoride. However, in the absence of fluoride, complete coverage took place after 3 minutes immersion as shown in Plate 25a and 25b.

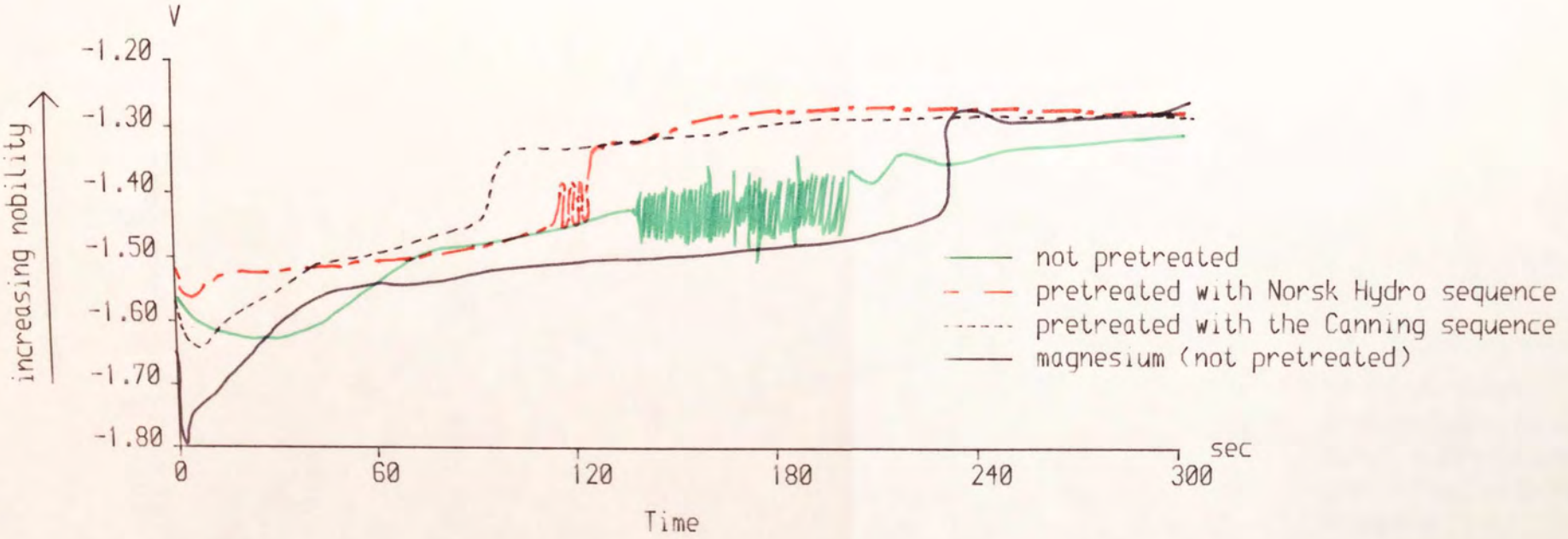


Fig.37 Potential-time curves recorded for alloy AZ61CC and magnesium during immersion in zincate solution minus lithium fluoride and sodium carbonate.

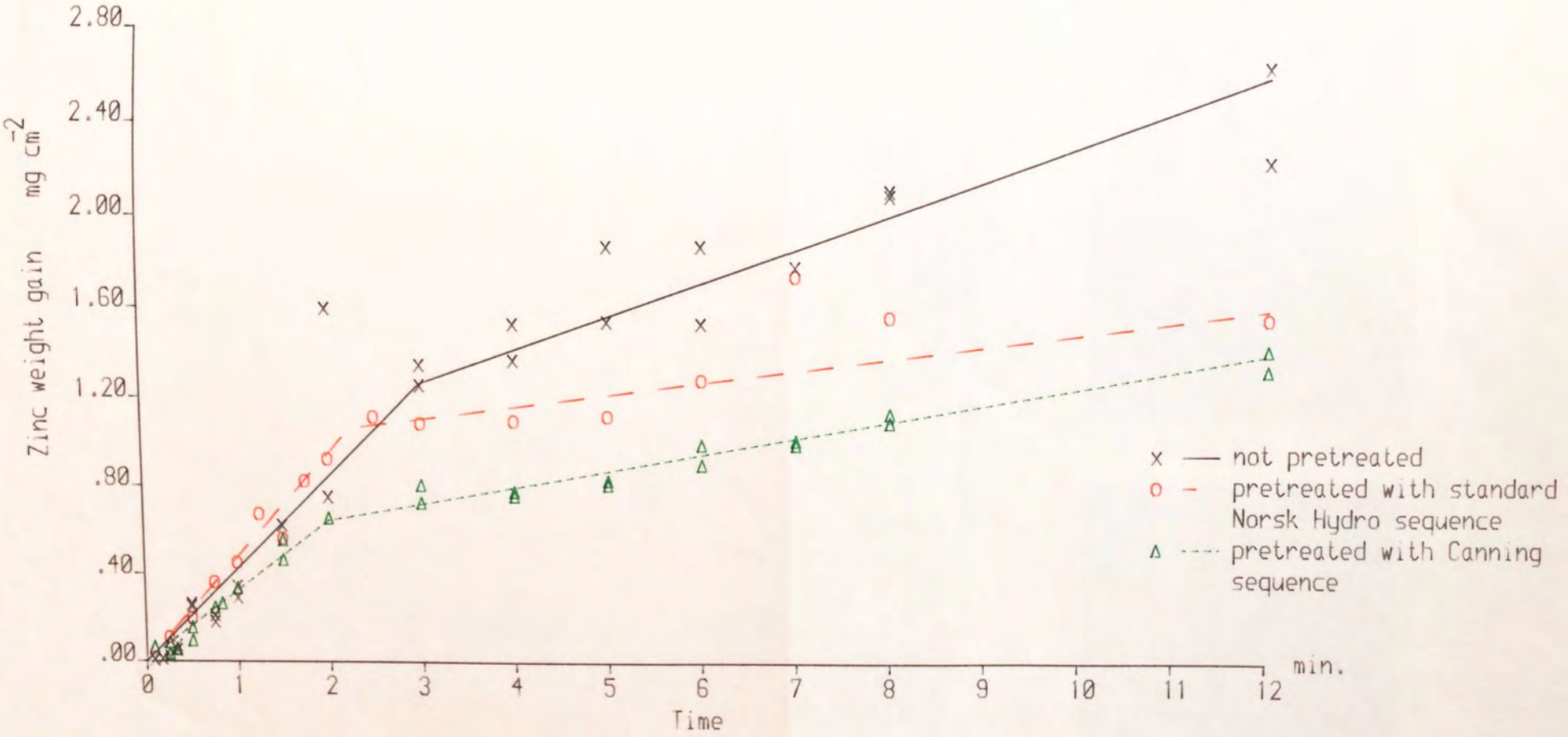


Fig.38 The change in zincate film weight with immersion time in zincate solution minus lithium fluoride and sodium carbonate for alloy AZ61CC, corresponding to Fig. 37.

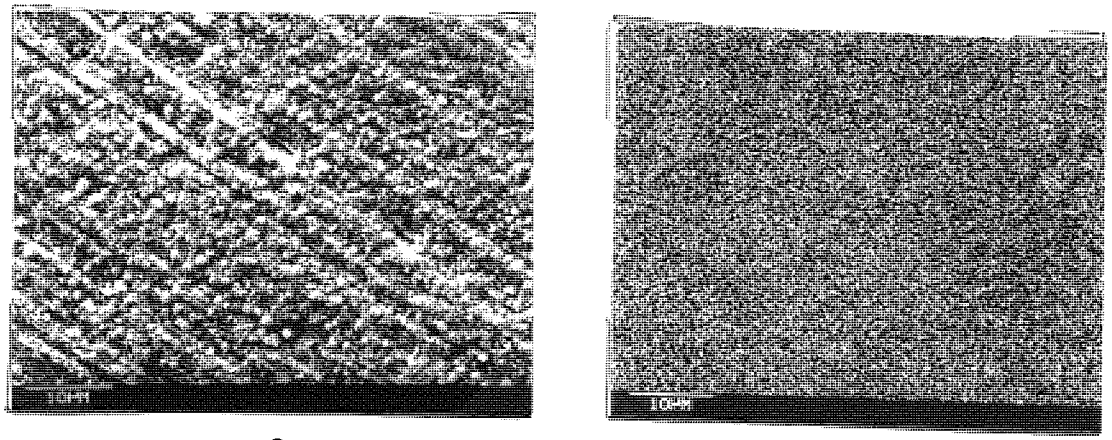

a b

Plate 25 Surface appearance of alloy AZ61CC after 3 min. immersion into the zincate solution which contains no fluoride.
a) After immersion zinc deposition for 3 min.
b) X-ray map showing distribution of zinc in 25a.

## 3.10 EXAMINATION USING AUGER ELECTRON SPECTROSCOPY

Samples of alloy AZ61CC and AZ91HC, designated 1 to 14 in Table 7, were examined using Auger electron spectroscopy to detect the presence of surface films during various stages of pretreatment. The elements which would inevitably be present, Mg and Al, were not included in the analysis. Oxygen was important since oxide and hydroxide films are significant in this investigation. The presence of fluoride was not definite in the case of samples 1, 2, 5 and 6, but significant amounts were detected on samples 7 to 14. Its presence on samples 7 and 8 illustrates that fluoride does remain on the surface after immersion in the Canning second stage solution, almost certainly as a magnesium/aluminium fluoride film.

Table 7 ANALYSIS OF AUGER ENERGY SPECTRUM, SAMPLES PRETREATED USING DIFFERENT SEQUENCE.

| sample no. | alloy | treatments | $O_2$ | F | P | B | Ca | K | Zn |
|---|---|---|---|---|---|---|---|---|---|
| 1 | 91 HC | zincated using the Norsk Hydro sequence | ✱ | Δ | x | x | x | ✱ | ✱ |
| 2 | 61 CC | 〃 | ✱ | Δ | x | x | x | ✱ | ✱ |
| 3 | 91 HC | oxalic etched/Norsk Hydro solution activated | ✱ | x | x | x | x | x | o |
| 4 | 61 CC | 〃 | ✱ | x | x | x | x | x | o |
| 5 | 91 HC | zincated with no prior chemical treatment | ✱ | Δ | x | x | Δ | Δ | ✱ |
| 6 | 61 CC | 〃 | ✱ | Δ | x | x | Δ | Δ | ✱ |
| 7 | 91 HC | oxalic etched/Canning solution activated | ✱ | o | x | x | x | x | o |
| 8 | 61 CC | 〃 | ✱ | o | x | x | x | x | o |
| 9 | 91 HC | zincated using the Canning sequence | ✱ | o | x | x | x | Δ | ✱ |
| 10 | 61 CC | 〃 | ✱ | o | x | x | x | Δ | ✱ |
| 11 | 91 HC | zinc deposit was stripped with $NH_4HF_2/H_3PO_4$ | ✱ | ✱ | x | x | x | x | o |
| 12 | 61 CC | 〃 | ✱ | ✱ | x | x | x | x | o |
| 13 | 91 HC | double zincate sequence | ✱ | ✱ | x | x | o | o | ✱ |
| 14 | 61 CC | 〃 | ✱ | ✱ | x | x | o | o | ✱ |

| | |
|---|---|
| not present | x |
| possibly small amount | Δ |
| present | o |
| plenty | ✱ |

## 3.11 EFFECT OF DOUBLE DIP PRETREATMENT SEQUENCE

The double dip sequence employed is shown in Fig. 39. A large amount of gas was liberated when the second immersion deposit was laid down after stripping the first one off in a phosphoric acid/ammonium fluoride solution. It was apparent that the zinc deposit did not completely cover the alloy surface and this was confirmed by S.E.M. examination. Plate 26 shows the surface effect of the double dip treatment on alloy AZ61CC at each stage after the first zincate dip.

When the first zinc coating was removed after the 90-second ammonium bifluoride immersion, the sample surface was left in a fairly smooth but porous condition (Plate 26a). It is demonstrated in Plate 26 b and c that the second coating of zinc is porous and patchy.

Fig. 40 shows the potential time curve recorded for alloy AZ61CC when its zinc coating was being removed in the ammonium bifluoride + phosphoric acid solution. It would seem that the formation of fluoride film is the cause of the increasing nobility.

Potential time curves recorded for alloy AZ61CC during the first and second immersion using the same zincating solution

are shown in Fig. 41. Equilibrium potential was reached more quickly during the first immersion. It indicates that the prior condition of the alloy influences the position of the step in the curve.

## THE DOUBLE DIP SEQUENCE

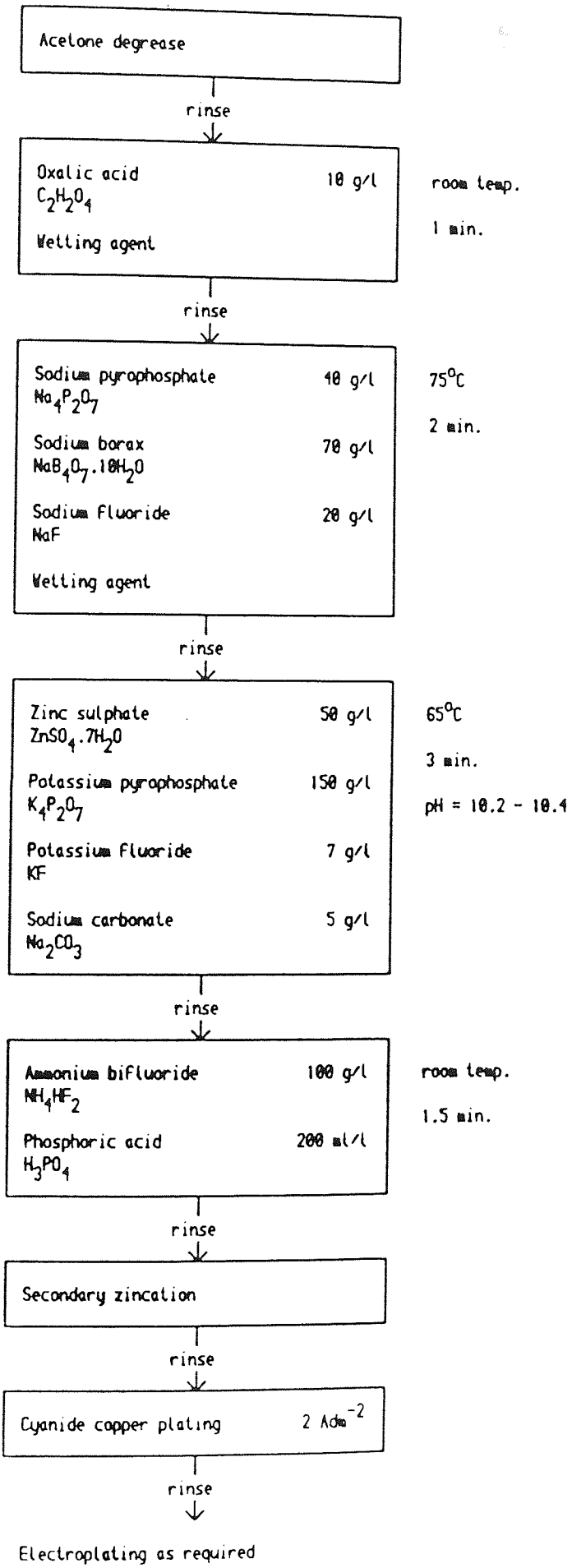


Fig.39 Flow chart for the double dip sequence.

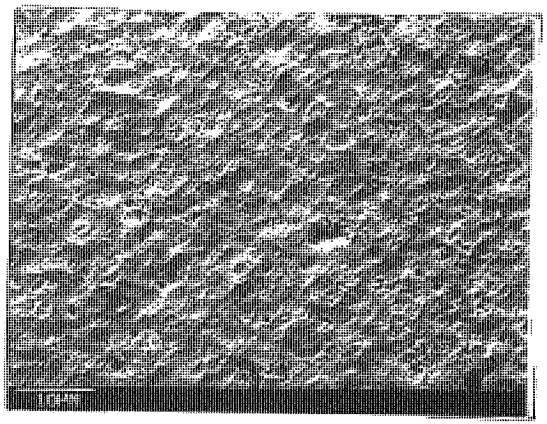

a

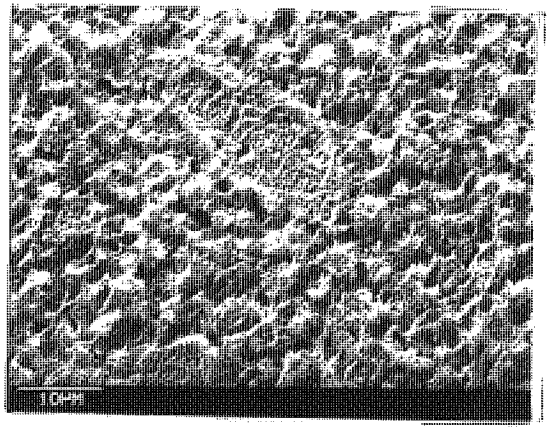

b

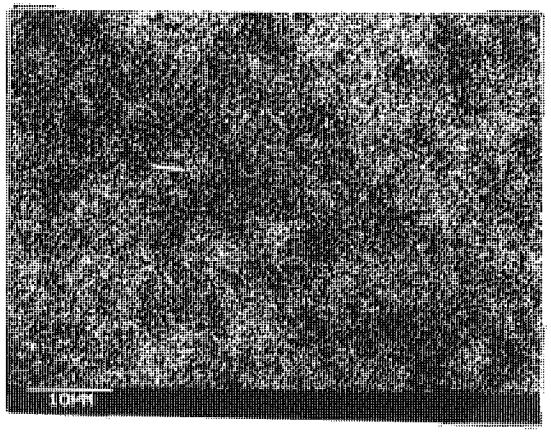

c

Plate 26 Effect of the Double dip treatment on alloy AZ61CC.

a) After 1½ min. ammonium bifluoride immersion. (where the first zinc coating was removed)

b) After 3 min. second immersion zinc deposition.

c) X-ray map showing distribution of zinc in 27b.

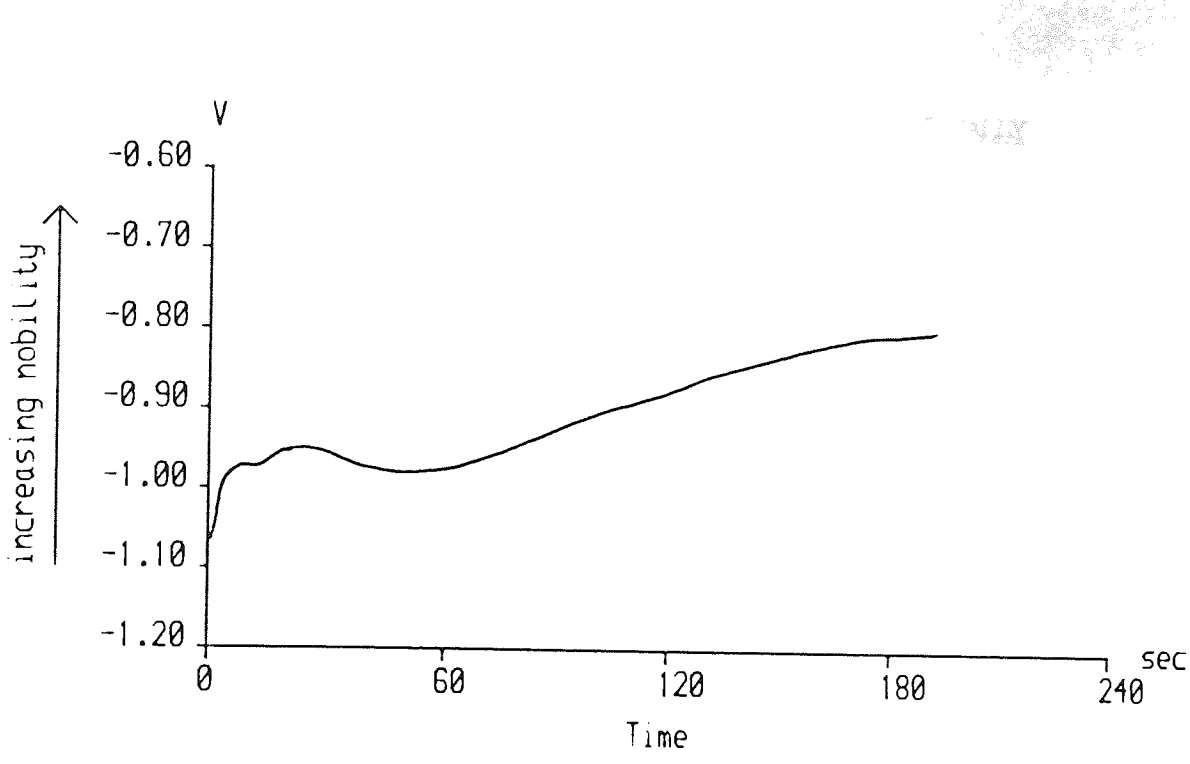


Fig.40 Potential-time curve recorded for alloy AZ61CC when its zinc coating was being removed in the ammonium bifluoride + phosphoric acid solution.

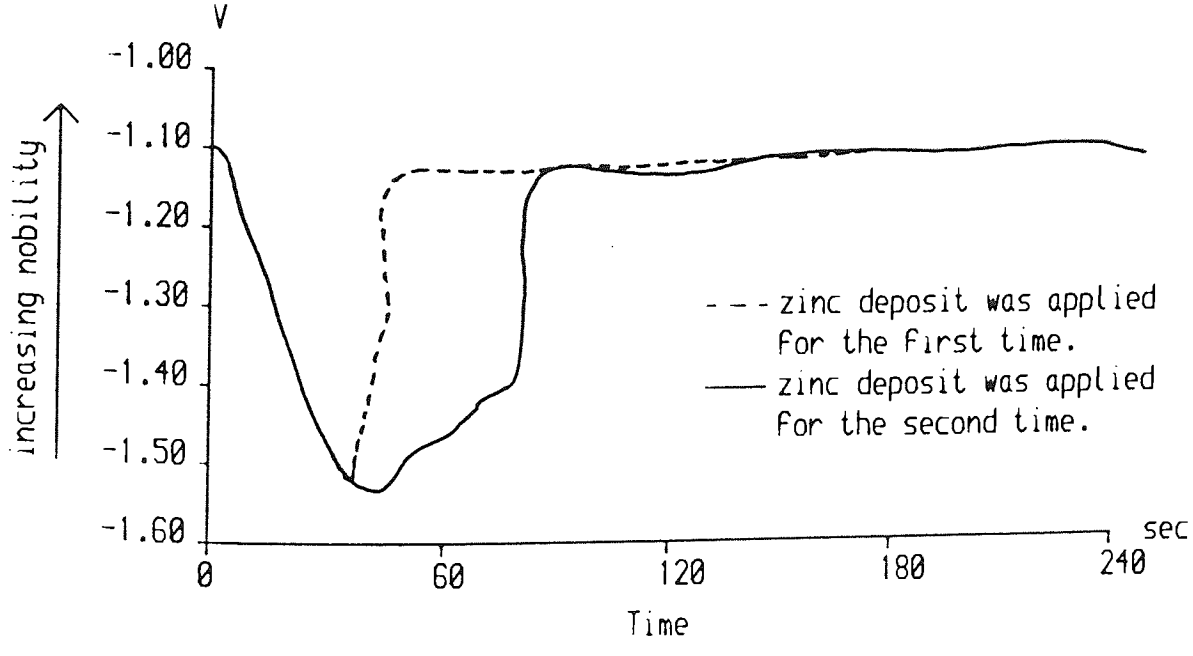


Fig.41 Potential-time curves recorded for alloy AZ61CC during the first and second zincating.

## 3.12 EFFECT OF OPERATING ZINCATE SOLUTION ELECTROLYTICALLY

Figs. 42, 43, and 44 show the relationship between film weight gain and immersion time for alloy AZ61CC when the zincate solution was operated electrolytically using 0.5, 1.0 and 2.0 $Adm^{-2}$ respectively. Two sets of samples were used with each current density. One set of samples was activated using the Canning sequence, and another set was activated using the Norsk Hydro sequence.

Samples pretreated with both sequences exhibited lower zinc growth rates with increase in time. It was also noted that when the electric current was increased, lower zinc deposits were obtained, contrary to expectations. This occurred with all the samples and under the two different conditions. However, samples maintained their characteristics in the various currents supplied. In order to show the effect of pretreatments, a sample which had no prior chemical treatment was used. Plate 27a shows the surface of an unpretreated alloy AZ61CC after a 5-minute electrolytic zinc deposition with a current density of 1.0 $Adm^{-2}$. Here, apparent complete zinc coverage was achieved and the zinc layer was thick and massive. However, traces of magnesium were still detected when the X-ray microanalysis of the surface was employed.

Contrasted against Plate 27 is Plate 27b, where the zinc deposit is very porous and sparing. The current density applied was 2.0 $Adm^{-2}$ and the sample was pretreated using the Canning sequence.

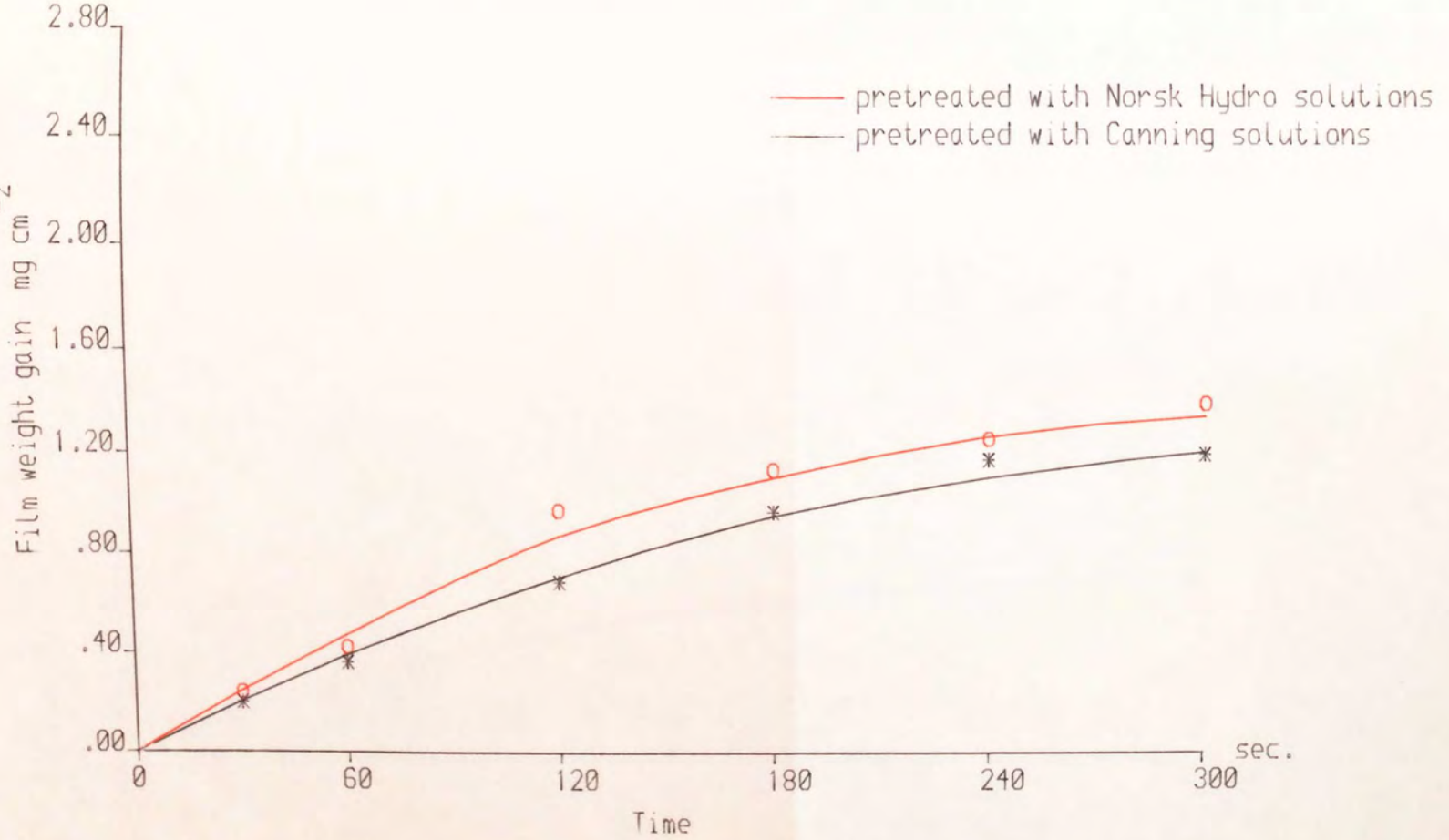


Fig.42 Relationship between film weight and immersion time for alloy AZ61CC pretreated using Norsk Hydro and Canning sequences with 0.5 A dm$^{-2}$ electrolytic immersion dips in zincate solution.

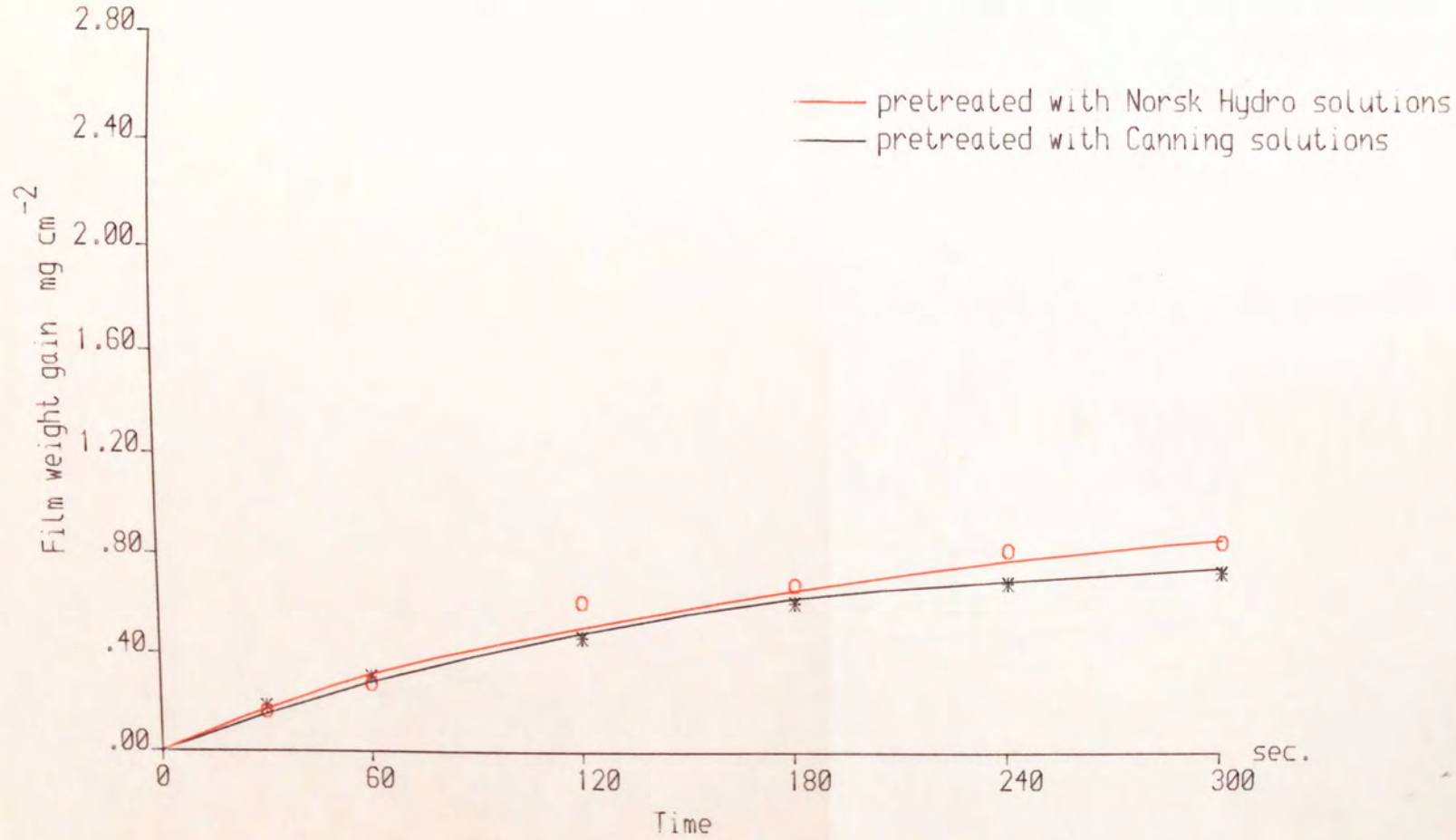


Fig.43 Relationship between film weight and immersion time for alloy AZ61CC pretreated using Norsk Hydro and Canning sequences with 1.0 A dm$^{-2}$ electrolytic immersion dips in zincate solution.

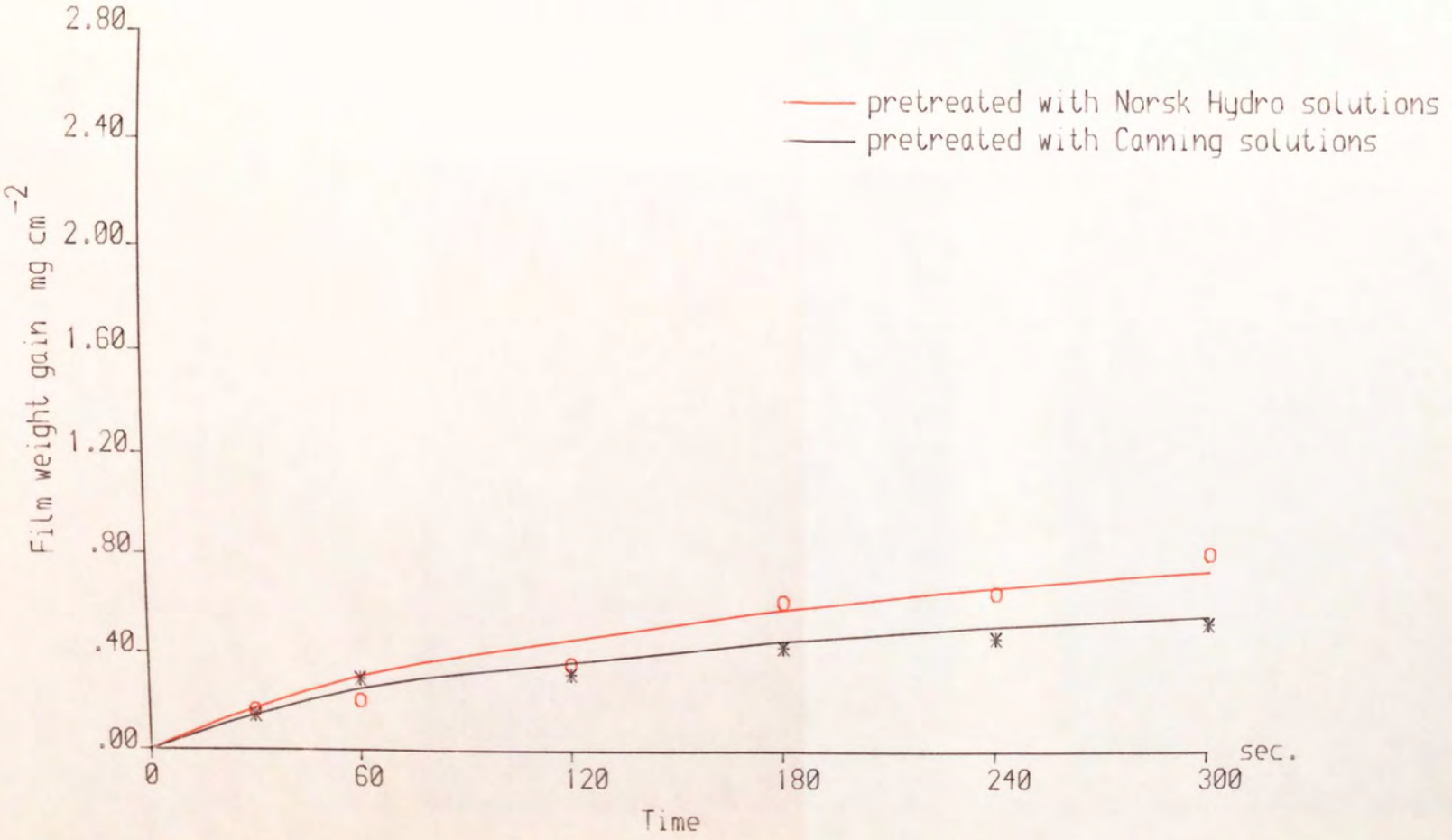


Fig.44 Relationship between film weight and immersion time for alloy AZ61CC pretreated using Norsk Hydro and Canning sequences with 2.0 A dm$^{-2}$ electrolytic immersion dips in zincate solution.

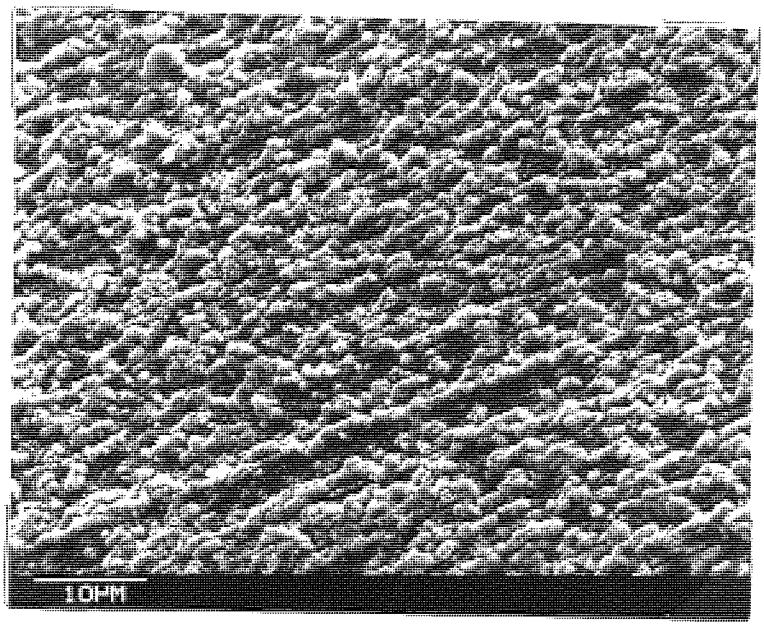


a

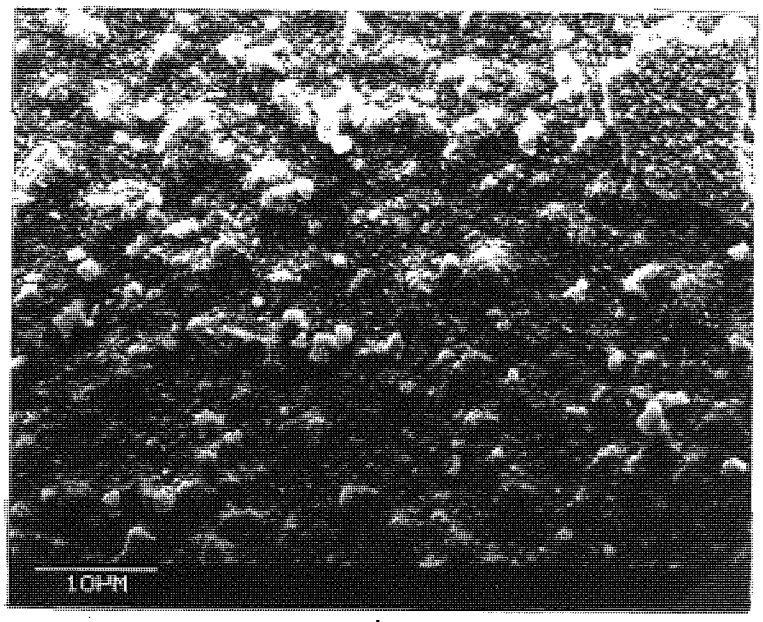


b

Plate 27 Surface appearance of alloy AZ61CC after 5 min. electrolytic zinc deposition.

a) Alloy AZ61CC received no prior chemical treatment and was immersed into the zincate solution for 5 min. operated electrolytically at 1.0 $Adm^{-2}$.
b) Alloy AZ61CC pretreated using Canning solutions and was immersed into the zincate solution for 5 min. operated electrolytically at 2.0 $Adm^{-2}$.

## 3.13 ADHESION TESTING

The samples for thermal cycling and peel testing were carefully pretreated and subsequently plated as described in Chapter 2.

### 3.13.1 THERMAL CYCLING TEST

The quality of the deposits on castings from all tests was evaluated, based on the following criteria:

(a) Visual appraisal of the Cu/Ni deposits immediately after deposition.

(b) Heat test at 250 °C for 20 minutes followed by quenching in water at 20-25 °C.

The evaluated samples were divided into 4 classes:

1. Deposits of good quality, e.g. no blistering and good brightness.
2. No blisters in the coating but dull surface.
3. Small blister formation.
4. Extremely poor adhesion, i.e. failure in the coating.

The results are shown in Table 8.

Table 8 QUALITY OF Cu + Ni COATING PRIOR TO AND AFTER THERMAL CYCLING TESTING

| Pretreatments | Alloy AZ61 cold chamber | | Alloy AZ91 cold chamber | | Alloy AZ91 hot chamber | |
|---|---|---|---|---|---|---|
| | Prior to heat test | Adhesion after heat test | Prior to heat test | Adhesion after heat test | Prior to heat test | Adhesion after heat test |
| Standard Dow | 2 | 3 | 2 | 3 | 2 | 4 |
| Modified Dow 1 | 2 | 2&3 | 2 | 2&3 | 2 | 2&3 |
| Modified Dow 2 | 3 | - | 3 | - | 3 | - |
| Standard Norsk Hydro | 1 | 1&3 | 1 | 1&3 | 1&3 | 3 |
| Canning | 1 | 1 | 1 | 1 | 1&3 | 1&3 |

These numbers are defined on page 173 in the text.

All alloys plated using the standard Dow process had a rather dull appearance after bright nickel plating even prior to the thermal cycling test. After thermal cycling small blisters occurred at the edges of alloy AZ61 and AZ91 cold chamber casting samples, whilst big bubbles and blisters occurred on alloy AZ91 hot chamber samples, indicating extremely poor adhesion.

Again, good brightness could not be achieved by using either of the modified Dow pretreatment processes. (oxalic $\longrightarrow$ Kelco $\longrightarrow$ $NH_4HF$ $\longrightarrow$ zincate, or oxalic $\longrightarrow$ Kelco $\longrightarrow$ HF $\longrightarrow$ zincate). With the first modification small blisters were normally formed on most of the samples after heating, even though a few samples did maintain their quality after quenching. Thermal cycling tests were not carried out on samples plated using the second modification of the standard Dow process since blisters had already appeared immediately after electroplating.

With the Norsk Hydro pretreatments, all alloy samples showed reasonably good brightness immediately after electroplating with bright nickel. However, inconsistent results were obtained with the alloy AZ91 and AZ61 cold chamber samples after the thermal testing, i.e. some samples maintained their good quality coating whereas others still showed small blisters especially at the edges. The AZ91 hot chamber samples pretreated with this process had in fact shown less

blister formation compared with the previous pretreatment samples.

The castings provided by the Promagco Ltd. in Worcester were AZ91 hot chamber door handles. All the castings showed unsatisfactory surface quality e.g. cracks and porosity prior to, and after plating. Adhesion tests were therefore not carried out.

3.13.1.1 QUALITY OF CU/NI COATING WITH VARIATION OF THE SECONDARY STEP IN THE STANDARD NORSK HYDRO PRETREATMENT SEQUENCE

Table 9 shows the quality of Cu/Ni coatings on the alloy samples with variations of the secondary activation step in the Norsk Hydro pretreatment process prior to, and after thermal cycling test. The variations of the secondary activation step were operated at:

(a) 10-200 g/l of potassium pyrophosphate.

(b) 0-50 g/l of sodium carbonate.

(c) 20-80 $^{o}$C.

It appears that the conditions at 200 g/l of potassium pyrophosphate + 50 g/l of sodium carbonate at temperature 75-80 $^{o}$C achieved the best results. Alloy AZ91 hot chamber

appeared to be the most difficult alloy on which to achieve good adhesion, whereas alloy AZ61 cold chamber exhibited higher adhesion with the coating and was even slightly superior to alloy AZ91 cold chamber in that respect.

Table 9 QUALITY OF Cu + Ni COATING WITH VARIATION OF THE SECONDARY ACTIVATION STEP IN THE NORSK HYDRO PRETREATMENT PRIOR TO AND AFTER THERMAL CYCLING TESTING.

| Test | Secondary activation step | | | Alloy AZ61 Cold Chamber | | Alloy AZ91 Cold Chamber | | Alloy AZ91 Hot Chamber | |
|---|---|---|---|---|---|---|---|---|---|
| | Conc. of $K_4P_2O_7$ g/l | Conc. of $NaCO_3$ g/l | Temp. $^oC$ | Prior | After | Prior | After | Prior | After |
| 1 | 10 | - | 55 | 1 | 3 | 1 | 3 | 1 | 3 |
| 2 | 10 | - | 80 | 1 | 1&3 | 1 | 1&3 | 1 | 1&3 |
| 3 | 60 | 15 | 55 | 1 | 1&3 | 1 | 1&3 | 1 | 1&3 |
| 4 | 60 | 15 | 80 | 1 | 1&3 | 1 | 1&3 | 1 | 1&3 |
| 5 | 110 | 30 | 55 | 1 | 1&3 | 1 | 1&3 | 2 | 2&3 |
| 6 | 110 | 30 | 80 | 2 | 2&3 | 2 | 2&3 | 2 | 2&3 |
| 7 | 160 | 40 | 55 | 1 | 3 | 2 | 2 | 2 | 3 |
| 8 | 160 | 40 | 80 | 2 | 2 | 2 | 2 | 2 | 2 |
| 9 | 210 | 50 | 55 | 1&2 | 1&2 | 1&2 | 1&2 | 1&2 | 1&2 |
| 10 | 210 | 50 | 80 | 1&2 | 1&2 | 1&2 | 1&2 | 1&2 | 1&2 |

These numbers are defined on page 173 in the text.

## 3.14 PEEL ADHESION TESTING

Plate 28 shows the Instron tensile testing machine, which is the instrument used for the peel adhesion tests. Peel tests were not carried out after the Dow pretreatment process because the adhesion level was very low. The results of the peel adhesion tests on the plated copper coating on the alloy test samples with different secondary activation conditions in the Norsk Hydro pretreatment sequence are shown in Table 10.

Test 1 was performed using low concentrations of potassium pyrophosphate and sodium carbonate whereas Tests 2 to 4 were all performed using the same chemicals but with higher concentrations. The latter tests, however, were performed at various temperatures. Test 5 was carried out using different chemicals at a temperature of 75 °C in the secondary activation step, and this was designated as the Canning process. The details of the process were described in previous sections.

From the results, it is apparent that higher adhesion values were obtained for alloy AZ91 cold chamber castings than for the alloy AZ91 hot chamber castings. This is consistent with the previous observation of the relatively better performance of the cold chamber AZ91 alloy castings in the thermal cycling tests discussed earlier (Section 3.7.1).

Comparing the adhesive performance of alloy AZ61 cold chamber castings with AZ91 cold chamber castings, it appeared that the former has been able to sustain a better adhesion (7.72 - 9.65 $KNm^{-1}$) with copper plating than the latter (7.33 - 8.88 $KNm^{-1}$).

It would also appear that performing the secondary activation step in the Norsk Hydro process at higher concentrations of potassium pyrophosphate (200 g/l) and higher temperatures gives slightly better adhesion (4.25-5.79) than at the recommended standard conditions of lower concentration and temperature, when adhesion values of *around 3.86* $KNm^{-1}$ were obtained. However, the appearance of the plated samples pretreated with the standard condition showed better brightness compared with those pretreated at the higher concentration and temperature.

It is apparent that all samples pretreated with the Canning process achieve the best peel adhesion values. The appearance of the failure surfaces after the adhesion test has been studied using the scanning electron micrographs. The results are reported below.

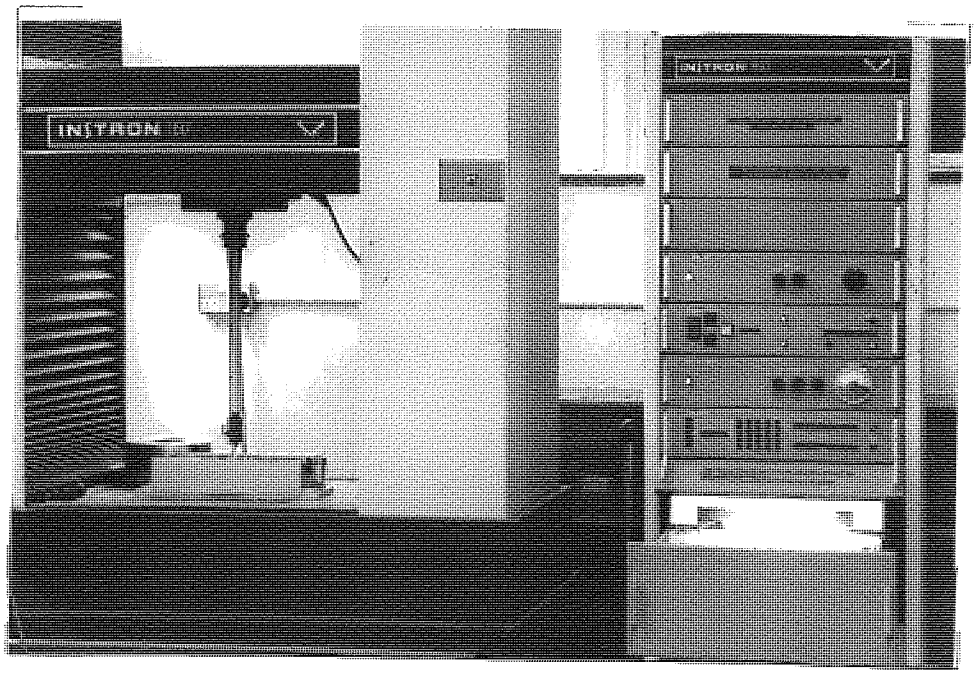


a

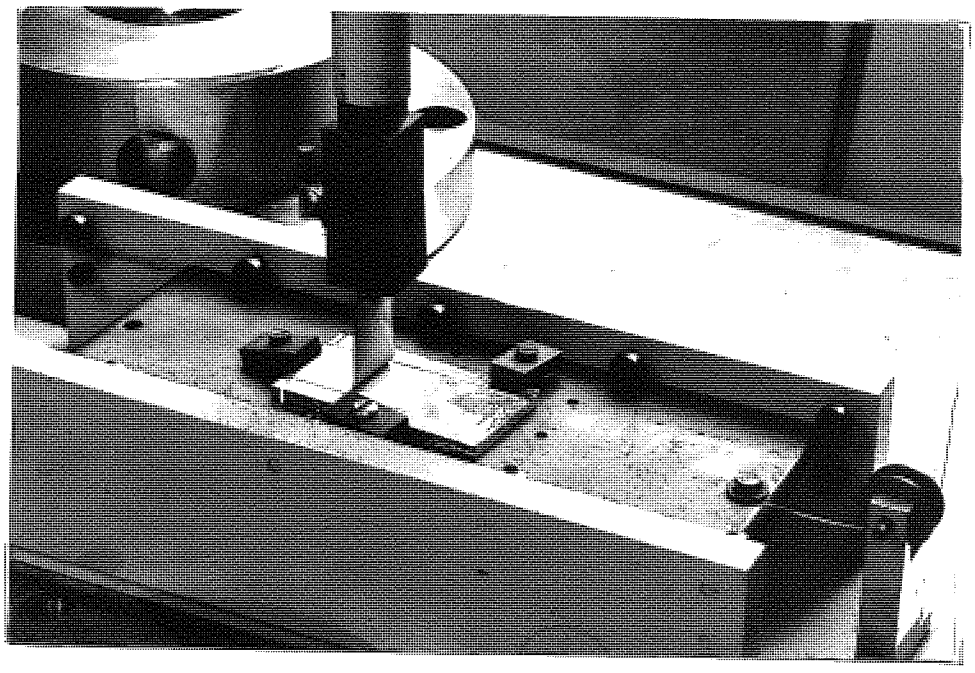

b

Plate 28 Peel adhesion test instrument.

a) Instron tensile testing machine connected with a chart recorder.
b) Peel adhesion test attachment used on 'Instron tensile testing machine.

Table 10 PEEL ADHESION VALUES OF COPPER COATING ON ALLOY SAMPLES WITH DIFFERENT PRETREATMENT PROCESS.

| Test | Process | Secondary activation condition | Alloy AZ61 cold chamber KN $m^{-1}$ | Alloy AZ91 cold chamber KN $m^{-1}$ | Alloy AZ91 hot chamber KN $m^{-1}$ |
|---|---|---|---|---|---|
| 1 | Standard Norsk Hydro | 60 g/l $K_4P_2O_7$ + 15 g/l $Na_2CO_3$ at temp. 55°C | 4.25 - 5.79 | 2.70 - 5.45 | 0.78 |
| 2 | Norsk Hydro | 210 g/l $K_4P_2O_7$ + 50 g/l $Na_2CO_3$ at temp. 20°C | 0.50 - 2.00 | 0.49 - 1.20 | 0.20 - 0.96 |
| 3 | Norsk Hydro | 210 g/l $K_4P_2O_7$ + 50 g/l $Na_2CO_3$ at temp. 55°C | 4.25 | 3.47 | 1.10 |
| 4 | Norsk Hydro | 210 g/l $K_4P_2O_7$ + 50 g/l $Na_2CO_3$ at temp. 80°C | 5.79 - 6.56 | 6.56 | 1.93 - 2.70 |
| 5 | Canning | 70 g/l NaBorax + 40 g/l $NaP_2O_7$ + 20 g/l KF at temp. 75°C | 7.72 - 9.65 | 7.33 - 8.88 | 1.54 - 5.01 |

### 3.14.1 APPEARANCE OF FAILURE SURFACES AFTER PEEL ADHESION TESTING

Micrograph (a) of Plate 29 shows the failure surface of the substrate after the peel adhesion test using a specimen of alloy AZ61 cold chamber casting which was pretreated with the Norsk Hydro process corresponding to Test 4 shown in Table 10. Micrograph (b) of Plate 27 shows the failure surface of the substrate after the peel adhesion test on the same alloy but pretreated with the Canning process corresponding to Test 5 in Table 10.

Both surfaces exhibit the characteristic of ductile failure, that is the crest-like features on the failure interfaces. X-ray spectra obtained with the aid of the X-ray analysis attachment show that failure took place in the sub-surface of the magnesium alloy substrate since only the presence of magnesium and aluminium could be detected.

The micrograph shown in Plate 29a illustrates that the foil had been peeled evenly from the substrate whilst micrograph 29b shows a comparatively rougher surface in that larger pieces of magnesium were peeled away from the substrate. The corresponding back surfaces of the copper foils are shown in Plates 30a and 30b respectively, although it was not possible to have them correspond exactly in location. Magnesium is present on both of the copper foil surfaces.

Depending on adhesion, differing amounts of substrate were detached on the back of the peeled foil.

The levels of adhesion for alloy AZ61 cold chamber castings using the Norsk Hydro process and the Canning process varied from 5.79 to 9.65 $KNm^{-1}$ respectively. Both samples revealed ductile failure characteristics.

Samples treated using the double dip sequence were plated with copper, and peel tests were carried out. Although the appearance was promising, the adhesion levels achieved were virtually zero. The failure surface of AZ61CC and its peeled off copper foil after peel adhesion testing are shown in Plates 31a and 31b respectively. The presence of magnesium on the back of the peeled off copper foil could not be detected.

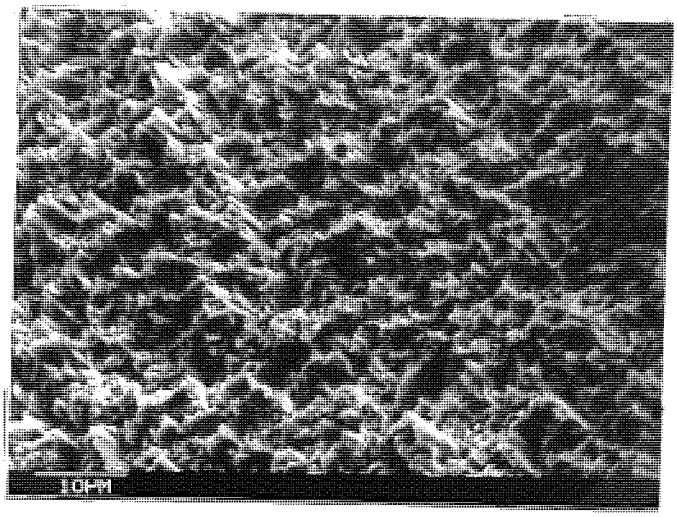


a

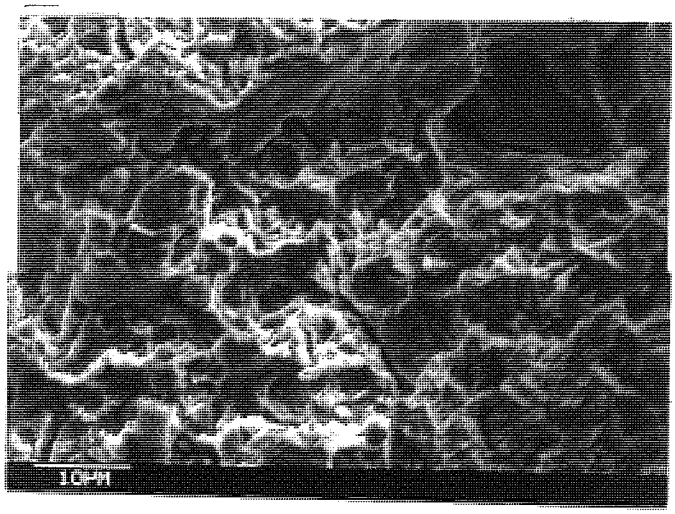


b

Plate 29 The failure surfaces of alloy AZ61CC after peel adhesion testing, corresponding to process 4 and 5 in table 10.

a) Norsk Hydro secondary activation at 80°C using a solution containing 210 g/l $K_4P_2O_7$ and 50 g/l $Na_2CO_3$ . Adhesion 5.79 $KNm^{-1}$.
b) Canning sequence. Adhesion 9.65 $KNm^{-1}$.

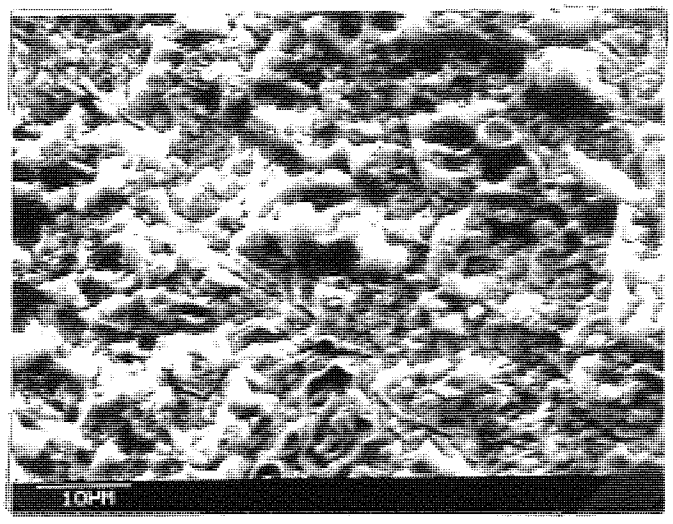


a

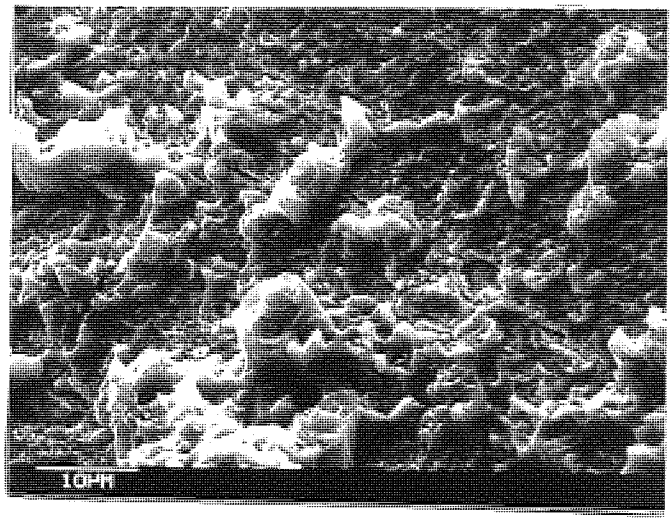


b

Plate 30 The back of the peeled copper foil after peel adhesion testing of alloy AZ61CC.

a) Norsk Hydro secondary activation at 80°C using a solution containing 210 g/l $K_4P_2O_7$ and 50 g/l $Na_2CO_3$. Adhesion 5.79 $KNm^{-1}$.
b) Canning sequence. Adhesion 9.65 $KNm^{-1}$.

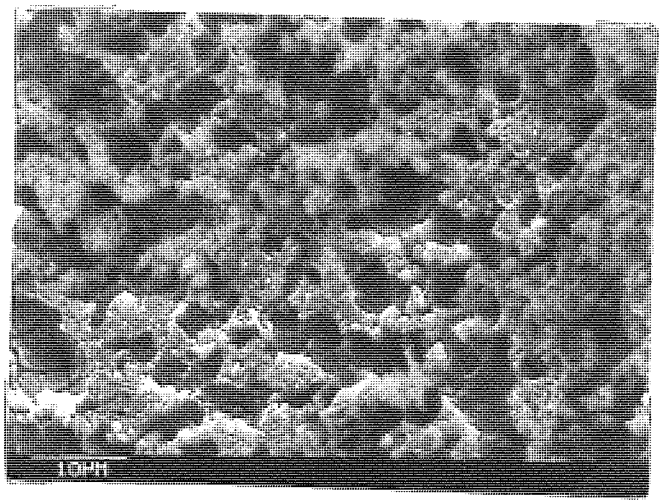


a

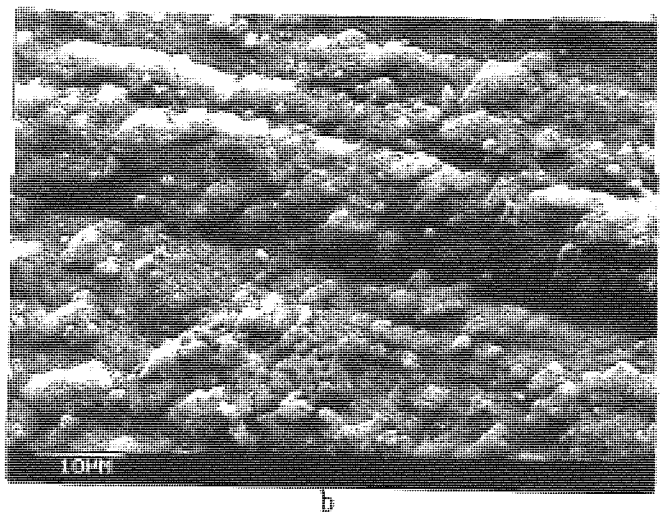


b

Plate 31 The failure surface of AZ61CC and its peeled off copper foil after peel adhesion testing. Nil adhesion value was recorded. The sample was pretreated using the double dip sequence.

a) The failure surface.
b) The back of the peeled off copper foil.

## 3.15 CORROSION TESTING

Three pretreatment processes were employed in this corrosion testing programme. They were: the Canning process coded as B1; the standard Norsk Hydro process coded as B2; and the Norsk Hydro process with the higher concentration and temperature secondary activation coded as B3. Four coating systems were applied as described in Section 2.11.2. Three types of alloys were involved. They are the AZ91 and AZ61 cold chamber casting panels and AZ71 hot chamber paper knives. For each coating system, 2 samples of each alloy were used.

Results are illustrated in Plates 32 to 37 where samples plated with the four different coating systems after 2 cycles (48 hours) of Copper Acetic Acid Salt Spray testing are displayed. The corresponding plated samples prior to corrosion testing are also shown.

### 3.15.1 ASSESSMENT OF CORROSION BEHAVIOUR

All the corroded samples were assessed visually using the A.S.T.M. B537-70 rating method as mentioned earlier in Section 2.14. Examples of the A.S.T.M. rating method are shown in Fig. 45. With reference to the AZ71 hot chamber

paper knives, only the blades of the knives were assessed because some polishing products left in the recessed areas of the indented handles were very resistant to removal. Spots or defects therefore resulted and it was decided that they should not be counted.

It was apparent that the samples pretreated with the Canning process achieved the best brightness compared with the other two processes. On the other hand, since the testing involved quite a few factors that may affect the appearance and the corrosion results, analysis of variance was applied with the aid of a computer.

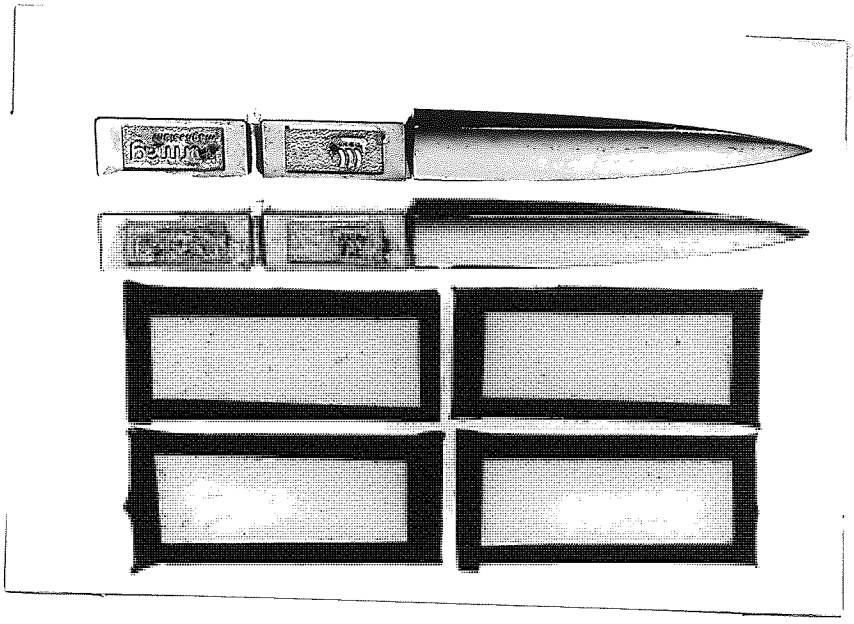

a

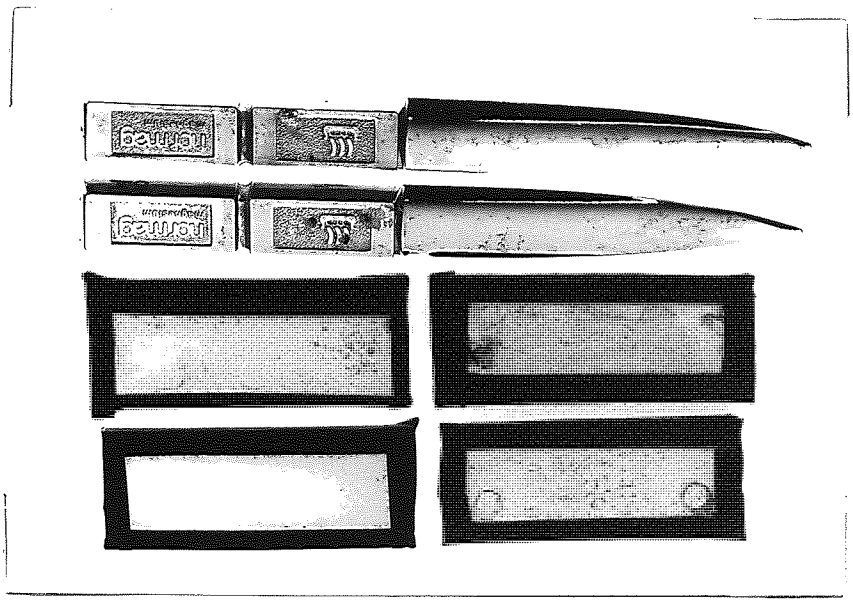

b

Plate 32 Appearance of alloys AZ61CC, AZ91CC and AZ71HC after 48 hours of CASS test, pretreated using Canning sequence.

a) Alloys coated with Bright Ni + decorative Cr.
b) Alloys coated with Bright Ni + microporous Cr.

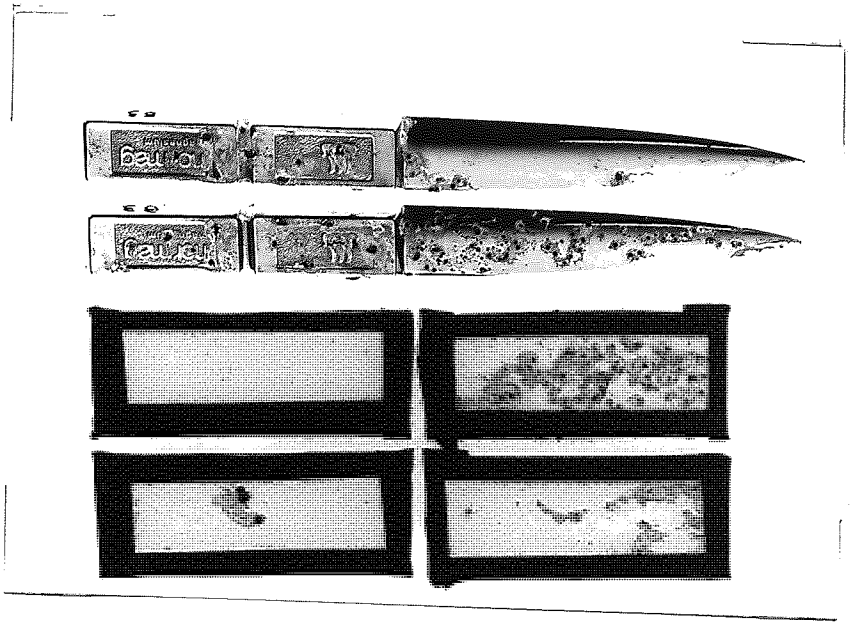

a

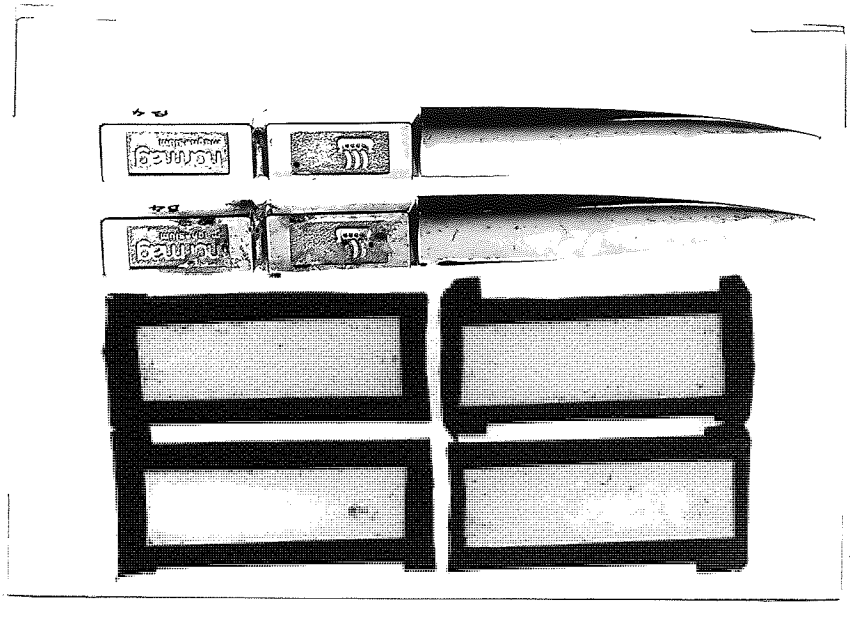

b

Plate 33 Appearance of alloy AZ61CC, AZ91CC and AZ71HC after 48 hours of CASS test, pretreated using Canning sequence.

a) Alloys coated with Duplex Nickel + decorative Cr.
b) Alloys coated with Semi-bright Ni + microporous Cr.

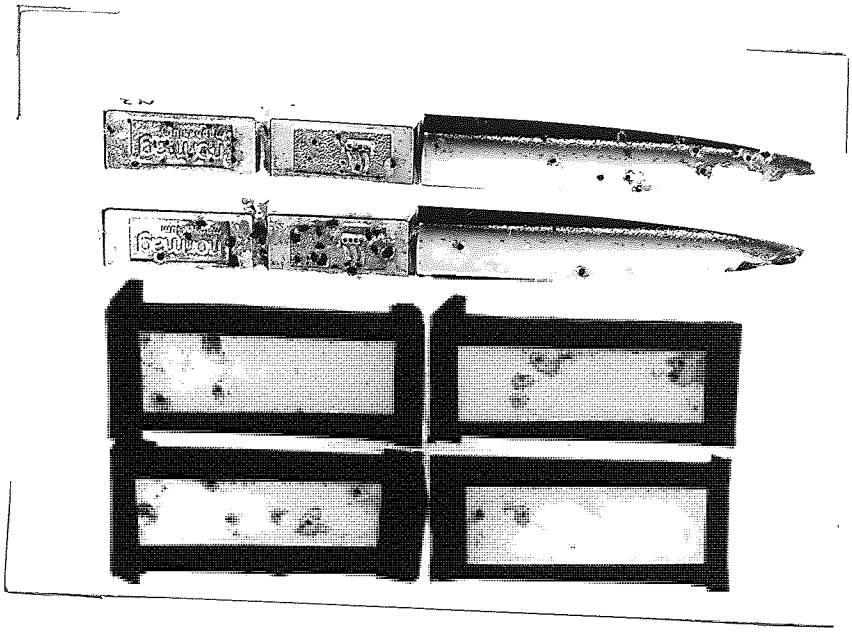

a

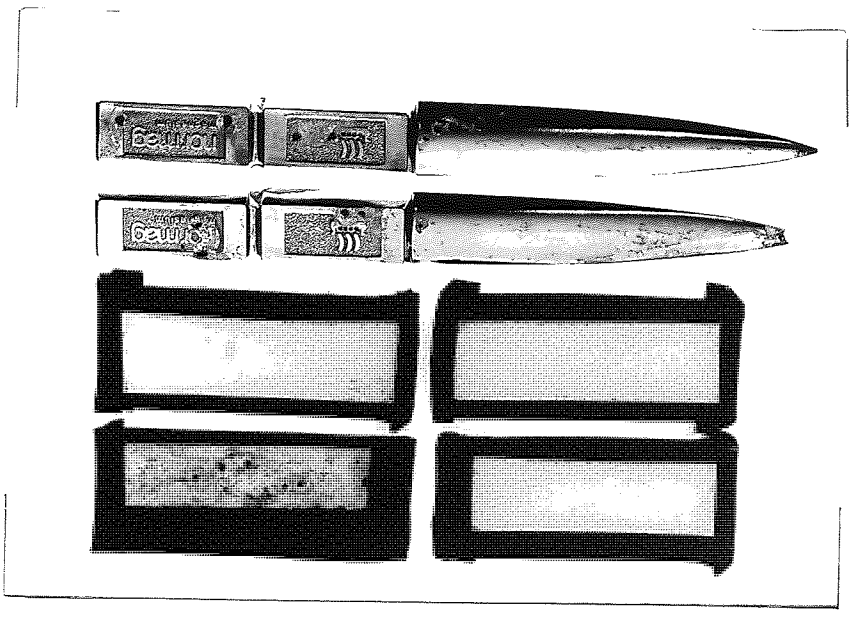

b

Plate 34 Appearance of alloys AZ61CC, AZ91CC and AZ71HC after 48 hours of CASS test, pretreated using Norsk Hydro sequence.

a) Alloys coated with Bright Ni + decorative Cr.
b) Alloys coated with Bright Ni + microporous Cr.

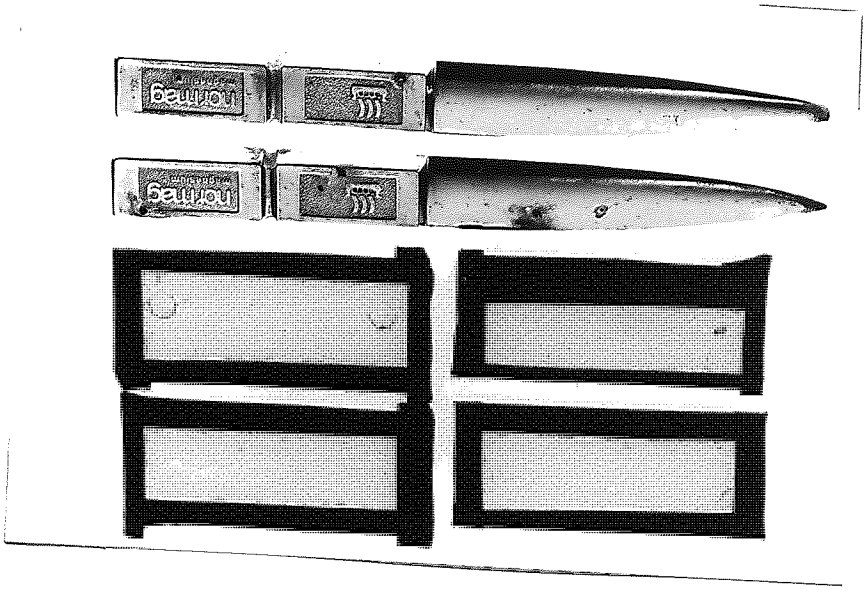

a

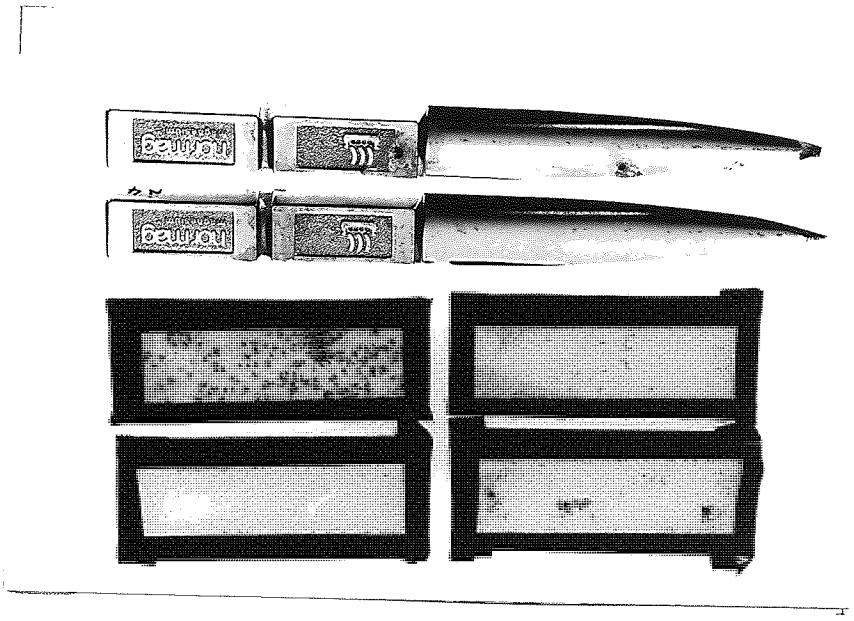

b

Plate 35 Appearance of alloys AZ61CC, AZ91CC and AZ71HC after 48 hours of CASS test, pretreated using Norsk Hydro sequence.

a) Alloys coated with Duplex Ni + decorative Cr.
b) Alloys coated with Semi bright Ni + microporous Cr.

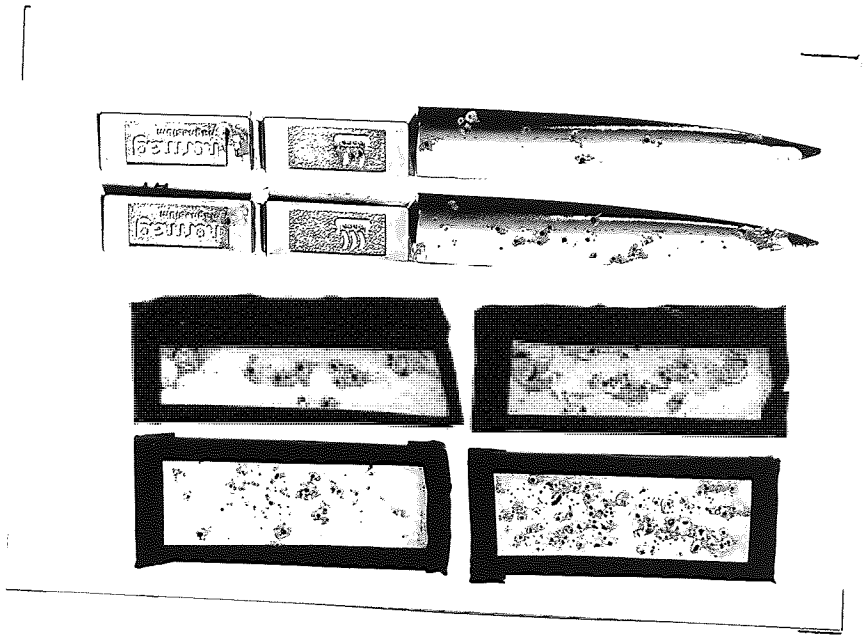

a

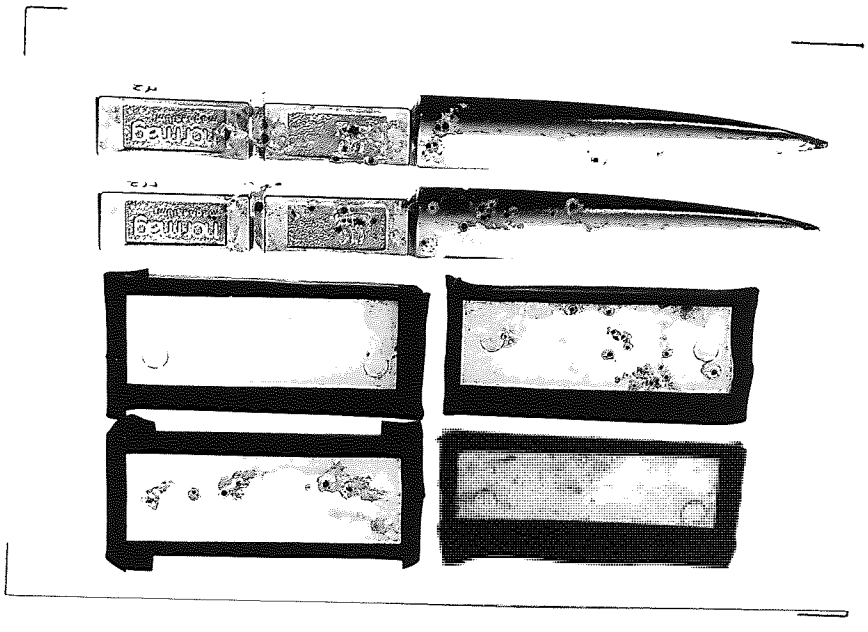

b

Plate 36 Appearance of alloys AZ61CC, AZ91CC and AZ71HC after 48 hours of CASS test, pretreated using Norsk Hydro sequence, operated at a higher temperature and concentration in the secondary activation stage.

a) Alloys coated with bright Ni + decorative Cr.
b) Alloys coated with bright Ni + microporous Cr.

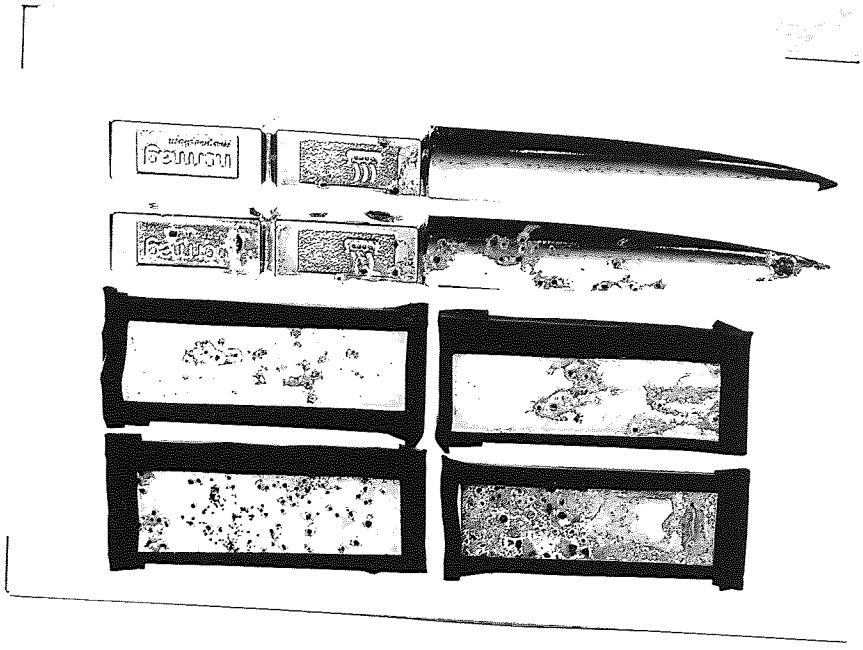

a

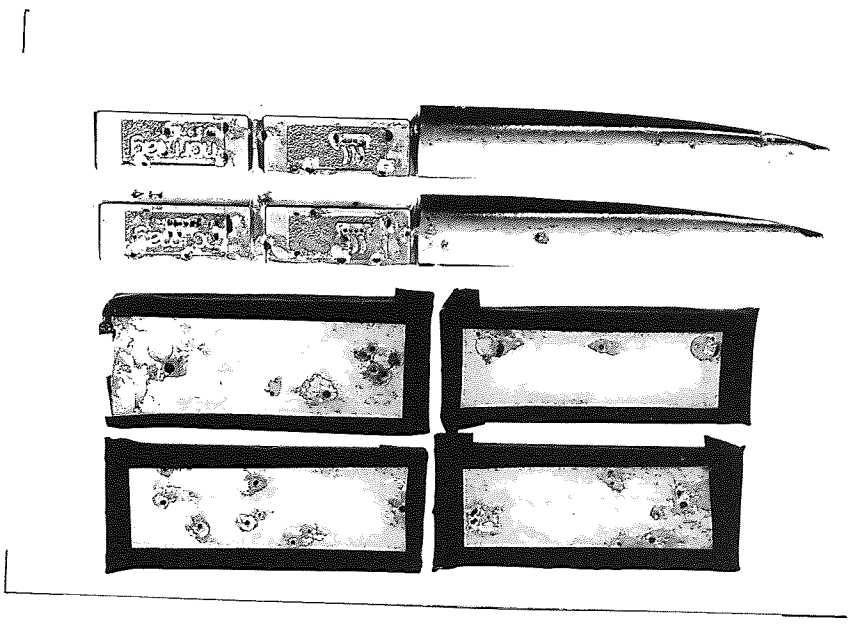

b

Plate 37 Appearance of alloys AZ61CC, AZ91CC and AZ71HC after 48 hours of CASS test, pretreated using Norsk Hydro sequence, operated at a higher temperature and concentration in the secondary activation stage.

a) Alloys coated with Duplex Ni + decorative Cr.
b) Alloys coated with semi bright Ni + microporous Cr.

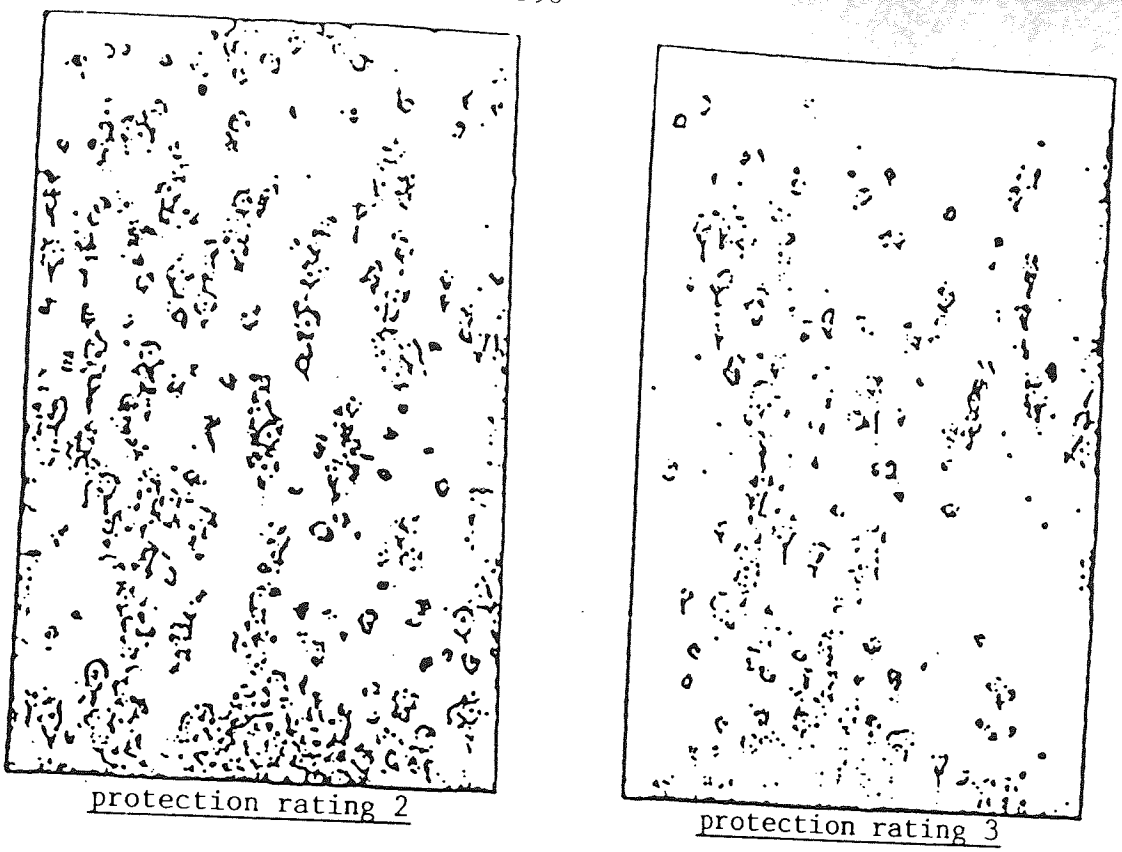


Examples of Corrosion Appearance.

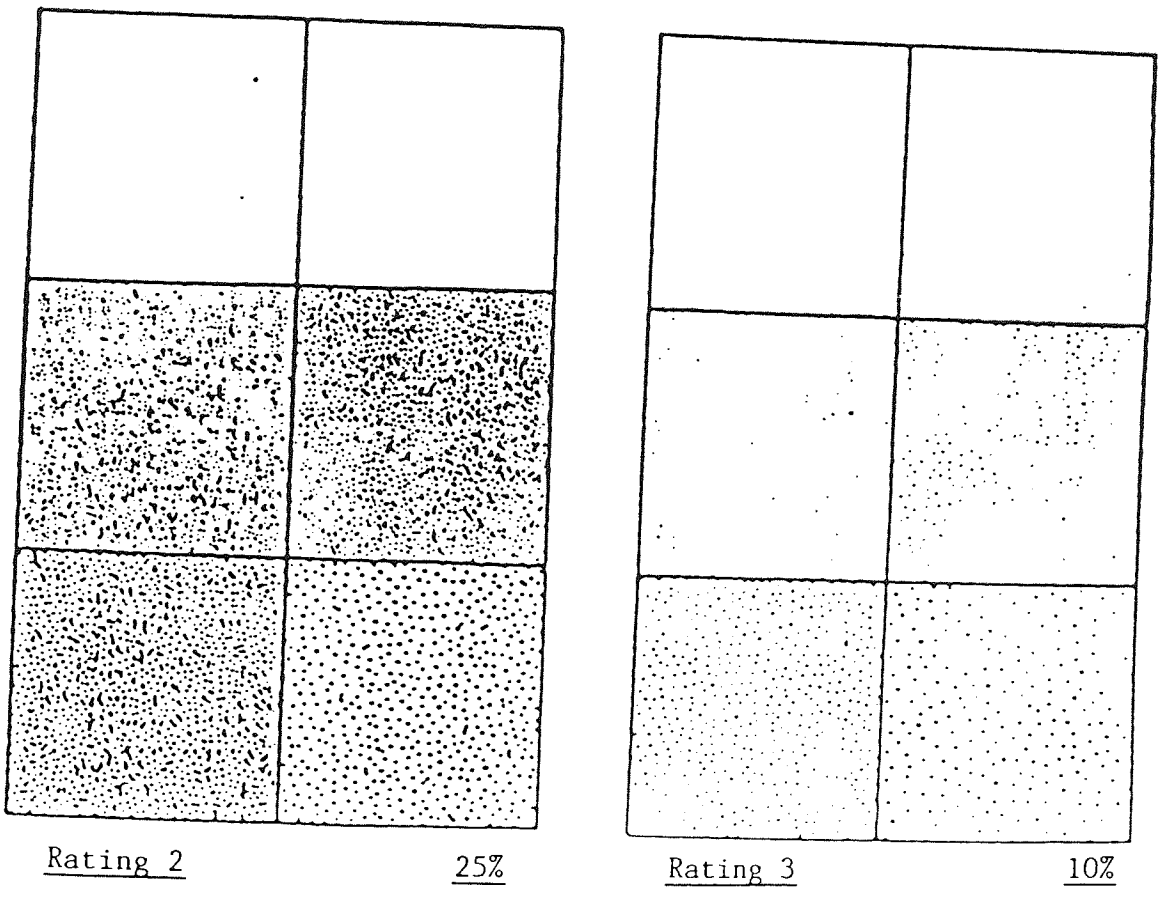


Examples of Dot Charts

Fig. 45 Examples of standards used for the ASTM Rating Method[102].

### 3.15.2 ANALYSIS OF VARIANCE

The overall objective of this analysis was to obtain a general idea of how the response variable is affected by changes in the different factors.

Factors involved with the corrosion test were:

1. Four coating systems, i.e. A has 4 levels.
2. Three pretreatments, i.e. B has 3 levels.
3. Three alloys, i.e. C has 3 levels.

The data were tabulated in Table 11 and the summary table is shown in Table 12. After the F-ratios had been calculated (as shown in Table 12), the significant factors were found to be the B factor and the AB factor.

B - pretreatment factor

AB - coating systems + pretreatment factors

Therefore, it indicates that the C factor (i.e. different alloys) had played a very insignificant role in this test. The Post-Hoc comparison for B and AB is shown below:

For variable = B

| VARIABLE | A | B | C | |
|---|---|---|---|---|
| LEVEL | 0 | 1 | 0 | mean = 9.25 |
| LEVEL | 0 | 2 | 0 | mean = 8.92 |
| LEVEL | 0 | 3 | 0 | mean = 7.63 |

FOR VARIABLE = AB

| VARIABLE | A | B | C | |
|---|---|---|---|---|
| LEVEL | 1 | 1 | 0 | mean = 10 |
| LEVEL | 1 | 2 | 0 | mean = 8.5 |
| LEVEL | 1 | 3 | 0 | mean = 5.67 |
| LEVEL | 2 | 1 | 0 | mean = 10 |
| LEVEL | 2 | 2 | 0 | mean = 8.67 |
| LEVEL | 2 | 3 | 0 | mean = 8.83 |
| LEVEL | 3 | 1 | 0 | mean = 7.17 |
| LEVEL | 3 | 2 | 0 | mean = 9.67 |
| LEVEL | 3 | 3 | 0 | mean = 7.83 |
| LEVEL | 4 | 1 | 0 | mean = 9.83 |
| LEVEL | 4 | 2 | 0 | mean = 8.83 |
| LEVEL | 4 | 3 | 0 | mean = 8.17 |

The 2 tables above can be shown graphically for comparison.

(see Figs. 46 and 47.)

As shown in Fig. 46, it is apparent that the Canning process is the best pretreatment process, and the average rating of 9.25 was achieved after the corrosion testing. The secondary activation of the Norsk Hydro process with the higher concentration and temperature had in fact achieved the lowest rating with an average of 7.63.

In Fig. 47, both A and B factors are involved. With reference to the B1 curve, (i.e. samples pretreated with the Canning process), a significant and unexpected decrease in rating was achieved with samples coated with the duplex system AS. However, the rest of the samples coated with A1, A2 and A4 systems have shown good corrosion resistance. On the other hand, samples coated with the same A3 systems but pretreated with the standard Norsk Hydro process (B2 curve) achieved the higher rating of 9.67 when compared with the samples coated with A1, A2 or A3 systems which obtained average ratings between 8.5 and 8.83. The lowest rating of average 5.67 was obtained with samples pretreated with the B3 process and coated with the A1 system (B3 being the Norsk Hydro process with the higher concentration and temperature secondary activation and A1 being the bright nickel + decorative chromium system). The rest of the samples coated with the A2, A3 and A4 systems showed better corrosion resistance, with average ratings between 7.83 and 8.83.

Table 11 RESULTS AFTER 48 HOURS OF CASS TESTS

| | Canning | | | Norsk Hydro | | | Norsk Hydro with Higher Temp | | |
|---|---|---|---|---|---|---|---|---|---|
| | AZ71HC | AZ61CC | AZ91CC | AZ71HC | AZ61CC | AZ91CC | AZ71HC | AZ61CC | AZ91CC |
| Bright Ni + decorative Cr | 10,10 | 10,10 | 10,10 | 8,9 | 9,8 | 8,9 | 8,7 | 5,3 | 4,7 |
| Bright Ni + microporous Cr | 10,10 | 10,10 | 10,10 | 9,9 | 10,5 | 10,9 | 9,8 | 10,8 | 10,8 |
| Duplex Ni + decorative Cr | 8,4 | 8,9 | 10,4 | 10,9 | 10,10 | 10,9 | 10,8 | 9,6 | 7,7 |
| Semi bright Ni + microporous Cr | 10,10 | 10,9 | 10,10 | 10,9 | 9,10 | 10,5 | 9,9 | 8,7 | 8,8 |

Table 12 SUMMARY OF THE ANALYSIS OF VARIANCE INVOLVED IN THE C.A.S.S. CORROSION TEST

| Source of variance | Sum of square, X | Degree of freedom, Y | Mean square, X/Y | F ratio | $\alpha$ = 0.05 | $\alpha$ = 0.01 |
|---|---|---|---|---|---|---|
| A | 15.82 | 3 | 5.27 | 2.55 | | |
| B | 35.36 | 2 | 17.68 | 8.54 | | |
| AB | 57.64 | 6 | 9.61 | 4.64 | | |
| C | 2.78 | 2 | 1.39 | 0.67 | | |
| AC | 7.89 | 6 | 1.31 | 0.63 | | |
| BC | 8.55 | 4 | 2.14 | 1.03 | | |
| ABC | 16.78 | 12 | 1.40 | 0.68 | | |
| Error | 74.50 | 36 | 2.07 | | | |

The significant factors in this case are the B factor and AB factor, i.e. pretreatment factor and coating system + pretreatment factor.

F ratio = (mean square) / (error of mean square)

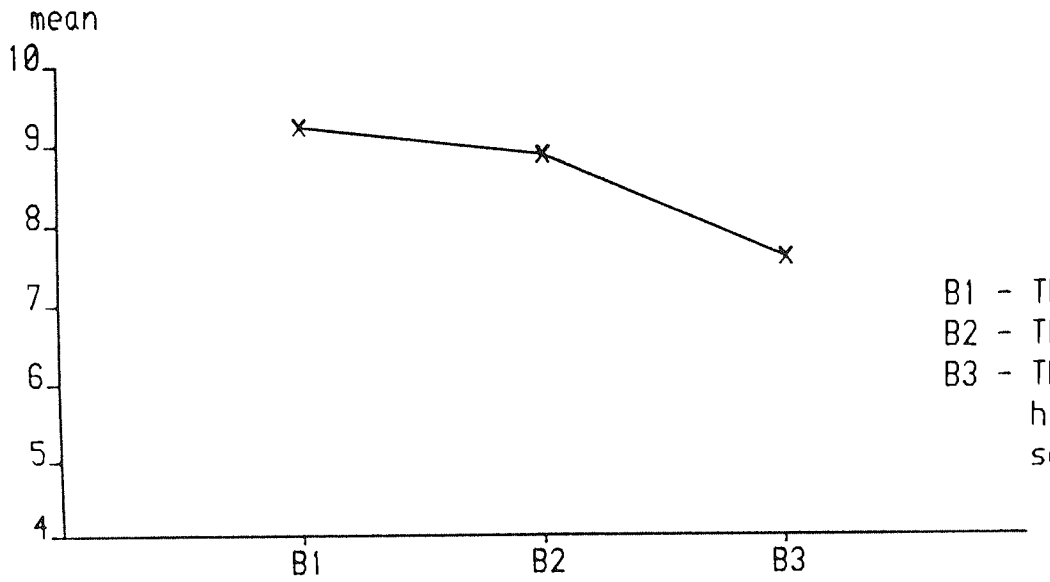


B1 - The Canning process.
B2 - The standard Norsk Hydro process.
B3 - The Norsk Hydro process with a higher concentration and temperature secondary activation step.

Fig.46 The post-Hoc comparison for factor B (pretreatment factor) which is one of the factors found to be significant in the C.A.S.S. corrosion test.

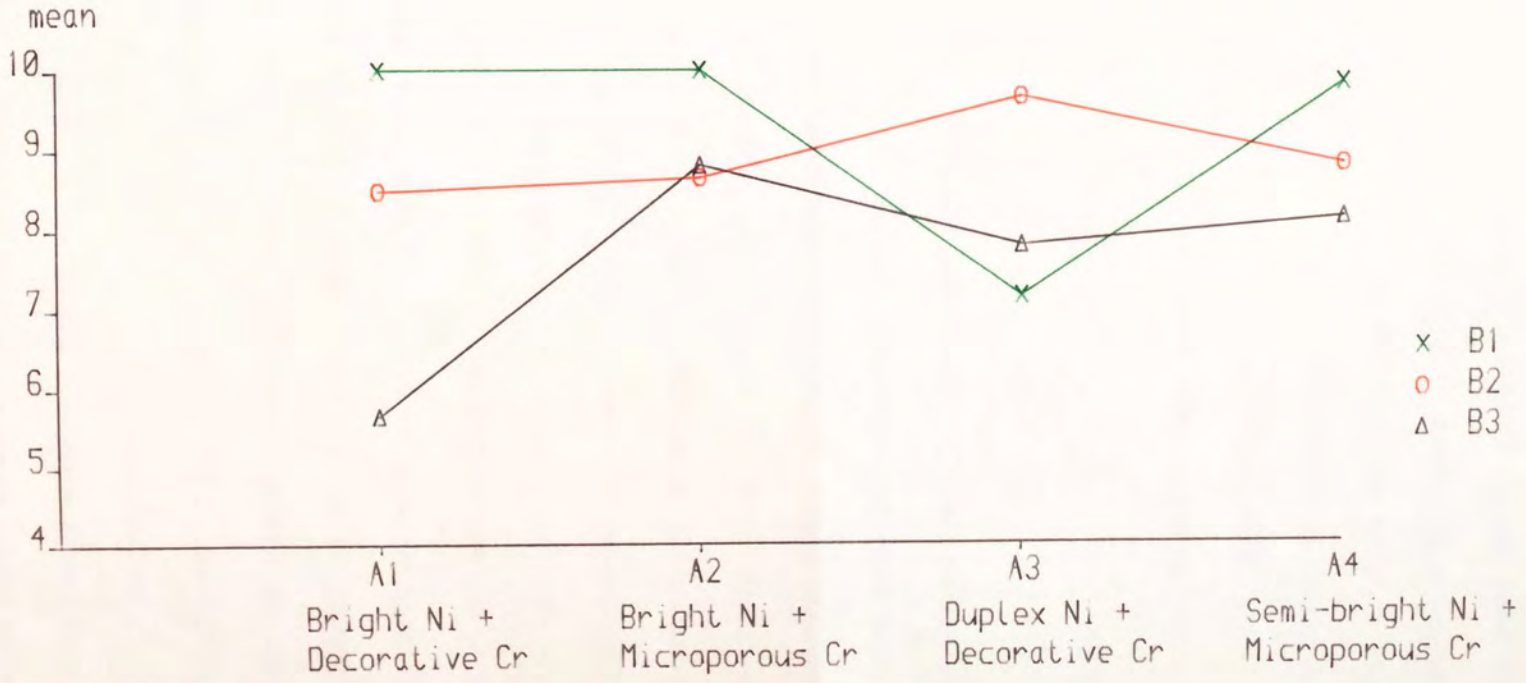


B1 - The Canning process.

B2 - The standard Norsk Hydro process.

B3 - The Norsk Hydro process with a higher temperature and concentration activation step.

Fig.47 The post-Hoc comparison for factor AB (coating systems + pretreatment factors) which is one of the factors found to be significant in the C.A.S.S. corrosion test.

### 3.15.3 EXAMINATION OF CORROSION TESTED SAMPLES

The plated samples of magnesium alloys were examined using the optical microscope and the scanning electron microscope. The large pits formed in some of the samples were studied in greater detail by the examination of cross-sections taken through pits. Sections through pits were made with a jeweller's hack saw and the samples were mounted in bakelite.

Plates 38a, b and c show some of the results of the optical microscopy examination, illustrating that most of the large pits formed were hemispherical in shape and that the attack was very severe and rapid in the underlying magnesium substrate. The attack started at different points at the top coating layer, and once it penetrated through the coatings, rapid preferential attack into the magnesium alloy took place, due to the large difference in nobility between substrate and coating. Plate 38 also clearly illustrates that the adhesion level was adequate to prevent exfoliation of the coating even when voluminous magnesium corrosion products were produced (Plate 39). The corrosion products formed were largely magnesium chloride which was identified with the aid of the X-ray analysis attachment. The cross-section of the AZ71 hot chamber paper knives (the blade part) shown in Plate 40 reveals the amount of porosity present within the casting itself.

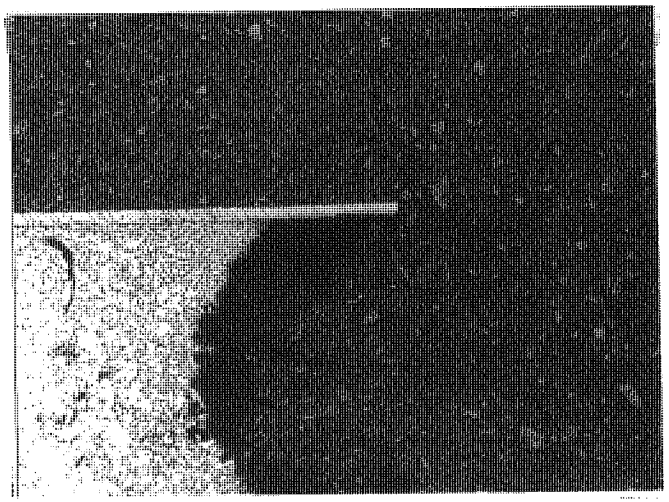

a

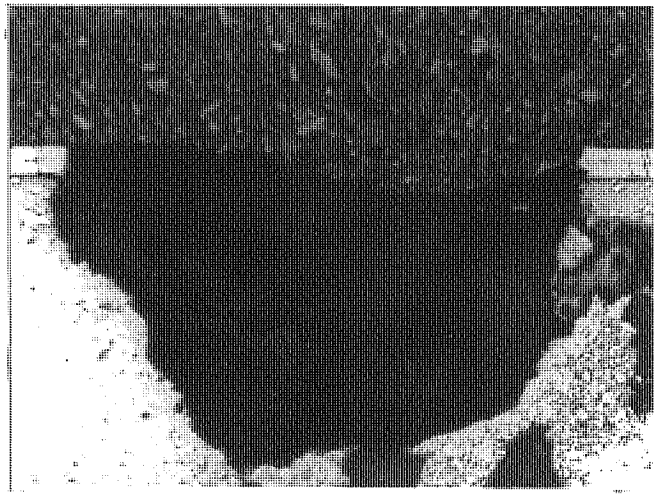

b

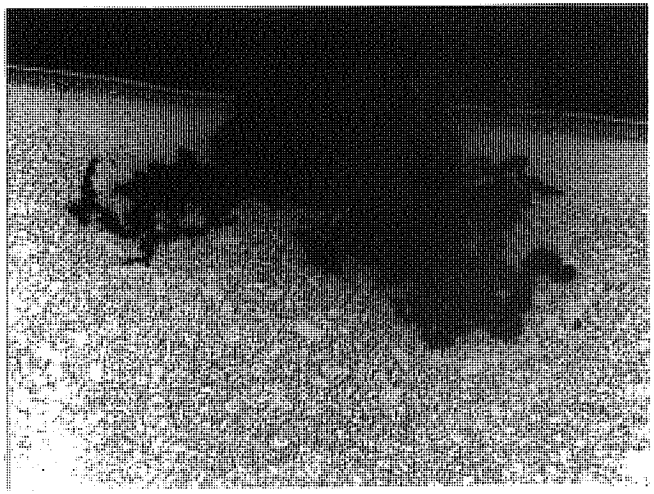

c

Plate 38 Cross sections of alloy samples after 48 hours of CASS test.

a) Alloy AZ61CC pretreated with Canning sequence and coated the Duplex system. (X35)

b) Alloy AZ91CC pretreated with Norsk Hydro sequence and coated with bright Ni + decorative Cr. (X80)

c) Alloy AZ91CC pretreated with Norsk Hydro sequence, operated at a higher temperature and concentration in the secondary stage, sample was coated with the duplex system. (X20)

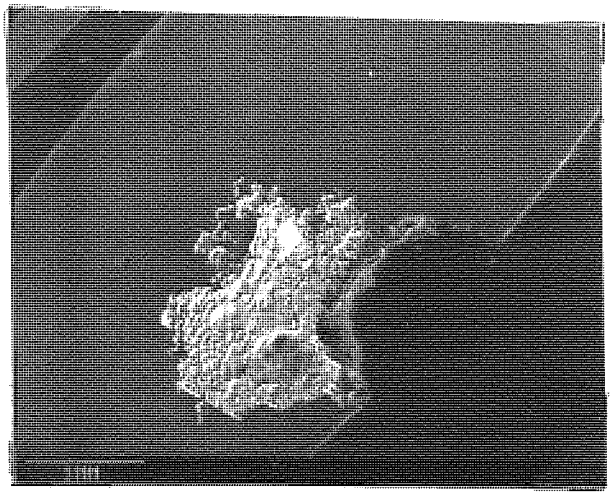

Plate 39 Corrosion products formed on alloy AZ91CC after 48 hours of CASS test, were found to be $MgCl_2$.

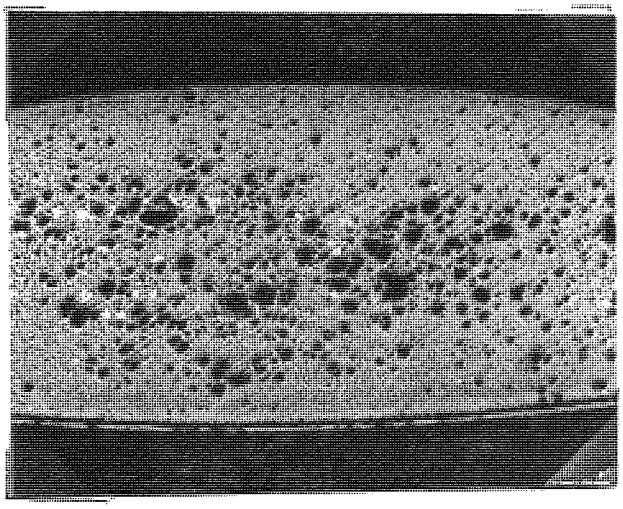

Plate 40 Cross section of AZ71HC knife showing porosity in the casting. (X30)

# CHAPTER 4 DISCUSSION OF RESULTS

Initial experiments were commenced using the published Dow and Norsk Hydro processing sequences. Various modifications were studied but ultimately the sequence termed Canning was found to be the most successful. The first three sections of the discussion deal with the effect of the various pretreatments.

## 4.1 THE DOW PROCESS

Each of the standard Dow pretreatment steps prior to the zincating, etched the sample surface to a certain extent, as shown in Plate 3 in Section 3.4. The chromic acid dip was to remove all the surface contaminants and the sample was then protected by the newly formed chromic oxide film, which was subsequenctly dissolved in the activation solution. It was observed that after 40-60 seconds of immersion in the activation solution, the sample surface became passive and further etching ceased. Formation of fluoride film was thought to be the reason for passivity.

The standard Dow zincating stage was in fact the basis of all the pretreatment processes employed. The zincating process involved a chemical reaction between magnesium and zinc ions in solution. The driving force for the reaction was the difference in their electrodepotentials. The specimen performed a dual role as a cathode and an anode. Zinc was deposited at cathodic regions on the surface while at anodic ones magnesium dissolution occurred, resulting in pitting.

In the modification of the Dow process, the 1% oxalic acid resulted in preferential attack on the magnesium-rich phases. The purpose of using Kelco in the cleaning stage was to clean and activate the aluminium constituents in the magnesium alloys. However, micrographs a and b in Plate 4 show further etching on magnesium-rich surfaces, revealing a greater concentration of aluminium-rich particles. The zinc coating deposited with this sequence was porous as shown in Plate 4d. In the second modification, 2% HF was used as the activating solution which resulted in patches, indicating a preferential attack on parts of the surface.

## 4.2 THE NORSK HYDRO PROCESS

It is mentioned in the Norsk Hydro patent (77) that either potassium pyrophosphate or sodium pyrophosphate can be used

in both the activation and zincating baths, but the initial experiments using sodium pyrophosphate were found to be unsatisfactory owing to the formation of patchy immersion zinc coatings. When the process was operated using potassium pyrophosphate in both the activation and zincating baths, visually good quality coatings on various alloy samples were obtained. It was observed that potassium pyrophosphate was more soluble in the solution compared with sodium pyrophosphate, especially in such quantity (65-150 g/l), and it may well be the reason for the better quality zinc coating obtained. During the oxalic acid cleaning stage, the surfaces of the alloys were cleansed of their oxide films by forming insoluble magnesium oxalate which was then subsequently washed off during rinsing. In the secondary activation, the surface hydroxide films which may be formed during rinsing could be removed by forming soluble complexes with the pyrophosphate ions.

$$2\,Mg(OH)_2 + X\,P_2O_7^{4-} \longrightarrow (Mg(P_2O_7)X)^{-2X}$$

However, after the zinc immersion stage, the zinc deposits were distributed irregularly in small patches over the surface. In order to improve the distribution of zinc, the secondary activation step in the standard Norsk Hydro pretreatment was operated at the higher temperature and concentration. Three types of alloy samples viz. AZ91, AZ61 cold chamber and AZ91 hot chamber, pretreated under the same

conditions and sequence were examined under the S.E.M. A finely divided and massive layer of zinc was deposited on each of the alloy sample surfaces. It appeared that the zinc deposits did cover most of the alloy surfaces, but the distribution was uneven. The zinc deposits were much thicker in some areas than in others. Preferential growth of zinc on the alloy surfaces was therefore believed to have taken place during the zincate process. The different alloy samples were found to be responding similarly in each stage.

## 4.3 THE CANNING PROCESS

The Canning sequence was introduced to further improve zinc distribution. The process was in fact very similar to the Norsk Hydro process, except that different chemical agents were employed in the secondary activation. The surface response at each stage is shown in Plate 9. After the final zincating process, the zinc deposits were found to be finely spread over the surface and no preferential growth on the more cathodic surface i.e. the aluminium rich area, was detected.

## 4.4 POTENTIAL MEASUREMENTS

### 1% OXALIC ACID ACTIVATION

The potential-time curves recorded for the three alloy samples (AZ91, AZ61 cold chamber panels and AZ91 hot chamber castings) were virtually identical indicating that the alloys behaved similarly to one another (Fig. 14). The curves had a shallow parabolic shape which is usually characteristic of the formation of a protective surface film. X-ray analysis confirmed the presence of magnesium oxalate which is relatively insoluble in water. The oxalic acid removed the surface oxide but this lead to the formation of an oxalate film which must subsequently be removed by very thorough swilling in water.

### THE SECONDARY ACTIVATIONS

The likely interpretation of the potential/time curves obtained in the secondary activation stage of the Norsk Hydro sequence (Fig. 17) is that first oxide or other surface contaminants are first removed (region A-B). Then from B to C it is suggested that a hydroxide film forms but at the same time the pyrophosphate forms soluble complexes, causing the potential to remain at a fairly base value.

The potential-time curves for the second stage in the Canning process (Fig. 18) show that a less base potential was reached, after a few seconds immersion, than in the case of the standard Norsk Hydro solution (Fig. 17). The equilibrium value also occurred at a more noble potential.

The function of each reagent in this activation solution was defined by the potential-time curves when each of the reagents was added successively to the solution (Fig. 19). Sodium borax with its pH ranging from 10.5 to 11.5 appeared to be working as a buffer. Addition of pyrophosphate ions has made the surface of the sample more active by forming soluble complexes with the surface hydroxide film. The presence of fluoride ions caused passivation of the magnesium alloy surface. These phenomena will be discussed in more detail in Section 4.6.

## THE ZINCATE IMMERSION

The outstanding feature of the potential-time curves obtained when immersing the magnesium alloys in the zincating solution is the sharp step prior to the establishment of an equilibrium value. This step was shown to coincide with the change in rate of zinc growth illustrated in Fig. 36. Initially, deposition of zinc was rapid because the surface was free of hydroxide but once the

hydroxide film covered the exposed magnesium surface the deposition rate slowed down. The likely steps in the sequence are as follows:

(i) Initially, immersion zinc deposits rapidly onto the magnesium alloy but magnesium also goes into solution to form a hydroxide film on the surface.

(ii) Dissolution occurs at the outer surface of the hydroxide film due to the presence of pyrophosphate and fluoride ions in the solution; soluble complexes form.

(iii) Zinc can diffuse through the hydroxide film to enable slow formation of the zinc coating. The dissolution of magnesium is controlled by the arrival of zinc ions since the driving force is the difference in potential between zinc and magnesium. The arrival of zinc ions is controlled by their rate of diffusion through the magnesium film and consequently is governed by the thickness of the hydroxide film. The pH and composition of the zincating solution influences the position and magnitude of the step in the curve as will be discussed in the following sections.

## 4.5 COMPARING AND CONTRASTING THE ZINCATING STAGE IN THE PRETREATMENT SEQUENCE OF ALUMINIUM AND MAGNESIUM

There is a similarity between the zincating of magnesium and the treatment of aluminium prior to plating and zincating, the latter of which has been extensively studied. High, uncontrolled rates of zinc deposition in the zincating of aluminium have been reported to give a coarse, non-adherent deposit of zinc, and therefore any deposit applied to it will have poor adhesion to the substrate [96,134]. Consequently various techniques have been adopted to limit the rate of growth of the zinc layer when applied to aluminium. Amongst the most important is the use of a very highly concentrated zincating solution of high viscosity so that zinc depletion occurs at the surface and diffusion controls the rate of zinc deposition [118]. A better method is the addition to a dilute zincating solution, of soluble complexes of metals which are more noble than zinc. These more noble metals diffuse to the growing zinc deposit, form an alloy immersion deposit, and so limit the growth of the crystals. They also limit dissolution, and thus reduce weakening of the aluminium substrate.

It is reasonable to suppose that the criteria for good adhesion of a subsequent deposit to a zincate treated magnesium substrate will be the same as those established

for aluminium, amongst which are :

a) a fine grained zinc deposit of reasonable mechanical strength.

b) absence of excessive weakening of the substrate by dissolution.

The zincating solution employed in this study contained zinc present in relatively labile complexes. The solution had a low viscosity and did not contain more noble metals such as those used to advantage in the treatments of aluminium. However, very good adhesion, judged by the accepted values for aluminium, was obtained provided fluoride containing pretreatment and zincating solutions were used. The test results are subsequently discussed in Sections 4.10 and 4.11.

## 4.6 THE ROLE OF FLUORIDE IONS IN THE PRETREATMENT SOLUTION

It is postulated that fluoride, present both in the treatment immediately prior to zincating, and in the zincating solution itself, limited the rate of zinc deposition. Magnesium fluoride is very sparingly soluble in water (87 mg/l at 18 C) (117) and is probably even less soluble in solutions containing an excess of fluoride ions.

The potential-time curves shown in Figs. 19, 21 and 22 illustrate the behaviour of magnesium alloys in various components of the second stage solution of the Canning sequence. In the fluoride solution, the potential became more noble with time of immersion for pure metals and the magnesium alloy. This is consistent with the surface becoming covered with a layer of the sparingly soluble magnesium fluoride and was confirmed by Auger analysis of the pretreated magnesium surface.

When the fluoride containing pretreatment was omitted, rapid complete coverage with zinc was obtained (see Plate 25), but adhesion of a subsequent electrodeposit was poor. This is consistent with the formation of a coarse, dendrite zinc deposit known to give poor adhesion on aluminium.

However, when the fluoride containing pretreatment was used, the zinc deposit formed rather slowly and failed to cover the magnesium surface completely. Nevertheless, excellent adhesion of the subsequent electrodeposit was obtained. It is suggested that such good adhesion was obtained in areas which received a zinc deposit, that the overall adhesion value, judged by the accepted values where aluminium is the substrate, was very good. The mean size of the uncoated areas is quite small in relation to the thickness of the electrodeposit, which would tend to grow laterally more rapid than normal to the surface, and so a continuous layer of copper would rapidly be formed in the

first electroplating stage. Another possible explanation is that the uncoated portions of the surface are protected by a fluoride film which is soluble in the cyanide electroplating solution thus enabling good adhesion by direct plating. In an attempt to confirm this an experiment was conducted in which a sample of alloy AZ61CC was dipped in the Canning second stage solution and then in a solution having the composition of the zincate solution except that the zinc sulphate was omitted. Consequently, no zinc layer was present when the alloy was plated in a cyanide copper bath. Some adhesion of the copper was achieved. This was much greater than that obtained if a fluoride containing stage is omitted.

The role of fluoride in the zincating solution may be to reduce the rate of dissolution of the magnesium fluoride formed in the pretreatment, to form and reinforce the layer if it is damaged and possibly, if uncoated areas represent permanent anodic sites in the zincating stage, to control the anodic current density and thus the rate of zinc deposition.

## 4.7 THE INFLUENCE OF pH IN THE ZINCATING STAGE

The Pourbaix diagram shown in Fig. 5 [39] indicates the electrochemical behaviour of magnesium in aqueous solution.

Magnesium dissolves readily as $Mg^{++}$ in solutions with a pH below 10 but since magnesium hydroxide is stable above a pH of 10.2-10.6, magnesium does not dissolve in strong bases.

Almost all organic and mineral acids attack magnesium and its alloys except hydrofluoric and chromic. The reaction with nitric and hydrochloric is quite violent. However, the resistance to attack by hydrofluoric acid is due to the formation of a relatively insoluble and protective film of magnesium fluoride. It is claimed that at concentrations above about 2% magnesium is not attacked to an appreciable extent (37). Fig. 15 shows the rate of attack on alloy AZ61CC in oxalic acid, which was the first activator. In the Canning second stage solution which contained fluoride, the rate of attack was small (Fig. 20). This small rate is presumably attributed to the formation of a fluoride film.

A complete explanation of the clearly defined step in the potential-time curves has still not been found since joint studies of these results and S.E.M. examination of the zinc coating has not provided a direct relation.

It is shown clearly that the time at which a step occurs is dependant on pH as illustrated in Figs. 25-35, but the corresponding scanning electron micrographs (Plates 11 to 22) taken shortly after the step occurred revealed that complete coverage of zinc was not achieved. Therefore it is

most likely that the step is concerned with the coverage of exposed magnesium alloy surface with a hydroxide film. Moreover, the potential-time result for magnesium (Fig. 37) illustrates that a step occurs in the curve even when fluoride is excluded from all stages of pretreatment. This suggests that on the immersion in zincate solution the step is due partly to hydroxide film formation but also fluoride zinc film formation.

## 4.8 EFFECT OF OPERATING ZINCATE SOLUTION ELECTROLYTICALLY

One would have expected that with the application of electrolysis, the result should be a greater zinc deposition (because of added electrolytic reaction), than just purely by galvanic reaction. However, a brief study discovered the opposite to be true (c.f. Fig. 36). In fact, when the current was increased, the deposition rate was even lower.

One explanation could be that electrolysis caused rapid coverage of the active areas which would reduce the galvanic reaction to a very slow rate, particularly if other areas were covered with fluoride film. In fact, the higher the current, the faster the coverage, resulting in a lower weight gain.

In view of the indication of poor adhesion obtained and the limited time available, it was not considered worthwhile to pursue further investigations on this aspect. In addition, the zincate solution was formulated only for use as a conventional immersion bath. Therefore, if more work is to be carried out to investigate this phenomenon, a solution formulated specifically for electrolytic operations may be necessary.

## 4.9 EFFECT OF THE DOUBLE DIP SEQUENCE

Potential-time curves for the first and second immersion using the same zincate solution are shown in Fig. 41. It illustrates that the prior condition of the alloy, in this case AZ61CC also influences the position of the step in the curve. Equilibrium potential was reached more quickly during the first immersion. This phenomenon is very similar to those observed in the plating of aluminium [75,118]. The corresponding micrographs shown in plate 27 reveals that the zinc deposit did not completely cover the alloy surface even after the second immersion.

Samples treated using the double dip sequence were plated with copper and peel tests carried out. Although the appearance was promising the adhesion levels achieved were virtually zero. The double dip procedure was not pursued

and further work is necessary to discover whether it really does have any prospects for commercial processing of die-cast magnesium alloys.

## 4.10 ADHESION TESTS

### THERMAL CYCLING TESTS

Most of the failures occurred by blister formation at the edges of the plated samples after quenching. Some of the bigger blisters formed after quenching (pretreated using the Standard Dow process) were examined using the S.E.M. together with the X-ray analysis attachment. Massive zinc deposits found on both sides of the failed surfaces indicated that the reason for blister formation was the failure in the zinc layer.

### PEEL ADHESION TESTS

Mathematical analysis of the peel tests used for determining the adhesion of electrodeposits to plastics indicated that the resulting numerical reading was not a true measure of adhesion. It has been claimed (98) to be a measure of a complex of factors including Young's modulus and tensile

strength of the substrate and coating. Applying the limited evidence available, it was believed that this study was also applicable to the peeling of electrodeposits from metal substrate.

Although the levels of adhesion using the canning process varied from 7.72 for alloy AZ61 cold chamber casting to 1.54 for alloy AZ91 hot chamber casting, all the alloys revealed ductile failure characteristics. The adhesion between two different materials is determined by the extent of chemical and mechanical bonding. Because of differences in the mechanical strengths of the alloys, it would be expected that differing percentages of perfect adhesion between substrate and coating would be required to obtain the same overall measured level of adhesion. Where the force or bond between the electrodeposit and substrate is greater than the cohesive forces between the atoms of the substrate, the adhesion value would depend only on the mechanical properties of the substrate, provided that the coating would withstand the peeling load involved.

A ductile copper coating was employed for the peel test instead of a bright or semi-bright nickel which would have been applied for most decorative application in commerce. Therefore, as in the case of plated plastics, it is a controversial matter whether the peel test on its own is a realistic measure of adhesion in relation to service performance.

CORROSION TESTING

Results are illustrated in Plates 32 to 37 where samples plated with the four different coating systems after 2 cycles of copper acetic acid salt spray testing are displayed. The plated samples prior to the corrosion test are also shown correspondingly. The analysed result indicates that there is no apparent difference between the alloys. As shown in Fig. 46 , it is apparent that the Canning process is the best pretreatment process, and the average rating of 9.25 was achieved after the corrosion tests. In Fig. 47 , with reference to the B1 curve, i.e. samples pretreated with the canning process, a significant and unexpected decrease in rating was obtained with samples coated with the duplex system. However, the rest of the samples coated with the other three systems have shown good corrosion resistance. It is suspected that poor quality of the castings may have ruined some of the results and therfore further investigation is necessary.

Optical microscopy and scanning electron microscope examinations show that most of the pits formed were hemispherical in shape and that the attack was very severe and rapid in the underlying magnesium substrate.

# CHAPTER FIVE CONCLUSIONS

1. Of all the pretreatment sequences investigated, the Canning process was the most successful one both from the point of view of adhesion and appearance after plating with decorative copper + nickel + chromium coatings. Samples pretreated with the standard Dow sequences all gave poor performance when subjected to thermal cycling tests. Fairly good brightness was achieved when samples were pretreated using the standard Norsk Hydro sequence but blisters occurred on thermal cycling. A high concentration and temperature in the secondary activation stage of the Norsk Hydro process is advantageous with respect to adhesion tests. However, comparatively dull surface appearance resulted after electroplating with bright nickel + decorative chromium.

2. Fluoride is an essential component of both the Canning second stage activation and the zinc immersion solution. It controls the rate of deposition of zinc from fluoride free zinc immersion solution (see Fig. 37).

3. The presence of fluoride in the immersion solution suppresses the rate of zinc deposition on the magnesium alloy surface.

4. In the zincating solution, pH and composition had a significant effect on the time taken to produce the step in the potential-time curve and hence the equilibrium potential.

5. Immersion zinc deposition occurred rapidly at first but then changed to a slower uniform rate at a point corresponding approximately to the step in the potential-time curve.

6. Alloys AZ61 and AZ91 whether hot or cold chamber castings, behaved in a similar manner in a particular processing solution. This was illustrated by potential-time results and zinc growth rate curves. However, the alloys behaved in a different manner in different processing sequences.

7. Peel tests illustrated that good adhesion levels could be achieved when samples were pretreated using the Canning sequence. The adhesion levels achieved were comparable with the levels achieved on many aluminium alloys. The comparatively poor adhesion achieved by the AZ91 hot chamber castings was due to its poor surface quality.

8. The best corrosion results, using copper + nickel + chromium coatings, were achieved with the Canning pretreatment sequence but corrosion results were not entirely reliable as many of the die castings were not of satisfactory standard. However, the adhesion level

was adequate since exfoliation did not occur even when large pits formed in the magnesium alloy substrates. Due to the difference in chemical activity between magnesium and the coating metals it is inevitable that large pits are formed in the substrate once the coating is penetrated.

9. Samples treated using the double dip sequence exhibited good appearance. However, the adhesion levels achieved were virtually zero.

10. It is essential that castings of higher quality should be available before plating of magnesium alloy die castings can be considered attractive commercially.

## SUGGESTIONS FOR FURTHER WORK

1. In view of the results obtained on the various magnesium alloys chosen, it would be worthwhile studying the behaviour of other alloys, in particular those used in the aviation industry.

2. To achieve a more universally applicable pretreatment, other zincate solutions should be developed. For example, the addition of metal ions and complexing agents similar to those used for producing immersion films on aluminium alloys may be effective in preventing rapid film growth instead of fluoride.

3. The double dip sequence operated in this programme resulted in zero adhesion. Phosphoric acid/ammonium bifluoride solution was employed as the stripping agent which was possibly too aggressive for the alloys. Other stripping agents need to be developed and hence further work is necessary to discover whether the double dip sequence does have any prospects for commercial processing of die-cast magnesium alloys.

4. Previously it has been reported that direct plating does not produce quite as high a level of adhesion as zinc immersion. However, recently J.Cl. Puippe (66) has claimed that good results have been obtained using electroless nickel plating. It is therefore suggested

that his work be followed up to determine whether his claims apply to all alloys or to only the ones that he used which were AZ61 and AZ81.

5. Electrolytic operation of the zincate solution did not achieve good adhesion for any of the alloys used. Since the solution was formulated only for use as a conventional immerson bath, further work should be undertaken to develop a solution specifically for electrolytic operation.

6. Peel tests have been carried out to assess adhesion and the associated failure surfaces examined. However, it is still difficult to understand the fundamental mechanisms connected with good peel adhesion. Therefore a much more detailed investigation concerning the various aspects of the peel test and other methods of evaluating adhesion is required.

7. It is questionable whether peel results give a good indication of behaviour in service and so work is necessary to correlate adhesion tests with service trials.

8. Conclusions concerning corrosion performance given in this study were derived from the results of C.A.S.S. testing. However, accelerated corrosion tests do not always give a realistic indication of service performance. A programme of static and mobile atmospheric exposure tests should be initiated.

APPENDIX 1

Chromating baths (44) :

1. The acid chromate bath

The bath consists of a solution in water of:

70 g sodium or potassium dichromate,
0.22 litres of concentrated nitric acid per litre of bath.

Good quality clean tap water should be used.
Items to be treated should be clean and free from grease. (Degreased and/or acid pickled if necessary.)
Items should be immersed for about 30 sec. to 1 min., drained completely, and immediately washed in several changes of clean water or by hosing.
After thoroughly drying (by warm air if possible), the film should not be capable of being easily rubbed off.
Note: This bath dissolves magnesium and too long an immersion period will affect the dimensions of the parts.

2. The Chrome-Manganese bath

The bath consists of a solution in water of:

0.1 kg sodium or potassium dichromate,
0.05 kg magnesium sulphate,
0.05 kg manganese sulphate per litres of bath.

Good quality clean tap water should be used.

The bath may be used at any temperature between 20 °C and boiling point, the immersion times vary from about two hours to a few minutes.
Items to be treated should be clean and free from grease and should be degreased if necessary. They should be immersed until a brown to black film is obtained. The actual colour will vary with the alloy. Pressure die castings and the cast skin of sand and die castings often show a patchy appearance. Results should be judged on machined surfaces but the film should not be capable of being easily rubbed off.
Components should be thoroughly washed, preferably in running water and dried quickly and completely.
Note: This bath causes no dimensional loss.

Data taken: Magnesium Industry Council, 'Magnesium in general engineering' (44).

APPENDIX II MATHEMATICAL ANALYSIS OF THE PEEL TEST FOR DETERMINING THE ADHESION OF ELECTRODEPOSITS TO PLASTICS. (REF. 89)

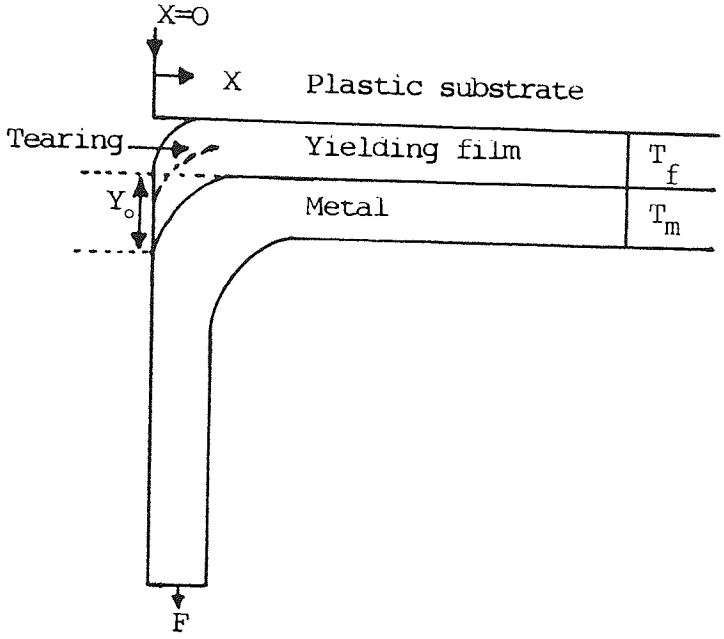


Nature of Jacquet tests

The electrodeposited coating is pulled at 90° angle from the underlying plastic substrate. Either the plastic substrate or the metallic film must yield plastically in order to permit the radius of curvature which results from pulling testing. It is assumed that both the plastic yielding substrate and the metallic film obey Hook's Law. The following definitions will be used.

$M$ = bending moment ($Nmm^{-1}$)
$S$ = stress on the plastic film ($Nmm^{-2}$)
$F$ = force applied to the metallic strip per unit length
$I_z$ = moment of inertia of the metallic strip relative to the Z-axis

$$= \frac{Wtm^3}{12} \quad (mm^4)$$

$$K = \frac{F}{tm^{\frac{3}{4}}}$$

$E_f$ = Young's Modulus for the plastic film ($Nmm^{-2}$)
$E_m$ = Young's Modulus for the metallic coating ($Nmm^{-2}$)
$\delta_f$ = tensile strength of the plastic-yielding film
$y$ = deflection of the plastic-yielding film under load (mm)

$t_f$ = thickness of the unstressed plastic-yielding film (mm)
$t_m$ = metallic coating thickness (mm)
w = width of the metallic strip in Z-plane (mm)
X,Y = planes are shown in above figure. Z-plane is perpendicular to the plane of the paper.

When the plastic-yielding film is subjected to a loading, Hook's Law being obeyed, the following relationship must hold:

$$E_f = \frac{S}{\frac{y}{t_f}} \qquad \frac{N\ mm^{-2}}{\frac{mm}{mm}} = N\ mm^{-2} \qquad (1)$$

If we assume that shear stresses in the plastic-yielding film are negligible, this means that the maximum stress in the plastic-yielding film is

$$S = -\frac{y}{t_f} E_f \qquad (2)$$

This stress must now be equated with the corresponding load on the metal strip being deflected. It is assumed that the radius of curvature is extremely small. This assumption leads to the boundary condition that the bending moment (M) is zero at X=0. The equation for a beam on an elastic foundation is therefore applied.

$$S = \frac{E_m I_z}{W} \frac{d^4y}{dx^4} \qquad (3)$$

Equating (2) and (3):

$$S = \frac{y}{t_f} E_f = \frac{E_m I_z}{W} \frac{d^4y}{dx^4} \qquad (4)$$

$$\text{Let } \alpha = \sqrt[4]{\frac{E_f}{4E_m} \frac{W}{I_z t_f}} = \sqrt[4]{\frac{E_f}{E_m} \frac{3}{Wtm^3 t_f}} \qquad (5)$$

Then integration of equation (4) leads to:

$$y = e^{\alpha x}(A\cos\alpha X + B\sin\alpha X) + e^{\alpha x}(C\cos\alpha X + D\sin\alpha X) \quad (6)$$

The previous assumptions lead to the following boundary conditions:

$$Fw\left(\frac{dM}{dx}\right)_{x=0} = E_m I_Z \left(\frac{d^3y}{dx^3}\right)_{x=0} \quad (7)$$

$$(M)_{x=0} = -E_m I_Z \left(\frac{d^2y}{dx^2}\right)_{x=0} = 0 \quad (8)$$

$$\left(\frac{dy}{dx}\right)_{x=0} = 0 \quad (9)$$

$$(y)_{x=0} = 0 \quad (10)$$

It can be shown that A and B are zero, and that C and D have finite values. This then leads to the following equation:

$$y = \frac{2\alpha F\, t_f}{E_f(\sinh^2[\alpha X_t]-\sin^2[\alpha X_t])} \text{ multiplied by}$$

$$[\sinh(\alpha X_t)\cos(\alpha X)\cosh(\alpha[X_t-X])\sin(\alpha X_t)\cosh(\alpha X)\cos(\alpha[X_t-X])] \quad (11)$$

If we consider $X_t$ (the total length of the strip) to be very greatly larger than the portion of the length of the metallic strip which is undergoing bending, equation (11) reduces to:

$$y_o = \frac{2F\alpha t_f}{E_f} \quad (12)$$

where $y_o$ is the maximum deflection at bursting of the plastic-yielding film (x=0).

Substituting for $\propto$ as above defined

$$y = \frac{2f(1.316)}{t_m^{\frac{3}{4}} t_f^{\frac{1}{4}}} \left(\frac{E_f}{E_m}\right)^{\frac{1}{4}} \left(\frac{t_f}{E_f}\right) \qquad (13)$$

Transforming:

$$F = 0.38\, y_o \left(\frac{E_m}{E_f}\right)^{\frac{1}{4}} t_m^{\frac{3}{4}} t_f^{\frac{1}{4}} \left(\frac{E_f}{t_f}\right) \qquad (14)$$

For a solid obeying Hook's Law, the maximum strain at rupture is:

$$\frac{y_o}{t_f} = \frac{\sigma_f}{E_f} \qquad (15)$$

where the tensile strength is equivalent to the maximum stress of equation (2).

Substituting equation (15) into (14)

$$F = 0.38\, \sigma_f \left(\frac{E_m}{E_f}\right)^{\frac{1}{4}} t_m^{\frac{3}{4}} t_f^{\frac{1}{4}} \qquad (16)$$

Equation (16) is the significant equation for the Jacquet test for adhesion of electroplated plastics.

It is possible to use equation (16) as a means of determining approximately the ultimate limit of bonding values for electroplated plastics despite the fact that it takes many surface and interfacial phenomena into account.

Note: All units has been changed to S.I. units.

ACKNOWLEDGMENTS

In producing this work I would like to express my gratitude to Dr. Keith Dennis whom I was most fortunate to have as my supervisor. His immense help and encouragement were instrumental in guiding me through to the completion of this thesis. Grateful thanks are also due to W. Canning Ltd. for their valuable advice and supply of materials, and to SERC for their finance. Finally I wish to thank Miss Julie Lai for her help in typing the thesis.

REFERENCES

1. C.J.P. Ball, The history of Magnesium, J. Inst. Met., 1955-1956, 84, p.399.

2. R.W. Bunsen, Ann. Chem. Pharm., 1852, 82, 137.

3. R.B. Ross, Metallic Materials Specification Handbook, 3rd Ed., E & F.N. Spon., New York, 1980, p.206.

4. B.S. 2970:1972 British Standards for Mg Castings.

5. B.S. 1490:1970 British Standards for Al Castings.

6. American Soc. For Metals, Metals Handbook, 9th Ed., American Soc. For Metals, Ohio, 1979, Vol.2, p.525.

7. E.V. Pannell,'Magnesium: Its production and use', Pitman, London, 1943, p.6

8. W.H. Dennis, Metallurgy of the Non-ferrous Metals, Pitman, London, 1954, p.432.

9. C.S. Roberts,'Magnesium and Its Alloys', 1960, John Wiley & Son, Inc., New York, 1960, p.17.

10. W.H. Rothery & G.V. Raynor, J. Inst. Metals, 1938, 63, 201-226.

11. N.S. Kurnakow & V.I. Miheeva, J. Inst. Metals, July 1938, 252.

12. A. Beck,'Technology of Magnesium and Its Alloys', 3rd Ed., Hughes, London, 1943, p.45-99.

13. E.F. Emley,'Principles of Magnesium Technology', 1st Ed., Pergamon Press Ltd., 1966, p.419.

14. American Soc. For Metals, Metals Handbook, 8th Ed., American Soc. For Metals, Ohio, 1978, Vol.1, p.1067.

15. J.D. Hanawalt, C.E. Nelson, & J.A. Peloubet, Trans, AIME, 1942, 147, 273.

16. K.E. Nelson,'The melting & refining of Mg', Trans, AIME, 1944, 59, 392.

17. Metal Bulletin Handbooks, year 1970-1982, 14th Ed., Metal Bulletin PLC, Surrey.

18. H.E. Elliott,'Casting High Quality Mg'. Modern Casting and AM Foundryman, July 1955.

19. A. Beck,'Technology of Mg & Its Alloys', 3rd Ed., Hughes, London, 1943, p.332-362.

20. A.W. Brace & F.A. Allen,'Magnesium Casting Technology'. Chapman & Hall, London, 1957, p.66-78.

21. American Soc. for Metals, Metals Handbook, 8th Ed., American Soc. for Metals, Ohio, 1982, Vol.5, p.433.

22. E.R. Petty, Physical Metallurgy of Engineering Materials, George Allen & Unwin Ltd., London, 1968, p.18-23.

23. F.L. Burhett, U.S. Patent no.2, 745, 153 (May 15,1956).

24. F.L. Burhett & F.C. Bennett, Trans.H.F.S. 1957, 65, 166.

25. F.C. Bennett,'For Mg: A Hot Chamber Die Casting Machine'. Modern Metals. Dec 1954.

26. A.F. Bauer, MOD. MET. 1950, Feb 17, Mar 27, Apr 30.

27. H.K. Barton & S. Bakui, Machinery, 1960, 96, 937-1183.

28. A.L. Olsen, W.H. Safranek, G.R. Kotler, Proceedings, International Mg. Association, May 1977, 39-43.

29. 'Standard Specification for Mg Alloy Die Casting', ASTM, B94-77.

30. B.S. 2L 126-128:1970. British Standards for Aerospace.

31. K.E. Mann,'Shrinkage & Crack Susceptibility of Mg Pressure Die Castings', Giesserei, 1957, 44, 301.

32. I.C. Hepfer, Light Metal Age, Oct. 1964, 4-7.

33. A.L. Olsen, Trans. Inst. Metal Finishing, 1980, 58, 29.

34. W.S. Loose, H.H. Uhlig, Editor,'Corrosion Handbook', John Wiley & Sons, Inc., New York, 1948, p.218-252.

35. G.D. Bengough & L. Whitby,'The corrosion & protection of magnesium & its light alloys', Trans. Inst. Chem. Eng. 1933, 11, 176-190.

36. L. Whitby. Trans. Faraday Soc. 1933, 29, 844.

37. L. Whitby in 'Corrosion resistance of metals & alloys' edited by F.L. LaQue and H.R. Capson, 2nd Ed., Chapman & Hall, London, 1963, p.169-180.

38. M. Pourbaix, Atlas of electrochemical equilibria in aqueous solutions, Pergamon press, 1966, p.70-83.

39. H.P. Godard,'Corrosion of light metals', J. Wiley & Son, New York, 1967. p.257-307.

40. R.J. Mckay & R. Worthington, 'Corrosion resistance of metals & alloys', Reinhold publishing Corp., New York, p.105-111.

41. C.V. King and W.H. Cathcart, J. Am. Chem. Soc., 1937, 59, 63-67.

42. L.F. Spencer, Metal Finishing, Sep 1961, 57, 56.

43. L.F. Spencer, Metal Finishing, Nov 1961, 59, 63.

44. Magnesium Industry Council,'Mg in general Engineering', 1968.

45. 'Standard Recommended Practices for Preparation of Mg alloy surface for painting', A.S.T.M. D 1732-67.

46. W.F. Higgins, Light Metals, 1956, 18, 264.

47. W.F. Higgins, Chem. & Ind., 1958, 49, 1604.

48. American Soc. for Metals, Metals Handbook, 9th Ed., American Soc. for Metals, 1982, Vol.5, p.629-649.

49. W.F.Higgins, Proceedings, International Mg. Association, 1959.

50. K. Huber, J. Electrochem. Soc., 1952, 100, 376

51. W.F. Higgins, Trans. Inst. of Metal Finishing, 1956, 33, 370.

52. L.F. Spencer, Metal Finishing, Oct. 1961, 58, 63.

53. G.L. Williams, U.S. Patent, 1, 562, 269 (8 May 1922).

54. I.A. Kenega, U.S. Patent, 1, 801, 629 (21 Apr, 1931).

55. Dow Chemical Co. Inc., U.S. Patent, 3, 152, 009 (6 Oct, 1964).

56. H. Richaud, U.S. Patent, 2, 965, 551 (20 Dec. 1960).

57. M. Jones, U.S. Patent, 1, 504, 061 (20 Feb. 1920).

58. A.C. Barlow, British Patent, 259, 307 (8 Oct. 1926).

59. E.I. DuPont, British Patent, 564, 823 (13 Oct. 1944).

60. W.F. Higgins, British Patent, 685, 219 (28 Dec. 1950).

61. Dow Chemical Co. Inc., U.S. Patent, 2, 526, 544 (17 Oct. 1950).

62. G.Bacquias, Trattamentie Finitura (Milano) 1981, 21, 49.

63. H.K.DeLong, Trans. Inst. Metal Finishing, 1953, 29, 201.

64. 'Standard Recommended Practice for Preparation of Mg & Mg alloys for electroplating', A.S.T.M. B480-68.

65. W.P. Innes, Modern Electroplating, 1974, p.601-607.

66. J.Cl. Puippe, Galvanotechnik, 1984, 75, 10.

67. H.K.DeLong, Trans. Inst. Metal Finishing, 1953, 29, 201.

68. H.K. DeLong, U.S. Patent, 2, 288, 995, (7 Oct. 1960).

69. L.F. Spencer, Metal Finishing, 1970, Dec., 32.

70. L.F. Spencer, Metal Finishing, 1971, Feb., 46.

71. Dow Chemical Company, Product & Process Bulletin, 147-43-67,'Plating Magnesium'.

72. H.K. DeLong, Metal Progress, 1955, April.

73. M.R. Caldwell, L.B. Sperry, L.M. Morse & H.K. DeLong, Plating, 1952, 39, p.142-148.

74. Canning Handbook on Electroplating, 22nd Edition.

75. J.W. Golby & J.K. Dennis, Surface Technology, 1981, 12, 141.

76. T.E. Such & A.E. Wyszynski, Plating, 1965, 52, 1027.

77. A.L. Olsen & S.T. Halvorsen, (Norsk Hydro AS), Euro Pat 030 305, (1981).

78. A.L. Olsen, Light Metal Age, 1977, August.

79. D. Davies & J.A. Whittaker, Metallurgical review, 12, no. 112.

80. J.K. Dennis & T.E. Such,'Nickel & Chromium Plating,' Butterworths, London, 1972, p.147-182.

81. K.L. Mittal,'Adhesion measurement, recent progress, unsolved problems and prospects,' ASTM, STD 640 1978 p.5-17.

82. B. Berdan, Chapter 15 in 'Electroplaters Process Control Handbook', edited by Foulke & Crane, New York, 1963.

83. K.L. Mittal, Electrocomponent Science & Technology, 1976, Vol.3, p.21-42.

84. K.L. Mittal in Properties of Electrodeposits: Their measurement & significance. Chapter 17, p.273-306. The Electrochemical Society.

85. 'Standard Test Methods for Adhesion of Metallic Coatings', A.S.T.M. B571-79.

86. S. Heiman, J. Electrochem. Soc., 1949, 95, 205.

87. W. Bullough & G.E. Gardam, J. Electrodep. Tech. Soc., 1947, 22, 169.

88. G.L.J. Bailey, J. Electrodep. Tech. Soc., 1951, 27, 233.

89. A.E. Wysjynski, Trans. Inst. Met. Fin., 1980, 58, 34.

90. A. Brenner & V.D. Morgan. Proc. American Electroplaters Soc., 1950, 37, 5.

91. E.A. Ollard, Trans. Faraday Soc., 1925, 21, 81.

92. G. Gugunishvili, Indust. Lab., 1958, 24, 333.

93. B.B. Knapp, Metal Finishing D 1949, 47, no 12, 42.

94. B.F. Ruthschlid, Products Finishing, 1969, 33, no 9, 66.

95. P.A. Jacquet, Trans. Electrochem. Soc., 1934, 66, 393.

96. T.E. Such & A. Wyszynski, Plating, 1956, 52, 1027.

97. J.W. Golby, Ph.D. Thesis, Dept. of Metallurgy, University of Aston in Birmingham, Oct. 1981.

98. E.B. Saubestre, L.J. Durney, J. Hajdu and E. Bastenbeck, Plating, 1965, Oct., p.982-1000.

99. E. Zmihorski, J. Electrodepositions Tech. Soc., 1947-48, 23, 203.

100. W.H. Dancy & A. Zavarella, Plating, 1965, 52, 1009.

101. 'British Specification for Electroplated Coatings of Nickel and Chromium', B.S. 1224:1970.

102. 'Acetic Acid Salt Spray Corrosion Testing for Metallic Coatings', A.S.T.M. B287-74.

103. P. Fintschenko & E.C. Groshart, Metal Progress, 1968, June, p.94-98.

104. 'Copper Acid Salt Spray Corrosion Testing for Metallic Coatings', A.S.T.M. B368-68.

105. J.K. Dennis & T.E. Such, Trans. Inst. Metal Finishing, 1963, 40, 60.

106. J.K. Dennis & T.E. Such,'Nickel & Chromium Plating', 1st Ed., Butterworth, London, 1972, Chapter 12, p.235-264.

107. 'Method for the Evaluation of Results of Accelerated Corrosion Tests on Metallic Coatings', B.S. 3745:1970.

108. 'Corrosion Testing of Decorative Chromium Electroplating by Corrodkote Procedure', A.S.T.M. B380-65.

109. 'Rating of Electroplated panels subjected to atmospheric exposure', A.S.T.M. B537-70.

110. W. Slavin,'Atomic Absorption Spectroscopy', John Wiley & Son, New York, 1978, p.6.

111. J.W.Robinson,'Atomic Absorption Spectroscopy', 2nd Ed., Marcel Dekker, Inc. New York, 1975, p.104-157.

112. Auger Electron Spectroscopy, Michael Thompson, Wiley, 1985.

113. A.E. Wyszynski, Trans. Inst. Met. Fin., 1967, 45, 147.

114. W. Canning Material Ltd. Canning microporous Nickel instrustruction sheet.

115. C. Chatfield, 'Statistics for technology', 2nd Ed., Chapman & Hall, John Wiley & Sons, New York, 1975, p.257-287.

116. J.K. Dennis & J.J. Fuggle, Trans. Inst. Metal Finishing, 1971, 49, 54.

117. C.R.C. Handbook of Chemistry and Physics. 62nd Ed., C.R.C. Press, Inc., 1981-1982, p.B111.

118. J.W. Golby, J.K. Dennis and A.E. Wyszynski, Trans, IMF, 1981, 59, 17.